A base station system study for LTE, UMTS and GSM/EDGE

Thesis

submitted in partial fulfillment of the
requirements for the degree of

Master of Science
in
Electrical Engineering

by
Sebastian-Ioan ENE BSc.
born in Bucharest, Romania
(E-mail: Ene.Sebastian@Gmail.com)
(Student ID: 4032179)

This work was performed in:

NXP Semiconductors

Gerstweg 2, 6534AE
Nijmegen, Gelderland
The Netherlands, EU

TU Delft Delft University of Technology

June 2011

Delft University of Technology

Printed in The Netherlands

Abstract

Communication systems evolve day after day at a very fast pace. People not only have high expectations in regard of the conversation quality, but they also need more data download speeds and better coverage. The industry tries to come and fill in this expectation by developing state-of-the art systems that are cost-effective and that ensure good profits.

Telecommunication operators require from vendors top class, cheap and reliable equipments for their sites. Vendors on the other hand try to cut down costs by simulating and then developing products. The aim of this project is to simulate three important wireless systems LTE, UMTS and GSM/EDGE (at physical layer level) for base stations, according to the implementations mentioned in the 3GPP standards. The most demanding requirements have been derived in this work for each of the transceiver systems and a realistic system description has been implemented in MatLab 2008b. The tolerance to RF imperfections (DC offset, I-Q amplitude & phase mismatch, cubic nonlinearity, frequency offset, phase noise, etc.) are taken into consideration. Also implementation specific RF imperfection, like the delay and amplitude misalignment in outphasing transmitters has been considered.

The RF imperfections have been considered in equal measures for both the transmitter and the receiver. The resulting study ensured a perfect calibration of the BER curves with the theoretical curves using the uncoded bits. The final system comparison in this thesis has been made only for the communication standard LTE, considering classical I-Q Tx configuration, a pure outphasing transmitter and an improved efficiency outphasing Tx. This in order to investigate which concept is more tolerant to RF impairments.

The parameters used in the simulations to check the system performances are: EVM, ACPR, scatter plots and BER. In conclusion, this study offers some suggestions for future research activities, related to topics like estimation, equalization, Rayleigh channels and Doppler affected Rayleigh channels.

Acknowledgements

I would like to start the list of acknowledgements with the professor that took me on this study trip, my Master thesis supervisor in TU Delft, Associate Prof. Leo C. N. de Vreede, for having the courage of taking me and for showing the confidence in the accomplishment of this work together with the great guidance for the implementation of the improved efficiency outphasing Tx. In an equal measure I would like to thank my mentor in NXP Semiconductors, Senior Principal System Architect Ir. Paul Mattheijssen for carefully guiding my work with patience, advices and understanding even when he was travelling on different continents.

I am grateful to the members of the dissertation committee for the time spent reviewing the content of the thesis: Prof. John R. Long for the valuable RF knowledge that he taught me in class, applied to parts of this project, Associate Prof. Robert B. Staszewski for advices on the transceiver imperfections division and 'Digital RF' knowledge and Associate Prof. Gerard J.M. Janssen for offering valuable advice regarding the equalization method for the Doppler shift case.

I am deeply indebted to the committee of the "*Promotion Top Talent Foundation*" of TU Delft that awarded me with a two years fellowship without which I would not have been able to properly concentrate on the Master of Science studies.

I would like to thank my colleagues in NXP Semiconductors: Dr. Spyros Vlachogiannatos for numerous precious advices on the system designs, Ir. Jawad Qureshi for valuable advice on the improved outphasing implementation, Ir. Rob Peters, Ir. Hasan Gul, Ir. Marcel Geurts for advices on subjects related to my project and Jos Coopmans for solving issues with the desktop computer and licenses. I also express my gratitude to the High Performance RF business line of NXP Semiconductors, Nijmegen, The Netherlands for the financial funding of this Master thesis project.

A considerable effort has been made by the MatLab support teams from Cambridge, United Kingdom and from Aachen, Germany for solving the bugs and offering support for the software implementations: Mr. Bastiaan Zuurendonk, Mr. Mahmoud Hammoud and Mr. David Yang helped me sort things out during various stages of the project, and their effort is acknowledged.

Moreover, I would like to thank my best friend, Alexandra Dobrescu MSc., for helping me with the relocation and accommodation to the Netherlands in general and for being a true friend on numerous occasions in special.

It has been a pleasure to study and have fun with new colleagues and new friends in the Netherlands: Paolo L. Schipani, Selcuk Ersoy, Alexandru Calu, Șerban A. Motoroiu, Andreea Ignat and Loup Balleyguier. I also appreciated the short time spent with my old friends in Romania.

I acknowledge here Mr. Boy and Mrs. Laila Lanée for proving to be great hosts here in Nijmegen and for unconsciously determining me call their historic house 'my home'.

Last but not least I would like to express my gratitude to my parents, brother and grandparents from Bucharest, Romania for encouraging me with the studies, for their love and support and to my uncles Dr. Irina-Margareta and Dr. Radu-Gabriel Dobrescu from Wiesbaden, Germany for their trust in my success and continuous encouragement.

Finally, I express my gratitude to God that gave me the opportunity and strength to study for this two year Master of Science degree and meet truly extraordinary people.

Sebastian-Ioan ENE BSc.
Nijmegen, The Netherlands
1st of June 2011

Contents

Abbreviations

3GPP	3rd Generation Partnership Project
ACLR	Adjacent Channel Leakage Ratio
ACPR	Adjacent Channel Power Ratio
AWGN	Additive White Gaussian Noise
BC2	Band Category 2
BS	Base Station
B_w	Unit of bandwidth occupied
CDMA	Code Divison Multiple Access
CP	Cyclic prefix
CRC	Cyclic Redundancy Check
CW	Continuous Wave
DCS 1800	Digital Cellular System 1800
DL-SCH	Downlink Shared Channel
DFT	Discrete Fourier Transformation
E-UTRA	Evolved UMTS Terrestrial Radio Access Network
E_b	Energy per bit
E_b/N_0	Signal to noise density ratio
EDGE	Enhanced Data rates for GSM Evolution
EVM	Error Vector Magnitude
FFT	Fast Fourier Transformation
HS-DSCH	High-Speed Downlink Shared Channel
IEEE	Institute of Electrical and Electronics Engineers
IC	Integrated Circuit
IL	Implementation Loss
GMSK	Gaussian Minimum Shift Keying
GSM	Global System for Mobile communications
LTE	Long Term Evolution
MLSE	Maximum likelihood sequence estimation
MSK	Minimum Shift Keying
N_0	Noise density
NA	Not Available
OFDM	Orthogonal Frequency Division Multiplex
PA	Power Amplifier
PCS 1900	Personal Communications System 1900
PDSCH	Physical Downlink Shared Channel
PSK	Phase-shift keying
QAM	Quadrature Amplitude Modulation
QPSK	Quadrature Phase-Shift Keying
R_b	Information bit rate
RE	Resource Element
RF	Radio Frequency
RMS	Root Mean Square (value)
RX	Receiver
RRC	Root Raised Cosine
SCH	Synchronization channel
SNR	Signal-to-Noise Ratio
T_c	Chirp time
TCH/F	Full-rate traffic channel
TX	Transmitter
UE	User Equipment
UEM	operating band Unwanted Emissions Mask
UMTS	Universal Mobile Telecommunications System

UTRAN	Universal Terrestrial Radio Access Network
UTRA-FDD	UMTS Terrestrial Radio Access - Frequency Division Duplexing
W-CDMA	Wideband Code Division Multiple Access

List of Figures

List of Tables

1. Introduction

1.1 Background

Today's world has a need for communication that was not encountered before. The main force that drives this need is probably the easiness with which people can now travel for business or for leisure. The way in which communication is made today is mostly wireless, without a wire, by making use of electromagnetic waves. Different connectivity scenarios exist: **fixed and wired** (a typical desktop computer in an office), **mobile and wired** (laptops in hotels), **fixed and wireless** (installed networks) and the most interesting case, **mobile and wireless** (no cables to restrict the user, roaming between wireless networks is possible). The applications range from vehicles to emergencies, business, and replacement of wired networks, infotainment in airplanes and cities and healthcare, just to name a few [**22**].

The increasing need for digital communications increases the need for high speed data and voice communication with high efficiency. Moreover, there are strict design rules and guidelines for RF IC designers, as they have to meet electrical industry standards.

Such standards are 3rd Generation Partnership Project (3GPP, www.3GPP.org) for Europe and Institute of Electrical and Electronics Engineers (IEEE www.iEEE.org) for USA. The standards have been developed by a group expert in order to assign frequency bands to different telecommunication systems to avoid interference. The standards impose limits to the most important RF system parameters, such as phase noise, linearity, frequency allocation, bit error rate (BER), error vector magnitude (EVM) or adjacent channel power ratio (ACPR).

1.2 Motivation

The mobile communications take part between a base station (the system that broadcasts to the users) and the handheld (the user that connects to the network of base stations). As mentioned above, the users require more and more data speed from their mobiles, the city centers are coming to a bottle neck in terms of mobile applications capacity, therefore newer and newer telecommunication systems are being introduced and standardized, this in order to be able to cope with higher data rates and capacity.

However, the network operators, such as Orange, KPN, Vodafone, T-Mobile (just to name a few) pay substantially for each base station that they replace with base stations complying with new standards, and this implies very high costs. Therefore, network operators prefer suppliers that can deliver cheap and easy to configure base stations, preferable by software. Suppliers try to reuse as many components of the old circuits for the new radio cards, or even implement the radio card with fewer components. Reusing the electronics that can be used for each of the systems, not only to reduce costs, but also because of space, weight and design considerations (in agglomerated city centers, it is not always easy to find a place for a base station, and space can pose problems for proper ventilation). The goal of this thesis is to simulate three systems at their physical level (PHY): LTE, UMTS, GSM/EDGE and investigate their tolerance to RF impairments. A goal of not less importance is to identify the most demanding hardware requirements for these standards. These requirements are to be met by the RF IC designers when they start defining the system architecture and their related circuit blocks.

1.3 Outline and Contributions

The emphasis of this master thesis is on system level simulations. This translates into the fact that the wireless circuits are mostly modeled using abstract models. For each of the three standards (LTE/UMTS/EDGE), the transmitter has been modeled using the European 3GPP specifications. The receiver architecture has been implemented by reversing the steps in the transmitter. In conclusion, several architectures that are of interest to the designers of wireless networks have been studied. The outline of the thesis is as follows:

Chapter 2: Multi-standards requirements

In this chapter, the most demanding requirements for multi radio systems have been derived using the latest[1] 3GPP standard [**2**].

Chapter 3: Linearity requirements

In this chapter, the intermodulation and ACLR requirements have been derived from the latest 3GPP standards [**3**, **4**, **5**] for LTE, UMTS and GSM/EDGE respectively.

Chapter 4: Phase noise requirements

In this chapter, the phase noise requirements have been derived from the latest 3GPP standards [**3**, **4**, **6**] for LTE, UMTS, GSM/EDGE respectively and WiMax [**7**].

[1] Latest version of the 3GPP standard available at the time of the derivation of the parameters, August 2010

Chapter 5: System performance evaluation

In this chapter, the transmitter and receiver of the LTE, UMTS and GSM/EDGE wireless systems are defined in conformance with the specifications at physical layer level as specified in the latest 3GPP standards [**8, 9; 10, 11, 12; 13, 14**].

Chapter 6: Simulation of LTE, UMTS&GSM/EDGE in AWGN channel (uncoded bits and MLSE equalization)

In this chapter, the three wireless systems are simulated in an AWGN channel. The bit error rate (BER) is calculated. Special attention is paid to the code validation, that is the curves of QSPK, 16QAM and 64QAM modulations match the theoretical curves for the uncoded bits of the system. The maximum likelihood sequence estimation (MLSE) equalizer is used to equalize the data affected by noise.

Chapter 7: Modeling of RF impairments

In this chapter, the RF impairments are modeled using blocks that have been verified for two tone signals. The RF impairments treated are: DC offset (in V), I-Q amplitude mismatch (in dB), I-Q phase mismatch (in deg), nonlinearity (IIP_3 given as an input in dBm), frequency offset (in Hz), phase noise (in RMS degrees) and all RF impairments in a chain. The parameters that are simulated are the BER, the error vector magnitude EVM and adjacent channel power ratio ACPR (AWGN noise has been skipped for these simulations). The objective is to see for each system which values of the RF impairments deviate the BER curve with 3 dB (as arbitrary assumption)) from the BER curve of the system with AWGN noise, in the ideal case with no RF impairments. A comparison is then made and the most demanding wireless systems and modulations are observed.

Chapter 8: LTE outphasing transmitter and comparison

In this chapter, apart from the classic I-Q LTE transmitter architecture that has been treated in chapter 5.2, two other transmitter architectures are considered. The first one is the classical outphasing implementation [**15**] and the second one is the improved efficiency outphasing transmitter which utilizes a threshold for the outphasing angle to improve its efficiency in power back-off operation. The relations from [**16**] are normalized to the maximum amplitude, in order for the cosine to cover the [-1, 1] range.

Chapter 9: Future research directions

In this chapter, directions and ideas for future investigations have been proposed. Because of time constraints, but also due to the requirements of the MSc. thesis in terms of content, not all ideas present have been implemented completely, nor has the study been completed for all three concepts and standards. For this reason a list of possible suggestions that could give useful results is included: a reception with multipath effects included, a reception in an environment in which the user is moving, introducing therefore signal fading, together with the assumption that the transmission channel coefficients are not known a-priori, therefore they have to be estimated.

The first direction is the study for the Rayleigh channel with multipath, but without Doppler shifts. The second direction is the Rayleigh channel that uses an equalizer to retrieve the information affected by multipath and Doppler shifts. The third direction is the estimation of the channel coefficients in multipath (and no Doppler shifts included) channels using two methods: the Toeplitz estimation and the FFT estimation method. The fourth section is related to the problems that the authors encountered during the implementation of the systems together with explanations.

Chapter 10: Conclusions

This chapter summarizes the main ideas of the work. It shows that the class B switched transmitter can provide better tolerance to all RF impairments and to nonlinearity and phase noise in special. The most intolerant system to RF impairments is underlined. A brief overview of each of the chapters of this study is given, along with conclusions of the study.

2. Multi-standards requirements

3GPP has worked on the standards of wireless systems since 1998 [**16**]. These are divided in specification series: requirements, service aspects, technical realization, signaling protocols, radio aspects, CODECs, data, programme management, subscriber identity module, security aspects (only for 3G and beyond), user equipment (UE) test specifications, security algorithms, LTE and LTE-Advanced radio technology and multiple radio access technology aspects. The security issue is considered in 2G and beyond systems, however for 2G systems, it is spread throughout several series.

Subject of specification series	3G and beyond / GSM (R99 and later)	GSM only (Rel-4 and later)	GSM only (before Rel-4)
General information (long defunct)			00 series
Requirements	21 series	41 series	01 series
Service aspects ("stage 1")	22 series	42 series	02 series
Technical realization ("stage 2")	23 series	43 series	03 series
Signalling protocols ("stage 3") - user equipment to network	24 series	44 series	04 series
Radio aspects	25 series	45 series	05 series
CODECs	26 series	46 series	06 series
Data	27 series	47 series (none exists)	07 series
Signalling protocols ("stage 3") -(RSS-CN)	28 series	48 series	08 series
Signalling protocols ("stage 3") - intra-fixed-network	29 series	49 series	09 series
Programme management	30 series	50 series	10 series
Subscriber Identity Module (SIM / USIM), IC Cards. Test specs.	31 series	51 series	11 series
OAM&P and Charging	32 series	52 series	12 series
Access requirements and test specifications		13 series (1)	13 series (1)
Security aspects	33 series	(2)	(2)
UE and (U)SIM test specifications	34 series	(2)	11 series
Security algorithms (3)	35 series	55 series	(4)
LTE (Evolved UTRA) and LTE-Advanced radio technolgy	36 series	-	-
Multiple radio access technology aspects	37 series	-	-

Figure 2-1 Specification numbering, image courtesy of [17]

Out of these standards in Figure 2-1, considered in this study are only the following chapters: radio aspects (for GSM, UMTS and LTE), LTE and LTE-Advanced radio technology, and multiple radio access technology aspects.

3GPP has worked on a standard [**2**] that deals with the minimum RF requirements for LTE, UMTS and GSM/EDGE multi-standard radio base stations.

These are given for downlink and are expressed using different specific terms. For convenience, the terms are put in tables and shown below.

In Table 2-1, important parameters defined in standard [**2**] are: **offset frequency** (gives a measure of the synchronization of the signals; it is the frequency offset from the carrier; for LTE it depends on bandwidth BW, for UMTS and GSM/EDGE it is fixed), **channel spacing** (it either depends on the carriers for LTE or is fixed for UMTS and GSM/EDGE, its importance is related to the frequency spectrum), **channel raster** (the centre frequency has to be an integer multiple of this value, it gives a measure of the smallest frequency division available in the system), base station output power tolerance (**BS P_{out} tolerance**, that gives a measure of the tolerance of the system to variations in terms of output power), dynamic range of the output power (**P_{out} dynamic range**, that gives an interval in dB for the output power variations), and error vector magnitude (**EVM**, which is a measure of how far the received points are in the constellation diagram from the ideal locations, thus one has the measure of the signal quality that will be used for decoding). P_{modMax} is the maximum power that depends on the modulation type used for GSM/EDGE (8PSK or GMSK) and is used in the calculation of P_{out} dynamic range.

System	F_{offset} [MHz]	Channel spacing [kHz]	Channel raster [kHz]	BS P_{out} tolerance [dB]	P_{out} dynamic range [dB]	EVM QPSK/16QAM/64 QAM [%]		
LTE	BW/2	$(BW_1+BW_2)/2$ [2]	100	+/-2.1	>20	17.5	12.5	8
UMTS	2.5	5000	200	+/-2.1	>18	17.5	12.5	-
GSM/EDGE	0.2	200	200	+/- 2	$>P_{modMax}-2N$ [3]	[8PSK] 9	NA	NA

Table 2-1 Frequency and power dynamics defined in the 3GPP standard [**2**]

[2] BW_1 and BW_2 are the channel bandwidths of the two LTE carriers [**2**]
[3] N is the radio frequency power step

Table 2-2: the parameters defined in the 3GPP standards [**2**, **3**, **5**] are the **time alignment** (delay between the signals from two antennas at the antenna ports, this measures the effectiveness of synchronization between the transmitted and received signal), the **frequency error** (frequency deviation from the carrier frequency, expressed in *ppm*: parts per million, this is a measure of the allowed deviation, usually caused by the tolerance of the components used for oscillators), **transmitter spurious emissions** (maximum interferer level at an offset from the carrier, these emissions mix with the signal and affect the linearity), and $\mathbf{P_{spurious}}$ for co-location of base stations with other base stations (requirements applied for the protection of the BS receivers when co-located with GSM900, DCS1800, PCS1900, GSM850, CDMA850, UTRA FDD and/or E-UTRA BS, spurious levels from other BS should not exceed this level). Considering the EVM values in Table 2-1, the GSM/EDGE is the most sensitive to errors and therefore has to have the best signal quality.

System	Time alignment	Frequency error [ppm]	Tx spurious emissions	$P_{spurious}$ for co-location of BS with other BS
LTE	<65 ns	0.05	Categ BC2[4]:-36 dBm [300 kHz]	-96 dBm [100 kHz]
UMTS	0.25-0.5 T_c	0.05	Categ BC2:-36 dBm [300 kHz]	-96 dBm [100 kHz]
GSM/EDGE	NA	0.1- 0.2	Categ BC2:-36 dBm [300 kHz]	-98 dBm [100 kHz]

Table 2-2 Spurious emissions data extracted from the 3GPP standard [**2**, **3**, **5**]

Table 2-3 specifies the **operating band unwanted emission mask** (specified only for LTE, for UMTS and GSM/EDGE, there is no specification, but the same mask can be considered as an alternative, it shows the maximum levels of emissions in the operating band), operating band unwanted emissions mask when co-located with a GSM/EDGE base station (**UEM in BC2 with GSM/EDGE adjacent BS** specified only for UMTS, therefore the limit for LTE and GSM/EDGE can be considered as such; different requirements apply when a BS is co-located with other types of BS, usually for protection of signal interference), $\mathbf{BW_{max}}$ (maximum channel bandwidth, important for issues related to spectrum).

[4] BC2 is Band category 2: Bands for E-UTRA FDD, UTRA FDD and GSM/EDGE operation [**2**]

System	Operating band unwanted emission mask	UEM in BC2 with GSM/EDGE adjacent BS	BW_{max} occupied
LTE	$-14dBm-15*(\frac{f_{offset}}{MHz}-0.215)dB$	NA	$BW_{channel}$
UMTS	$-14dBm-15\cdot\left(\frac{f_{offset}}{MHz}-2.715\right)dB$	$5dBm-60*(\frac{f_{offset}}{MHz}-0.015)dB$	5 MHz
GSM/EDGE	NA	NA	200 kHz [**15**]

Table 2-3 Operating band UEM from the standard [**2**]

In case of GSM/EDGE, the bit error rate BER should be smaller than 0.01% for GMSK up to -40dBm and maximum 0.1% for GMSK for power levels bigger than -40 dBm. The limit is 0.01% for 8PSK/QPSK, or 16QAM/32QAM.

In Table 2-4, Adjacent Channel Leakage power Ratio (**ACLR**, the ratio between the filtered mean power of the carrier channel frequency to the filtered mean power centered on an adjacent channel frequency situated at a frequency offset, it gives a measure of power leakage from the adjacent channels), the reference sensitivity power level ($\mathbf{P_{refsens}}$, the minimum mean power received at the antenna connector at which a reference performance requirement shall be met for a specified reference measurement channel [**2**]), **dynamic range** (a measure of the capability of the receiver to receive a wanted signal in the presence of an interfering signal inside the received channel bandwidth).

System	ACLR [dBc]	$P_{refsens\ Rx}$@ BW_{chan} [dBm@ Mhz]	Dynamic range & Interferer [dBc@ dBm]
LTE	45 or -13dBm/ 1 MHz	-106.8@ 1.4 -103@ 3 -101.5@ 5;10;15	-70.2/-76.4 dBm
UMTS	45 dB@ 5 MHz $channel_{offset}$ 50 dB@ 10 MHz $channel_{offset}$	-121 @ 12.2 kbps	12.2 kbps//wanted: -91 dBm//interfering: -73 dBm/3.84 MHz
GSM/EDGE	NA	-104 dBm	NA/same as above

Table 2-4 Tx ACLR and Rx sensitivity, dynamic range defined in the standard [**2**]

In Table 2-5 the Rx **in-band selectivity** and **in-band blocking** characteristics are given. These are measures of the receiver ability to receive a wanted signal while

considering an unwanted interferer inside the operating band. Two situations can be encountered: a (wideband) and a narrowband blocking requirement.

System	Rx in-band blocking	Rx in-band narrowband blocking
LTE	$P_{refsens}$+6dB/ $P_{avg\ interferer}$: -43 dBm	$P_{refsens}$+6dB / $P_{avg\ interferer}$: -49 dBm
UMTS	$P_{refsens}$+6dB/ $P_{avg\ interferer}$: -40 dBm	$P_{refsens}$+6dB / $P_{avg\ interferer}$: -49 dBm
GSM/EDGE	$P_{refsens}$+3dB/ $P_{avg\ interferer}$: -35 dBm	$P_{refsens}$+3dB / $P_{avg\ interferer}$: -49 dBm

Table 2-5 Rx wideband and narrowband blocking parameters defined in the standard [**2**]

In Table 2-6 are given the **out-of-band blocking** characteristics. This is a measure of the receiver ability to receive a wanted signal in the presence of an unwanted interferer outside the operating band. A special case is considered, that is when the base station is co-located with another base station.

System	Rx Out-of-band-blocking [CW carrier]	Rx Blocking requirements co-location
LTE	$P_{refsens}$+6dB/ $P_{avg\ interferer}$:-15 dBm	$P_{refsens}$ + 6 dB/ +16 dBm
UMTS	$P_{refsens}$+6dB/ $P_{avg\ interferer}$:-15 dBm	$P_{refsens}$ + 6 dB/ +16 dBm
GSM/EDGE	$P_{refsens}$+3dB/ $P_{avg\ interferer}$:-15 dBm	$P_{refsens}$ + 3 dB/ +16 dBm

Table 2-6 Rx blocking requirements out-of-band from the standard [**2**]

In Table 2-7 are given the strictest **receiver spurious emissions** limits in dBm, for a range of frequencies, at a frequency offset from the downlink operating band edge and in a specified measurement bandwidth.

System	Rx spurious emissions limit [dBm]//frequency range [MHz]// f_{offset}[MHz]// BW[kHz]
LTE	-57// 30-1000// 10-30// 300; 1000; 3000
UMTS	-57// 30-1000// 10-30// 300; 1000; 3000
GSM/EDGE	-57// 30-1000// 10-30// 300; 1000; 3000

Table 2-7 Rx spurious emissions limits extracted from the standard [**2**]

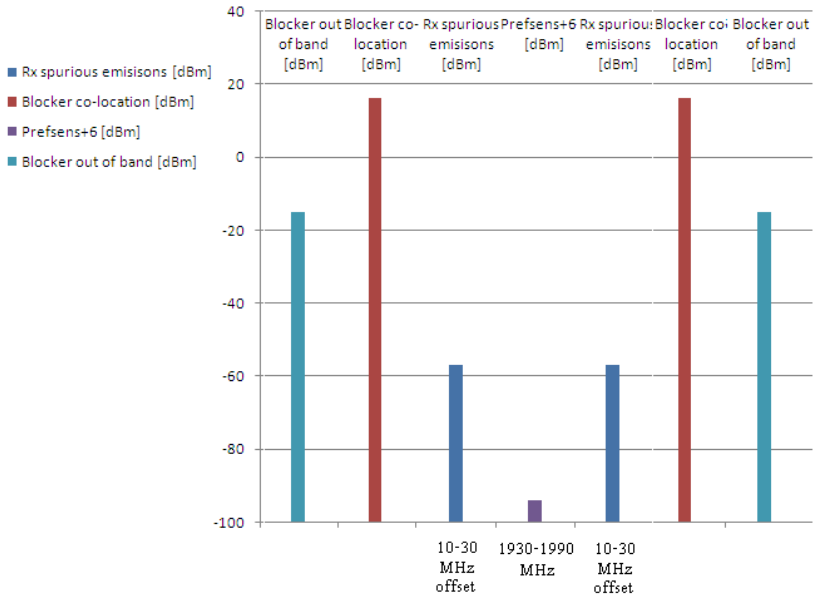

Figure 2-2 Plot of the signal powers, assuming $P_{refsens}$= -100 dBm

In Table 2-8 are given the receiver **intermodulation** (narrowband) **minimum requirements** (third and higher order mixing of two interfering RF signals produce an interfering signal in the band of the channel; the intermodulation response rejection shows the capability of the receiver to receive a wanted signal on its channel frequency in the presence of two interfering signals which have a specific frequency relationship to the wanted signal).

System	Rx intermodulation minimum requirement@ mean power of interfering signals	Narrow Rx narrow intermodulation @ mean power of interfering signals	Performance requirement SNR [dB]
LTE	$P_{refsens1}$+6dB/ -48 dBm	$P_{refsens1}$+6dB/ -52 dBm	18.8
UMTS	$P_{refsens2}$+6dB/ -48 dBm	$P_{refsens2}$+6dB/ -52 dBm	11.9
GSM/EDGE	$P_{refsens3}$+3dB/ -48 dBm	$P_{refsens3}$+3dB/ -52 dBm	9 [5]

Table 2-8 Rx intermodulation parameters defined in the standard [**2**]

[5] This is the strictest requirement from the table

3. Linearity requirements

A system can be considered as a function that maps an input to an unique output. Mathematically, this can be translated to the relation:

$$y(t)= T[x(t)] \quad [3.1]$$

where x(t) is the input or (excitation), y(t) is the output (or response) and *t* is the variable that usually represents time. *T* is the operation performed by the system.

A system is linear if and only if the output is expressed as a linear combination of responses to linear inputs:

$$T[a_1x_1(t) + a_2x_2(t)] = a_1T[x_1(t)] + a_2T[x_2(t)] \quad [3.2]$$

where $a_1$and a_2 are arbitrary scalars. A system that does not satisfy condition (3.2) is defined as *nonlinear* [**18**].

3.1. LTE

3.1.1 LTE Tx

Using the data in the tables specified in [3], one can derive the required output second order intercept point (OIP_2), output third order intercept point (OIP_3) and adjacent channel power ratio (ACPR) parameters using the data from spectral mask, out-of-band spectral emission, and parameters from ACLR requirements, respectively. The derivation below is done using the following procedure: as the wanted power is 43 dBm measured in 1.08 MHz bandwidth, and the interferer is 30 dB below the power of the carrier, and as P_{IM3} is -13 dBm in a 1 MHz bandwidth, the power density P_{wanted}= 43- 10*$\log_{10}$(1.08E6)= -17.3 dBm/Hz, the coupling loss between the transmitter and receiver is 30 dB (chapter 6.6.4.4 of [3]), then $P_{coupling\ loss}$ is -17.3-30 dB, which yields -47.3 dBm/Hz (the power density sensed by the receiver), and P_{IM3}= -13dBm-10*$\log_{10}$(1E6)= -73 dBm/Hz. The formulas used for the output third and second order intercept point are defined below and the corresponding figure is Figure 3-1:

$$OIP_3 = \mathrm{P}_{\mathrm{coupling\,loss}} + \frac{\mathrm{P}_{\mathrm{coupling\,loss}} - (P_{maxspurr} - 10log_{10}(BW_{spurr}))}{2}\ dBm \quad [3.3]$$

$$OIP_2 = \mathrm{P}_{\mathrm{coupling\,loss}} + \frac{\mathrm{P}_{\mathrm{coupling\,loss}} - (P_{maxspurr} - 10log_{10}(BW_{spurr}))}{1}\ dBm \quad [3.4]$$

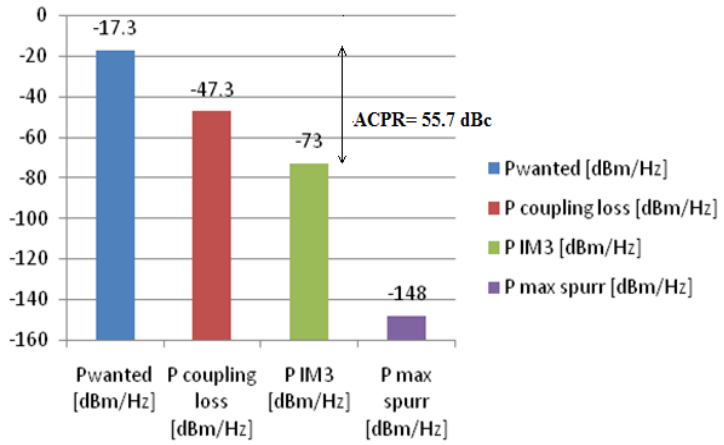

Figure 3-1 Plot of the spectrum requirements for LTE Tx

The term $P_{maxspurr}$ is the maximum emission power level of -98 dBm at 100 kHz. BW_{spur} is the measurement bandwidth in which the spurious limits have been measured in case the base station is co-located with another base station, 100 kHz. Both terms have been considered from Table 6.6.4.4.1-1 of [**3**]. ACPR= P_{wanted}- $P_{IM3.}$
The results are shown in Table 3-1, in the case of the transmitter.

P_{wanted}	[dBm/Hz]	-17.3
$P_{coupling\ loss}$	[dBm/Hz]	-47.3
P_{IM3}	[dBm/Hz]	-73
OIP_3	**[dBm]**	**63.3**
OIP_2	**[dBm]**	**113.7**
ACPR	**[dBc]**	**55.7**

Table 3-1 LTE Tx: derived OIP_3, OIP_2 and ACPR

The other set of parameters is determined using the power of ACLR, which for LTE is specified as 45 dBc.

$$OIP_3 = P_{wanted\ dBm/Hz} + 10\log_{10}(1.08MHz) + \frac{\text{ACLR}}{2}\ dBm \quad [3.5]$$

$$OIP_2 = P_{wanted\ dBm/Hz} + 10\log_{10}(1.08MHz) + ACLR\ dBm \quad [3.6]$$

OIP_3 is derived from ACLR by first converting the power density P_{wanted} to power and then adding the ACLR value divided by 2. The same procedure is applied for OIP_2 the difference being that in this case, ACLR is not divided anymore in half when adding. P_{IM3} is found by substracting from P_{wanted}[dBm] the ACLR value. The results are shown in Table 3-2.

OIP_3	**[dBm]**	**65.5**
OIP_2	**[dBm]**	**88**
P_{IM3}	**[dBc]**	**-2.3**

Table 3-2 LTE Tx: OIP_3, OIP_2 and ACPR derived from ACLR requirements

3.1.2 LTE Rx

For the receiver, different specifications have been calculated. These requirements have been computed considering an interferer standing at 52 dBc below the P_{wanted}, which is the $P_{reference\ sensed}$ with 6 dBm added.

The parameter P_{wanted} is the value higher with 6 dB compared to the lowest sensitivity level P_{sensed} equal to -106.8 dBm. The interferer mean power $P_{interferer}$ is extracted from chapter 7.5.1 of the standard [**3**], and is equal to -52 dBm. P_{IM3} is 3 dB below P_{wanted}. As $P_{interferer}$ is bigger than P_{wanted}, the term $P_{interferer}$ replaces P_{wanted} in formulas (3.3, 3.4):

$$OIP_3 = P_{interferer} + (P_{wanted} - P_{IM3})/2 \quad [3.7]$$

The same reasoning applies for OIP_2, therefore

$$OIP_2 = P_{interferer} + (P_{wanted} - P_{IM3})/1 \quad [3.8]$$

$$ACPR = P_{wanted} - P_{IM3} \quad [3.9]$$

P_{wanted}	[dBm]	-100.8
$P_{interferer}$	[dBm]	-52
P_{IM3}	[dBm]	-103.8
OIP_3	**[dBm]**	**-50.5**
OIP_2	**[dBm]**	**-49.0**
ACPR	**[dBc]**	**3**

Table 3-3 LTE Rx: OIP_3, OIP_2, ACPR from channel selectivity, blocking requirements [**3**]

Considering the strictest case (co-location with other BS) in which the mean $P_{interferer}$ is 30 dB below 16 dBm, this case yields -14 dBm. The blocking requirement from general blocking requirements is not that strict, as it is -43 dBm. P_{wanted} is 6 dB above $P_{refsens}$= -106.8 dBm, which is the sensitivity limit derived from chapter 7.7 Rx spurious emissions [**3**]. P_{IM3} is specified at 3 dB below P_{wanted}. As the mean power $P_{interferer}$ is bigger than the sensed mean power P_{wanted}, the same formulas as for Table 3-3 apply.

P_{wanted}	[dBm]	-100.8
$P_{interferer}$	[dBm]	-14
P_{IM3}	[dBm]	-103.8
OIP_3	**[dBm]**	**-12.5**
OIP_2	**[dBm]**	**-11.0**
ACPR	**[dBc]**	**3**

Table 3-4 LTE Rx: OIP_3, OIP_2 and ACPR derived from blocking requirements [**3**]

3.2 UMTS

3.2.1 UMTS Tx

Using the data in the tables specified in [**4**], one can derive the OIP_2, OIP_3 and ACPR parameters using the data from the transmitter spectral mask and out-of-band spectral emissions. The mean power P_{wanted} of 43 dBm is measured in a 3.84 MHz bandwidth, therefore P_{wanted}[dBm/Hz]= 43- $10\log_{10}(3.84E6)$= -22.84. In Table 3-5 it is derived the strictest power density of emissions. The emission limit is the strictest value considered from the transmitter's spectrum emission mask:
$P_{max\ emission}$[dBm/Hz]= -13- $10*\log_{10}$ (1E6)= -73.

BW_{meas} [Hz]	**f_{offset} [Hz]**	**$P_{max\ emission}$ [dBm]**	**$P_{max\ emission\ density}$ [dBm/Hz]**
30000	2500000	-14	-58.77
1000000	**7500000**	**-13**	**-73.00**

Table 3-5 UMTS Tx: Derivation of the strictest power density of emissions

The third order intercept point P_{IM3} is 3 dB lower than the mean power P_{wanted}. As the maximum power of any spurious emission shall not exceed -98 dBm (measured in 100 kHz bandwidth) in the case of co-location of a BS with another BS, the formulas used are described below:

OIP_3 [dBm]= P_{wanted} + ($P_{interferer}$-(-98-$10\log_{10}$(100kHz)))/2+$10\log_{10}$(3.84E6) [3.10]

OIP_2 [dBm]= P_{wanted} + ($P_{interferer}$-(-98-$10\log_{10}$(100kHz)))/1+$10\log_{10}$(3.84E6) [3.11]

ACPR [dBc]= P_{wanted}- P_{IM3} [3.12]

The results are synthesized in Table 3-6:

P_{wanted}	[dBm/Hz]	-22.8
$P_{max\ emission\ density}$	[dBm/Hz]	-73
P_{IM3}	[dBm/Hz]	-25.8
OIP_3	**[dBm]**	**80.5**
OIP_2	**[dBm]**	**118**
ACPR	**[dBc]**	**3**

Table 3-6 UMTS Tx: OIP_3, OIP_2 and ACPR parameters

There are two cases depending on the value of ACLR: one case in which ACLR= 45 dBc (Table 3-7), and the other case in which ACLR is 50 dBc (Table 3-8). The formulas used for derivation of the parameters are given below:

$$OIP_3\ [dBm] = P_{wanted} + ACLR/2 + 10*\log_{10}(3.84E6) \quad [3.13]$$

$$OIP_2\ [dBm] = P_{wanted} + ACLR/1 + 10*\log_{10}(3.84E6) \quad [3.14]$$

$$P_{IM3}\ [dBm] = P_{wanted} - ACLR + 10*\log_{10}(1E6) \quad [3.15]$$

$$ACPR[dBc] = P_{wanted} - ACLR + 10*\log_{10}(1E6) \quad [3.16]$$

OIP_3	**[dBm]**	**65.5**
OIP_2	**[dBm]**	**88**
P_{IM3}	**[dBm]**	-7.8
ACPR	**[dBc]**	**3**

Table 3-7 UMTS Tx: OIP_3, OIP_2 and ACPR derived from ACLR= 45 dB

OIP_3	**[dBm]**	**68**
OIP_2	**[dBm]**	**93**
P_{IM3}	**[dBm]**	-12.8
ACPR	**[dBc]**	**3**

Table 3-8 UMTS Tx: OIP_3, OIP_2 and ACPR derived from ACLR= 50 dB

3.2.2 UMTS Rx

For the receiver, different values for OIP_3 and OIP_2 have been calculated from intermodulation requirements. The interferer is at -47 dBc below P_{wanted}, as the strictest case is found for narrowband intermodulation. The sensitivity level P_{wanted} is taken from the blocking level power specification of -115 dBm. The $P_{interferer}$ is taken from the narrowband blocking performance. P_{IM3} is 3 dB below P_{wanted}. The same set of formulas (3.7-3.9) applies for the parameters in Table 3-9 and Table 3-10.

P_{wanted}	[dBm]	-115
$P_{interferer}$	[dBm]	-47
P_{IM3}	[dBm]	-118
OIP_3	**[dBm]**	**-45.5**
OIP_2	**[dBm]**	**-44**
ACPR	**[dBc]**	**3**

Table 3-9 UMTS Rx: OIP_3, OIP_2, ACPR from narrowband intermodulation requirements

The strongest interferer is found at -14 dBm, as the coupling loss is 30 dB and the carrier is situated at 16 dBm in the case of blocking performance requirement. This is the strictest requirement, compared to -15 dBm and -47 dBm, obtained from the blocking performance requirements or from general minimum emissions spurious requirement, respectively. P_{IM3} is 3 dB below P_{wanted}. The derived parameters are found in Table 3-10:

P_{wanted}	[dBm]	-115
$P_{interferer}$	[dBm]	-14
P_{IM3}	[dBm]	-118
OIP_3	**[dBm]**	**-12.5**
OIP_2	**[dBm]**	**-11**
ACPR	**[dBc]**	**3**

Table 3-10 UMTS Rx: OIP_3, OIP2 and ACPR derived for co-located base stations

3.3 GSM/ EDGE

3.3.1 GSM/EDGE Tx

Using the data in the tables specified in [**5**], one can derive the OIP_3, OIP_2 and ACPR parameters using the data from the transmitter spectral mask and out-of-band spectral emissions (as $P_{coupling\ loss}$ between the transmitter and receiver is 30 dBm, therefore from P_{wanted}= 33 dBm (most demanding requirement from [**5**] is for the 8PSK modulation) one subtracts 30 dB, as from chapter 4.7.1 [**5**] which refers to intermodulation) and from Adjacent Channel Leakage power Ratio (ACLR) requirements, respectively. P_{IM3}= P_{wanted}-70-3= -40 dBm, as the exceptions within the relevant transmit band may be up to 70 dBc relative to the carrier measured in a bandwidth of 100 kHz. This relation is derived using the information given in chapter 4.2.1.4.2 of [**5**], the special case of multicarrier BTS. The formulas (3.10 and 3.11) are modified into (3.17) and (3.18) as the power limit for spurious

emissions for BS co-location with a 3G BS is -96 dBm measured in a bandwidth of 100 kHz. These formulas are then applied in Table 3-11 for the computation of OIP_3, OIP_2 and ACPR.

OIP_3 [dBm]= P_{wanted} + ($P_{interferer}$-(-96-10$\log_{10}$(100kHz)))/2+10$\log_{10}$(200E3) [3.17]
OIP_2 [dBm]= P_{wanted} + ($P_{interferer}$-(-96-10$\log_{10}$(100kHz)))/1+10$\log_{10}$(200E3) [3.18]

P_{wanted}	[dBm/Hz]	-20.01
$P_{coupling\ loss}$	[dBm/Hz]	-50.01
P_{IM3}	[dBm]	-40
OIP_3	**[dBm]**	**80.99**
OIP_2	**[dBm]**	**128.99**
ACPR	**[dBc]**	**73**

Table 3-11 GSM/EDGE Tx: OIP_3, OIP_2 and ACPR parameters

Deriving the requirements from the ACLR specifications, one can consider two sets of rules: '*Continuous modulation spectrum*' and '*Switching transients spectrum*'. They are shown in Table 3-13 and Table 3-14, respectively. P_{wanted} as power density is determined from the measurement bandwidth of 300 kHz (chapter 4.5.1 of [**5**]) with the formula $P_{wanted\_density}$= P_{wanted}- 10*$\log_{10}$(300kHz).

f_{offset}[kHz]	*100*	200	250	400	900	1500	3900	6000
BW [kHz]	*30*	30	30	30	30	30	100	100
Power [dBc]	***0.5***	-30	-33	-56	-70	-73	-75	-80

Table 3-12 Interferer power for continuous modulation spectrum

The strongest interferer is found at a frequency offset of 100 kHz and has a mean power equal to 0.5 dBm measured in a bandwidth of 30 kHz. The power density of the wanted power is P_{wanted}[dBm/Hz]= 33-10$\log_{10}$(200E3). The power density of the interferer is $P_{interferer\ density}$[dBm/Hz]= P_{wanted}+0.5-10$\log_{10}$(30E3). P_{IM3}[dBm/Hz]= P_{wanted}-70-3. Formulas (3.17-3.18) are applied for the parameters P_{IM3}, OIP_3 and OIP_2 from Table 3-13. The conversion from power density to power is made after adding 10*$\log_{10}$(200E3) to OIP_3 and OIP_2.

In Table 3-13 is given the synthesis of the parameters P_{wanted}, $P_{interferer}$, P_{IM3} in power densities, together with OIP_3 and OIP_2 and ACPR.

$P_{wanted\ density}$	[dBm/Hz]	-20.0
$P_{interferer\ density}$	[dBm/Hz]	-64.3
$P_{IM3\ density}$	[dBm/Hz]	-93.0
OIP_3	**[dBm]**	**51.4**
OIP_2	**[dBm]**	**114.7**
ACPR	**[dBc]**	**73**

Table 3-13 GSM/EDGE Tx: OIP_3, OIP_2 and ACPR derived from ACLR specifications in case of '*Continuous modulation spectrum*'

$P_{interferer\ density}$= P_{wanted}-57-10log$_{10}$(300E3), as the maximum level indicated for switching transients is -57 dBc measured in a 300 kHz bandwidth.

P_{wanted}	[dBm/Hz]	-20.0
$P_{interferer\ density}$	[dBm/Hz]	-131.8
P_{IM3}	[dBm/Hz]	-93
OIP_3	**[dBm]**	**40.1**
OIP_2	**[dBm]**	**47.2**
ACPR	**[dBc]**	**73**

Table 3-14 GSM/EDGE Tx: OIP_3, OIP_2 and ACPR derived from ACLR specifications in case of '*Switching transients spectrum*'

3.3.2 GSM/EDGE Rx

For the receiver, different specifications have been calculated from intermodulation requirements. The wanted mean power P_{wanted} is given at -104 dBm (Table 6-1 b of [**5**], case of multi-standard radio BS) and the mean power of the interferer $P_{interferer}$ is at -43 dBm (chapter 5.1.3 of [**5**]). P_{IM3} is at 3 dB below P_{wanted}. For OIP_3, OIP_2 and ACPR, formulas (3.7-3.9) are applied. The resulting table is Table 3-15 given below:

P_{wanted}	[dBm]	-104
$P_{interferer}$	[dBc]	-43
P_{IM3}	[dBm]	-104
OIP_3	**[dBm]**	**-41.5**
OIP_2	**[dBm]**	**-40**
ACPR	**[dBc]**	**3**

Table 3-15 GSM/EDGE Rx: OIP_3, OIP_2 and ACPR derived for $P_{interferer}$= -43 dBm

Analyzing the specifications given in the blocking requirements (chapter 5.1.4 of [**5**]), the strictest requirements are for a $P_{interferer}$ of -13 dBm (strictest BS requirement from Table 5-2a) at a desired power of -104 dBm. The applied formulas are the same as for Table 3-15

and synthesized in Table 3-16. The $P_{interferer}$ in the case in which the base station is co-located with other base stations equals 16 dBm- 30dBm= -14 dBm, as P_{wanted} is 16 dBm and 30 dB above the interferer.

P_{wanted}	[dBm]	-104
$P_{interferer}$	[dBm]	-14
P_{IM3}	[dBm]	-107
OIP_3	**[dBm]**	**-12.5**
OIP_2	**[dBm]**	**-11**
ACPR	**[dBc]**	**3**

Table 3-16 GSM/EDGE Rx: OIP_3, OIP_2 and ACPR derived for $P_{interferer}$= -14 dBm

3.4 Conclusion

The linearity computed data has been synthesized in Table 3-17. The strictest requirements have been derived, and the most demanding ones have been written with bolded font.

	LTE Tx	**LTE Rx**	**UMTS Tx**	**UMTS Rx**	**GSM Tx**	**GSM Rx**
P_{IM3} [dBm/Hz]	-73/*-62.3*		-25.8/-12.8		-93/-93	
P_{IM3}[dBm]		***-85.6***/-103.8		-118/-118		-107/-106
OIP_3[dBm]	63.3/65.5	-50.5/-12.5	80.5/*68*	-45.5/-12.5	**81**/51.4	-41.5/-12.5
OIP_2[dBm]	113.7/88	-49/-11	118/93	-44/-11	**129**/114.7	-40/-11
ACPR[dBm]	55.7/55.7	3/3	3/3	3/3	**73**/73	3/3

Table 3-17 LTE, UMTS, GSM/EDGE systems linearity results

As one can observe from above, the linearity is the most important factor for the GSM/EDGE system (compared to LTE and UMTS), and therefore the power amplifiers will have to be state-of-the-art in order to be able to satisfy these requirements of the 2G system. Moreover, the most stringent parameter, for example OIP_3, equal to 96 dBm, is too high to be met without a predistortion circuit. Using a pre-distorer before the, the linearity of the power amplifier is improved. The ACPR is the most demanding requirement in the case of GSM/EDGE. This chapter treated the most important linearity requirements for LTE, UMTS and GSM/EDGE. The conclusion is that the GSM/EDGE system is the most sensitive to linearity as overall, whereas the LTE is the most tolerant.

4. Phase noise requirements

4.1 LTE

4.1.1 LTE Tx

Transmitter in-band unwanted emissions

We first consider the case for bands below 1 GHz for LTE. For this case, the P_{wanted}= 43 dBm and BW_{meas} is 100 kHz. $P_{emission\ max}$ is derived using the formulas in the chapter 6.6.3.1 of the standard [**3**], SNR is from chapter 8.2.1 of [**3**].

$P_{emission\ max}$ [dBm/Hz]	$f_{offset\ average}$ [Hz]	$f_{offset\ boundaries}$ [MHz]	$f_{offset\ min}$ [Hz]
-56	750000	0.05--->1.45	50000
-61	2150000	1.45--->2.85	1450000
-63	6425000	2.85--->10.0	2850000
-60.5	2550000	0.05--->5.05	50000
-64	*7550000*	*5.05--->10.05*	*5050000*
-63	15025000	10.05-->20	10050000
-56	750000	0.05--->1.45	50000
-61	2150000	1.45--->2.85	1450000
-63	6425000	2.85--->10.0	2850000
-60.5	2550000	0.05--->5.05	50000
-64	7550000	5.05--->10.05	5050000
-63	15025000	10.05-->20	10050000
-63	10525000	1.05-->20	1050000
-63	10525000	1.05-->20	1050000
-63	10525000	1.05-->20	1050000
-63	10525000	1.05-->20	1050000

Table 4-1 LTE Tx strictest in-band phase noise for LTE bands < 1 GHz

The strictest requirement is found to be -100.70 dB at an offset of 7.55 MHz for a SNR of 19.7 dB at a throughput of 70 %. The formula used is:

$$\mathbf{PN_{with\ margin} = P_{wanted} - 10*\log_{10}(BW_{meas}) + P_{emission\ max} - SNR - Margin} \quad [4.1]$$

where SNR is given in Table 4-2, and the margin is taken as 10 dBc/Hz. $PN_{with\ margin}$ is the phase noise with the noise margin of 10 dBc/Hz included and is given in Table 4-2.

$f_{offset\ max}$ [Hz]	SNR [dB]	$BW_{frequency}$ [Hz]	Throughput [%]	Phase noise [dBc/Hz]	$PN_{with\ 10\ dBc\ margin}$ [dBc/Hz]
1450000	18.6	1400000	70%	-81.60	-91.60
2850000	18.6	1400000	70%	-86.60	-96.60
10000000	18.6	1400000	70%	-88.60	-98.60
5050000	19.7	20000000	70%	-87.20	-97.20
10050000	*19.7*	*20000000*	*70%*	*-90.70*	***-100.70***
20000000	19.7	20000000	70%	-89.70	-99.70
1450000	4.4	1400000	30%	-67.40	-77.40
2850000	4.4	1400000	30%	-72.40	-82.40
10000000	4.4	1400000	30%	-74.40	-84.40
5050000	4.7	20000000	30%	-72.20	-82.20
10050000	4.7	20000000	30%	-75.70	-85.70
20000000	4.7	20000000	30%	-74.70	-84.70
20000000	18.6	entire range	70%	-88.60	-98.60
20000000	19.7	entire range	70%	-89.70	-99.70
20000000	4.4	entire range	30%	-74.40	-84.40
20000000	4.7	entire range	30%	-74.70	-84.70

Table 4-2 LTE Tx strictest in band phase noise for LTE bands < 1 GHz

BW_{meas} [Hz]	$P_{emission\ max}$ [dBm/Hz]	$f_{offset\ average}$ [Hz]	SNR [dB]
100000	-56	750000	18.6
100000	-61	2150000	18.6
1000000	-73	6650000	18.6
100000	-60.5	2550000	19.7
100000	-64	7550000	19.7
1000000	-73	15025000	19.7
100000	-56	750000	4.4
100000	-61	2150000	4.4
1000000	-73	6650000	4.4
100000	-60.5	2550000	4.7
100000	-64	7550000	4.7
1000000	-73	15250000	4.7
1000000	-73	10750000	18.6
1000000	-73	10750000	19.7
1000000	-73	10750000	4.4
1000000	-73	10750000	4.7

Table 4-3 LTE Tx strictest in band phase noise for LTE bands > 1 GHz

In the tables above and below, the case in which the LTE bands are higher than 1 GHz is considered. For this case, P_{wanted}= 43 dBm and the measurement bandwidth is either 100 kHz, either 1 MHz. The strictest requirement is found as -119.70 dB at average frequency offsets of 15.025 MHz and 10.075 MHz for a SNR of 19.7 dB and at a throughput of 70%, the same formula (4.1) has been applied. $P_{emission\ max}$ is computed using the relations from the same chapter of the standard, chapter 6.6.3.1 of [**3**].

$BW_{frequency}$ [Hz]	**Throughput [%]**	**Phase noise [dBc/Hz]**	**$PN_{with\ 10\ dBc\ margin}$ [dBc/Hz]**
1400000	70%	-81.60	-91.60
1400000	70%	-86.60	-96.60
1400000	70%	-108.60	-118.60
20000000	70%	-87.20	-97.20
20000000	70%	-90.70	-100.70
20000000	*70%*	*-109.70*	***-119.70***
1400000	30%	-67.40	-77.40
1400000	30%	-72.40	-82.40
1400000	30%	-94.40	-104.40
20000000	30%	-72.20	-82.20
20000000	30%	-75.70	-85.70
20000000	30%	-94.70	-104.70
entire range	70%	-108.60	-118.60
entire range	*70%*	*-109.70*	***-119.70***
entire range	30%	-94.40	-104.40
entire range	30%	-94.70	-104.70

Table 4-4 LTE Tx strictest in band phase noise for LTE bands > 1 GHz

Transmitter out-band unwanted emissions

For the computation of the strictest phase noise, a P_{wanted}= 43 dBm and a variable bandwidth frequency were considered. The most demanding phase noise value is obtained: -109.7 dBc/Hz. It is found by measuring in a bandwidth of 1 MHz for a SNR of 19.7 dB at a 70% throughput. $P_{emission\ max}$ is derived from the transmitter spurious emissions chapter 6.6.4 of [**3**]. The formula used for the phase noise computation is:

$$\mathbf{PN = P_{wanted} - 10*\log_{10}(BW_{meas}) + P_{emission\ max} - SNR} \quad [4.2]$$

BW [Hz]	$P_{emission\ max}$ [dBm/Hz]	BW_{freq} [Hz]	Throughput [%]	SNR [dB]	Phase noise [dBc/Hz]
1.00E+03	-43	1400000	70%	18.6	-48.60
1.00E+04	-53	1400000	70%	18.6	-68.60
1.00E+05	-63	1400000	70%	18.6	-88.60
1.00E+06	-73	1400000	70%	18.6	-108.60
1.00E+03	-43	20000000	70%	19.7	-49.70
1.00E+04	-53	20000000	70%	19.7	-69.70
1.00E+05	-63	20000000	70%	19.7	-89.70
1.00E+06	*-73*	*20000000*	*70%*	*19.7*	**-109.70**
1.00E+03	-43	1400000	30%	4.4	-34.40
1.00E+04	-53	1400000	30%	4.4	-54.40
1.00E+05	-63	1400000	30%	4.4	-74.40
1.00E+06	-73	1400000	30%	4.4	-94.40
1.00E+03	-43	20000000	30%	4.7	-34.70
1.00E+04	-53	20000000	30%	4.7	-54.70
1.00E+05	-63	20000000	30%	4.7	-74.70
1.00E+06	-73	20000000	30%	4.7	-94.70

Table 4-5 LTE Tx strictest out-band phase noise

4.1.2 LTE Rx

Rx spurious emissions

For the receiver of LTE, the derivation of the spur limit is done. The computation takes into account the thermal noise power (-174 dBm), the signal to noise ratio SNR, the implementation loss (IL), the noise figure (NL) and the bandwidth (BW_{freq}).

SNR [dB]	BW_{freq} [Hz]	Throughput [%]	NF [dB]	IL [dB]	$Spur_{limit}$ [dB]
18.6	1400000	70%	5	3	-85.94
19.7	1400000	70%	5	3	-84.84
4.4	20000000	30%	5	3	-88.59
4.7	20000000	30%	5	3	-88.29

Table 4-6 LTE Rx spurs limit derivation

The formula used for the derivation of the $Spur_{limit}$ is shown below:

$$\mathbf{Spur_{limit} = P_{thermal\ noise} + 10*\log_{10}(BW_{freq}) + SNR + NF + IL} \quad [4.3]$$

P_{wanted} [dBm]	BW_{meas} [Hz]	SNR [dB]	BW_{freq} [Hz]	Throughput [%]
-85.94	1.00E+05	18.6	1400000	70%
-85.94	1.00E+05	18.6	1400000	70%
-84.84	1.00E+05	19.7	20000000	70%
-84.84	1.00E+05	19.7	20000000	70%
-88.59	1.00E+06	4.4	1400000	30%
-88.59	1.00E+06	4.4	1400000	30%
-88.29	1.00E+06	4.7	20000000	30%
-85.29	1.00E+06	4.7	20000000	30%

Table 4-7 LTE Rx phase noise calculation part one

$P_{spurious\ max}$ [dBm]	$P_{spurious\ max\ density}$ [dBm/Hz]	Phase noise [dBc/Hz]	$PN_{with\ 10\ dBc\ margin}$ [dBc/Hz]
-57	-107	-40.40	-50.40
-57	*-107*	*-40.40*	*-50.40*
-57	-107	-50.85	-60.85
-57	-107	-50.85	-60.85
-47	-107	-43.05	-53.05
-47	-107	-43.05	-53.05
-47	-107	-54.30	**-64.30**
-47	-107	-51.30	-61.30

Table 4-8 LTE Rx phase noise calculation part two

It is shown in Table 4-8 that the strictest phase noise requirement is at -115.94 dBc/Hz. This value has been derived using the SNR from chapter 8.2.1 of [**3**] and using the formula

$$PN_{with\ margin} = P_{wanted} - 10*\log_{10}(BW_{freq}) + 10*\log_{10}(BW_{meas}) - P_{spurious\ max} - Margin \quad [4.4]$$

4.2 UMTS

4.2.1 UMTS Tx

SNR for out-of-band spurious emissions of the Tx

Using the formula (4.26) from [**15**] (rewritten in equation 4.5 of this work), the SNR is computed for each of the modulation types (QPSK, 16QAM, 64QAM), having as reference the signal-to-noise density ratio E_b/N_0, where E_b is the energy per bit and N_0 is the noise density. E_b/N_0 is taken as the most demanding value extracted from Table 8.3 of chapter 8.3.1.1 of [**4**]. R_b is the information bit rate and B_w is the unit bandwidth occupied.

Modulation type	E_b/N_0 [dB]	M	R_b/B_w [bps/Hz]	SNR [dB]
QPSK	19.1	4	2	**21.1**
16QAM	19.1	16	4	23.1
64QAM	19.1	64	6	25.1

Table 4-9 UMTS Tx SNR calculation

where **$SNR = (E_b/N_0)*(R_b/B_w)$** [4.5]

For the tables below, P_{wanted} is taken equal to 43 dBm and SNR is taken equal to 21.1dB (for Table 4-10), 23.1 dB (for Table 4-11) and 25.1 dB (for Table 4-12). The spectrum emission mask values have been derived from chapter 6.6.2.1 of [**4**].

Modulation type	BW_{meas} [Hz]	$P_{emission\ max}$ [dBm/Hz]	$f_{offset\ average}$ [Hz]	Phase noise [dBc/Hz]	$PN_{with\ 10\ dBc\ margin}$ [dBc/Hz]
	3.00E+04	-58.77	2615000	-81.64	-91.64
	3.00E+04	-64.77	3115000	-87.64	-97.64
	3.00E+04	-70.77	3757500	-93.64	-103.64
QPSK	1.00E+06	-73.00	7000000	-111.10	**-121.10**
additional bands	3.00E+04	-59.77	3015000	-87.66	-97.66
	1.00E+06	-73.00	7000000	-106.55	-116.55
	3.00E+04	-59.77	3015000	-87.66	-97.66
	1.00E+05	-63.00	6775000	-96.41	-106.41
	3.00E+04	-57.77	2565000	-86.96	-96.96
	1.00E+05	-63.00	6325000	-75.01	-85.01

Table 4-10 UMTS Tx Phase noise calculation for QPSK modulation

Modulation type	BW_{meas} [Hz]	$P_{emission\ max}$ [dBm/Hz]	$f_{offset\ average}$ [Hz]	Phase noise [dBc/Hz]	$PN_{with\ 10\ dBc\ margin}$ [dBc/Hz]
	3.00E+04	-58.77	2615000	-83.64	-93.64
	3.00E+04	-64.77	3115000	-89.64	-99.64
	3.00E+04	-70.77	3757500	-95.64	-105.64
16QAM	1.00E+06	-73.00	7000000	-113.10	**-123.10**
additional bands	3.00E+04	-59.77	3015000	-89.66	-99.66
	1.00E+06	-73.00	7000000	-108.55	-118.55
	3.00E+04	-59.77	3015000	-89.66	-99.66
	1.00E+05	-63.00	6775000	-98.41	-108.41
	3.00E+04	-57.77	2565000	-88.96	-98.96
	1.00E+05	-63.00	6325000	-75.01	-85.01

Table 4-11 UMTS Tx Phase noise calculation for 16QAM modulation

Modulation type	BW_{meas} [Hz]	$P_{emission\ max}$ [dBm/Hz]	$f_{offset\ average}$ [Hz]	Phase noise [dBc/Hz]	$PN_{with\ 10\ dBc\ margin}$ [dBc/Hz]
	3.00E+04	-58.77	2615000	-85.64	-95.64
	3.00E+04	-64.77	3115000	-91.64	-101.64
	3.00E+04	-70.77	3757500	-97.64	-107.64
64QAM	1.00E+06	-73.00	7000000	-115.10	**-125.10**
additional bands	3.00E+04	-59.77	3015000	-91.66	-101.66
	1.00E+06	-73.00	7000000	-110.55	-120.55
	3.00E+04	-59.77	3015000	-91.66	-101.66
	1.00E+05	-63.00	6775000	-100.41	-110.41
	3.00E+04	-57.77	2565000	-90.96	-100.96
	1.00E+05	-63.00	6325000	-75.01	-85.01

Table 4-12 UMTS Tx Phase noise calculation for 64QAM modulation

The most demanding requirement from Table 4-9, Table 4-10 and Table 4-11 is 64QAM with a phase noise value (including the margin of 10 dB) of -125.10 dBc/Hz, where formula (4.1) is applied.

UMTS Tx spurious emissions (not including out-of-band emissions)

Modulation type	BW_{meas} [Hz]	$P_{emission\ max}$ [dBm/Hz]	SNR [dB]	Phase noise [dBc/Hz]	$PN_{with\ 10\ dBc\ margin}$ [dBc/Hz]
QPSK	1.00E+03	-43	21.1	-51.10	-61.10
	1.00E+04	-53	21.1	-71.10	-81.10
	1.00E+05	-63	21.1	-91.10	-101.10
	1.00E+06	-73	21.1	-111.10	-121.10
16QAM	1.00E+03	-43	23.1	-53.10	-63.10
	1.00E+04	-53	23.1	-73.10	-83.10
	1.00E+05	-63	23.1	-93.10	-103.10
	1.00E+06	-73	23.1	-113.10	-123.10
64QAM	1.00E+03	-43	25.1	-55.10	-65.10
	1.00E+04	-53	25.1	-75.10	-85.10
	1.00E+05	-63	25.1	-95.10	-105.10
	1.00E+06	-73	25.1	-115.10	**-125.10**

Table 4-13 UMTS Tx Phase noise calculation for QSPK, 16QAM, 64QAM

In Table Table 4-12 is computed with the same formula (4.1) the phase noise including the margin of 10 dBc/Hz. The most demanding modulation is 64QAM not only for the out-of-band emissions, but also for the in-band emissions. The value is -125.10 dBc/Hz.

4.2.2 UMTS Rx

UMTS Rx Spurs calculation

It is considered here that the implementation loss is 3 dB, the bandwidth for the considered frequency is 3.84 MHz and the noise figure 5 dB. In the table below, $Spur_{limit}$ is derived using formula (4.3).

Modulation type	E_b/N_0 [dB]	M	R_b/B_w [bps/Hz]	$Spur_{limit}$ [dB]
QPSK	19.1	2	21.1	-79.06
16QAM	19.1	4	23.1	**-77.06**
64QAM	19.1	6	25.1	-75.06

Table 4-14 UMTS Rx spurs calculation for QSPK, 16QAM, 64QAM

Modulation type	P_{wanted} [dBm]	BW [Hz]	SNR [dB]	$Limit_{spur}$ [dBc]	$Limit_{spur2}$ [dBm/Hz]	Phase noise [dBc/Hz]	$PN_{with\ 10\ dBc\ margin}$ [dBc/Hz]
QPSK	-79.06	1.00E+05	21.1	-57	-107	-82.06	-92.06
16QAM	-77.06	1.00E+05	23.1	-57	-107	-80.06	-90.06
64QAM	-75.06	1.00E+05	25.1	-57	-107	-88.06	-98.06
QPSK	-79.06	1.00E+06	21.1	-47	-107	-92.06	-102.06
16QAM	-77.06	1.00E+06	23.1	-47	-107	-90.06	-100.06
64QAM	*-75.06*	*1.00E+06*	*25.1*	*-47*	*-107*	*-135.06*	***-145.06***

Table 4-15 UMTS Rx Phase noise for QSPK, 16QAM, 64QAM

The calculated minimum required power density has the same value (-77.06 dB) for QPSK, 16QAM and 64QAM and it gives the strictest value for the phase noise: -107.06 dBc/Hz in the case of 16QAM modulation and of an SNR of 25.1 dB. The formula used for the phase noise calculation is:

$$PN_{with\ margin} = P_{wanted} - 10*\log_{10}(1MHz) - P_{spur2} + 10*\log_{10}(BW) - Margin \quad [4.6]$$

4.3 GSM/ EDGE

4.3.1 GSM/EDGE Tx

Using the data in the standards [**5, 6**], the SNR is computed in order to calculate the phase noise requirements for the transmitter. The considered bandwidth is 100 kHz (chapter 4.2.1.1 general requirements for all types of base stations BS and mobile stations MS, the case of BTS at 1800 kHz and above [**5**]), the maximum spurious emission level is -96 dBm (Table 4-10 of [**5**]), R_b is 270.8 kbps and R_b is 4E-21 [**15**].

The SNR_{linear} is $P_{spurious\ max}[W]/(N_0*BW_{meas})$ and $SNR[dB]= 10*\log_{10}(SNR_{linear})$.

BW_{meas} [Hz]	$P_{spurious\ max}$ [dBm]	$P_{spurious\ max}$ [W]	R_b [bits/s]	N_0 [W/Hz]	SNR [dB]
100000	-96	2.51E-13	270800	4.00287E-21	**27.98**

Table 4-16 GSM/EDGE Tx SNR calculation

Tx Spurious emissions inside the BTS transmit band (from chapter 6.6.1 and 6.5.1.3 of [6])

It is considered below that P_{wanted}= 43 dBm. BW_{meas} and $P_{emission\ table}$ are taken from Table 5 of chapter 6.5.1.3 [**6**].

$$P_{emission\ density} = P_{emission\ table} - 10*\log_{10}(BW_{meas}) \quad [4.7]$$

$PN_{with\ margin}$ is computed using formula (4.1). Below is given the table with results, the smallest noise requirement is found for a frequency offset of 6 MHz, that gives a maximum spur power of -80 dBc. The same approach is used for spurious emissions outside BTS transmit band (Table 4-17 and Table 4-18).

BW_{meas} [Hz]	f_{offset} [Hz]	$f_{offset\ boundary}$ [kHz]	$P_{emission\ table}$ [dBm]	$P_{emission\ density}$ [dBc/Hz]	Phase noise [dBm/Hz]	$PN_{with\ 10\ dBc\ margin}$ [dBc/Hz]
30000	100000	100	0.5	-44.27	-74.02	-84.02
30000	200000	200	-30	-74.77	-104.52	-114.52
30000	250000	250	-33	-77.77	-107.52	-117.52
30000	400000	400	-56	-100.77	-130.52	-140.52
30000	900000	900	-70	-114.77	-144.52	-154.52
30000	1500000	1200-->1800	-73	-117.77	-147.52	-157.52
100000	3900000	1800-->600	-75	-125.00	-159.98	-169.98
100000	*6000000*	*6000*	*-80*	*-130.00*	*-164.98*	***-174.98***

Table 4-17 GSM/EDGE Tx Phase noise with margin calculation

Tx Spurious emissions outside the BTS transmit band (from 9 kHz to 1 GHz)

BW_{meas} [Hz]	f_{offset} [Hz]	$P_{emission}$ [dBm]	$P_{emission\ calc}$ [dBm/Hz]	Δf [MHz]	Phase noise [dBc/Hz]	$PN_{with\ 10\ dBc\ margin}$ [dBc/Hz]
30000	2000000	-35	-79.77	2	-109.52	-119.52
100000	5000000	-30	-80.00	5	-114.98	-124.98
300000	*10000000*	*-36*	*-90.77*	*10*	*-130.52*	***-140.52***

Table 4-18 GSM/EDGE Tx Phase noise calculation outside transmit band (from 9KHz to 1GHz)

The table above is made from the synthesized data found in Table 9e of chapter 6.6.2.7.3 [6]. Δf is the frequency offset from the edge of the relevant Tx band [6].

Tx Spurious emissions outside the BTS transmit band (from 1 GHz to 12.75 GHz)

BW_{meas} [Hz]	f_{offset} [Hz]	$P_{emission}$ [dBm]	$P_{emission\ calc}$ [dBm/Hz]	Δf [MHz]	Phase noise [dBc/Hz]	$PN_{with\ 10\ dBc\ margin}$ [dBc/Hz]
30000	2000000	-30	-74.77	2	-104.52	-114.52
100000	5000000	-25	-75.00	5	-109.98	-119.98
300000	10000000	-30	-84.77	10	-124.52	**-134.52**

Table 4-19 GSM/EDGE Tx Phase Noise calculation outside transmit band (from 1 GHz to 12.75 GHz)

4.3.2 GSM/EDGE Rx

Using the data in the standard, the SNR is computed in the same way as for the GSM/EDGE transmitter. This will be needed for the computation of the phase noise requirements for the receiver.

BW_{meas} [Hz]	$P_{spurious\ max}$ [dBm]	$P_{spurious\ max}$ [W]	R_b [bits/s]	N_0 [W/Hz]	SNR [dB]
200000	-84	3.9811E-11	270800	4.00287E-21	**36.97**

Table 4-20 GSM/EDGE Rx SNR calculation

It is considered in Table 4-21 that the noise figure NF is 5 dB and the insertion loss IL is 3 dB. The data is synthesized from chapter 7.9.3 of [**6**].

P_{sensed} [dBm]	BW_{meas} [Hz]	f_{offset} [Hz]	$P_{spurr\ emissions}$ [dBc]	$P_{spurr\ emissions\ density}$ [dBm/Hz]	Phase noise [dBc/Hz]	$PN_{with\ 10\ dBc\ margin}$ [dBc/Hz]
-76.02	2.00E+05	2.00E+06	-57	-62.30	-66.73	-76.73
-79.03	1.00E+05	5.00E+06	-57	-62.00	-67.03	-77.03
-74.26	3.00E+05	1.00E+07	-57	-62.48	-66.56	-76.56
-69.03	1.00E+06	2.00E+07	-47	-53.00	-76.03	-86.03
-64.26	3.00E+06	3.00E+07	-47	-53.48	**-75.56**	**-85.56**

Table 4-21 GSM/EDGE Rx phase noise calculation for spurious emissions

$$P_{sensed} = P_{thermal\ noise} + 10*\log_{10}(BW_{freq}) + SNR + NF + IL \quad [4.8]$$

$$\text{Phase noise} = P_{sensed} - 10*\log_{10}(BW_{meas}) - P_{spurr\ emissions\ density} \quad [4.9]$$

4.4 WiMAX

Although the WiMAX system is not implemented in MatLab code because of time and work load constraints, the specifications for this system have been derived, for future use. The maximum SNR is 21 dB. P_{wanted}= 43 dBm. The bandwidth of the channel is 2.8 MHz (Table 244 from chapter 8.1.8.2.2 of [**7**]).

4.4.1 WiMAX Tx

Tx phase noise constraints for spurious emissions

$Spur_{limit}$ [dBc]	$P_{spurr\ max}$ [dBm]	f_{offset} [MHz]	Phase noise [dBc/Hz]	$PN_{with\ 10\ dBc\ margin}$ [dBc/Hz]
0	-43.00	13	-85.47	-95.47
-15	-58.00	14	-100.47	-110.47
-20	-63.00	14.4	-105.47	-115.47
-28	-71.00	14.8	-113.47	-123.47
-34	-77.00	22.4	-119.47	-129.47
-42	-85.00	28	-127.47	-137.47
-52	-95.00	56	-137.47	-147.47
-52	-95.00	70	-137.47	**-147.47**

Table 4-22 WiMAX Tx phase noise calculation for spurious emissions

$$PN_{with\ margin} = P_{wanted} - 10*\log_{10}(BW_{channel}) + P_{spurr\ max} - SNR - Margin \quad [4.10]$$

Tx phase noise constraints from spectral mask

In this case, the bandwidth of the channel is 100 kHz instead of 2.8 MHz, however P_{wanted} has the same value of 43 dB, and the same formula (4.10) is applied.

f_{offset} [Hz]	$Spur_{limit}$ [dBc]	$P_{spurr\ max}$ [dBm]	SNR [dB]	Phase noise [dBc/Hz]	$PN_{with\ 10\ dBc\ margin}$ [10 dBc/Hz]
9500000	0	-43	21.00	-71	-81.00
10900000	-25	-68	21.00	-96	-106.00
19500000	-32	-75	21.00	-103	-113.00
29500000	*-50*	*-93*	*21.00*	*-121*	***-131.00***

Table 4-23 WiMAX Tx phase noise calculation from spectral mask requirements

4.4.2 WiMAX Rx

Rx P_{ref} determination

SNR_{Rx} [dB]	Base frequency [Hz]	n	f_{sample} [Hz]	N_{used}	N_{FFT}	$N_{subchan}$	P_{ref} [dBm]
5	*1250000*	*1.15*	*1440000*	*200*	*256*	*24*	***-93.73***
5	1500000	1.15	1720000	200	256	24	-92.96
5	1750000	1.14	2000000	200	256	24	-92.30
5	2000000	1.14	2280000	200	256	24	-91.73
5	2750000	1.15	3160000	200	256	24	-90.31

Table 4-24 WiMAX Rx P_{ref} calculation from spectral mask requirements

The parameter **n** is the sampling factor that determines the subcarrier spacing and the useful symbol time, f_{sample} is the sampling frequency, N_{used} is the number of used subcarriers, N_{FFT} is the smallest power of two greater than N_{used}, $N_{subchan}$ is the number of subchannels.

$$P_{ref}\ [dBm] = -101 + SNR_{Rx} + 10*\log_{10}(f_{sample\ MHz} * N_{used} / N_{FFT} * N_{subchan} / 16) \quad [4.11]$$

Relation (4.11) is derived in chapter 8.3.11.1 of [**7**].

Rx phase noise determination

P_{ref} [dBm]	Base frequency [MHz]	n	BW [Hz]	f_{offset} [Hz]	SNR [dB]	Phase noise [dBc/Hz]	$PN_{with\ 10\ dBc\ margin}$ [10 dBc/Hz]
-93.73	1.25	1.15	3.00E+04	2.00E+06	5.00	**-**118.96	**-128.96**
-92.96	1.5	1.15	1.00E+05	5.00E+06	5.00	-112.96	-122.96
-92.30	1.75	1.14	3.00E+05	1.00E+07	5.00	-107.53	-117.53
-91.73	2	1.14	1.00E+06	2.00E+07	5.00	-101.73	-111.73
-90.31	2.75	1.15	3.00E+06	3.00E+07	5.00	-95.54	-105.54

Table 4-25 WiMAX Rx Phase noise calculation from spectral mask requirements

Phase noise= P_{ref}- 10*log$_{10}$(10MHz)+ 10*log$_{10}$(BW) [4.12]

The value of 10MHz is the channelization space derived in Table 549 of chapter 8.5.1 of [**7**].

4.5 Conclusion

This chapter treated the phase noise requirements of four wireless systems: LTE, UMTS, GSM/EDGE and WiMAX. The computations of the phase noise requirements took into account the different spurious emissions (be it in-band or out-of-band), spectral masks and ACLR requirements. The most demanding requirements have been written in bold, and a 10 dBc margin has been taken into account for the physical implementation of the integrated circuits.

The wireless system that has the strictest requirements for Tx phase noise is GSM, followed by WiMax, UMTS and LTE. For the receiver, the most demanding system is UMTS, followed by WiMax, GSM and LTE.

As a general conclusion, LTE is the most tolerant to phase noise, given the specifications. The following three chapters will deal with the implementation of LTE, UMTS and GSM/EDGE in MatLab code.

5. System performance evaluation

5.1 Introduction

This chapter presents the LTE, UMTS and GSM/EDGE implementations made in software (in MatLab) at protocol level, in conformance with the specifications of the constituent blocks defined in the 3GPP standards. The objective of this chapter is to present a basis for system simulations, the skeleton of the transceivers (including the code validation), and then, in chapter 6, to add RF impairments and observe each system's tolerance to them. The aim is to obtain an arbitrary offset of 3 dB from the ideal BER curve, using different values of the RF impairments. An important aspect is the code validation; a set objective is to have a perfect match between the theoretical BER curve and the one that is obtained through simulations, along with the correct spectrum graphs which are to be found in the Appendix.

The schematic of a classical I-Q upconverter is shown in Figure 5-1 I-Q upconverter.

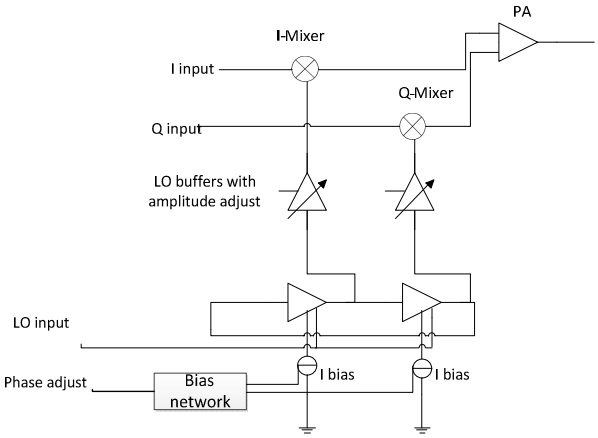

Figure 5-1 I-Q upconverter

5.2 LTE transceiver system design

LTE is the acronym of *Long term evolution*, which refers to the evolution of the universal terrestrial radio access network (UTRAN) which at its turn is an evolution of the wideband code division multiple access (W-CDMA) system; the most widely adopted third generation air interface technology for mobile communications.

It uses novel techniques, such as orthogonal frequency-division multiplexing (OFDM) modulation and spread spectrum techniques, that allow higher data rates and a higher capacity, which are very close to the Shannon limit [**19**] of the channel.

The implementation of the LTE transmitter is described at physical level (CRC calculation, channel coding, rate matching, code block concatenation) in chapters 5.1 and 5.3 of [**9**].

The implementation of the standard has been done in MatLab R2008b and followed the implementation described in Figure 5-2:

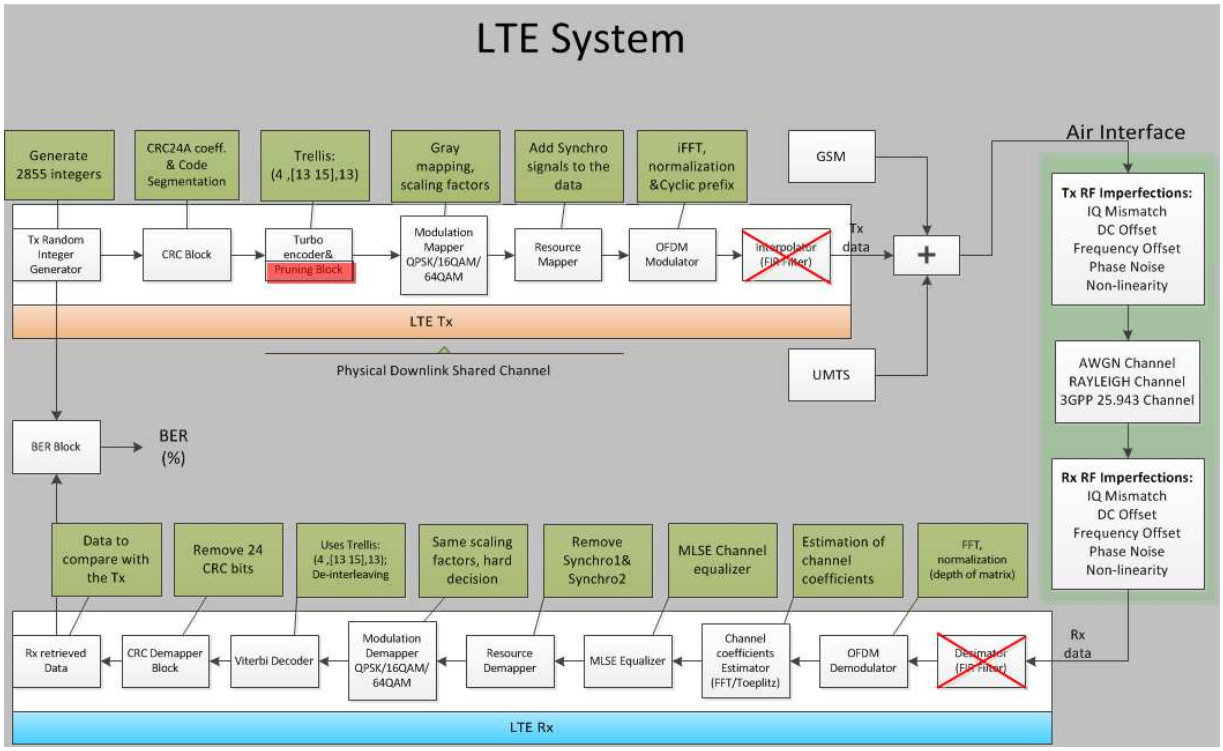

Figure 5-2 System implementation of LTE

The first block is the *random integer generator*, which generates in a pseudo-random order the integers that will be used for encoding and transmission over the air interface. It is the data that will be transmitted and received, and which will be used to compute the bit error rate (BER) of the system.

The second block is called *CRC calculation block*, which adds cyclic redundancy check (CRC) bits to the data block, in order to help correcting the accidental changes on the data block that was transmitted. It is described by a generation polynomial, and in the considered case, in which the downlink channel PDSCH (Physical downlink shared

channel)/DL-SCH (*Downlink Shared Channel*) is used for downlink transmission, the CRC polynomial generator is (D is the unit delay):

$$g_{CRC24A}(D) = [D^{24} + D^{23} + D^{18} + D^{17} + D^{14} + D^{11} + D^{10} + D^7 + D^6 + D^5 + D^4 + D^3 + D + 1].$$

The third block is the code segmentation block. Its purpose is to divide the generated block of data into blocks of a specified dimension *Z*. In case the last block has a length smaller than *Z*, then the block is filled with zero values. Although the functionality of the segmentation of data has been successfully proved during tests and verification, *Z* has been as such in order to have only one block to transmit. This is because it does not matter for the bit error rate (BER) computation if only one block is transmitted in a "for loop" or four blocks in another "for loop" that would have a four times smaller number of iterations.

The fourth block is the channel coding block. The bits are encoded either using 1/3 rate convolutional encoding, either using 1/3 turbo coding. The downlink channel that is considered in this system study uses 1/3 turbo encoding. The turbo encoder uses a transfer function given by $G(D) = \left[1, \frac{g_1(D)}{g_0(D)}\right]$, where

$$g_0(D) = 1 + D^2 + D^3,$$

$$g_1(D) = 1 + D + D^3.$$

The polynomials above are defining the *octals* that define the trellis. The *octals* are defined as the coefficients of *D* in decreasing order, and taken in groups of three, adding zeros from left to right if not able to make groups of three, then convert each group from binary values to decimal values. For the above mentioned polynomials, the bits:

$D^3\ D^2\ D^1\ D^0$→ zero add→grouping→decimal conversion:

$g_0(D) = 1 + D^2 + D^3$→1 0 1 1→**00** 1001→**00**1 001→13

$g_1(D) = 1 + D + D^3$→1 1 0 1→**00** 1101→**00**1 101→15

The turbo encoder is made of two feedback convolutional encoders and an interleaver (only for the second encoder). Each convolutional encoder has two outputs, one is the input data just copied at the output, and the other is the encoded data. These convolutional encoders give four outputs x_k, z_k, z'_k, x'_k. Out of these four outputs, only the first three will be taken for transmission over the air. Details are to be found in Figure 5-3 [**9**]:

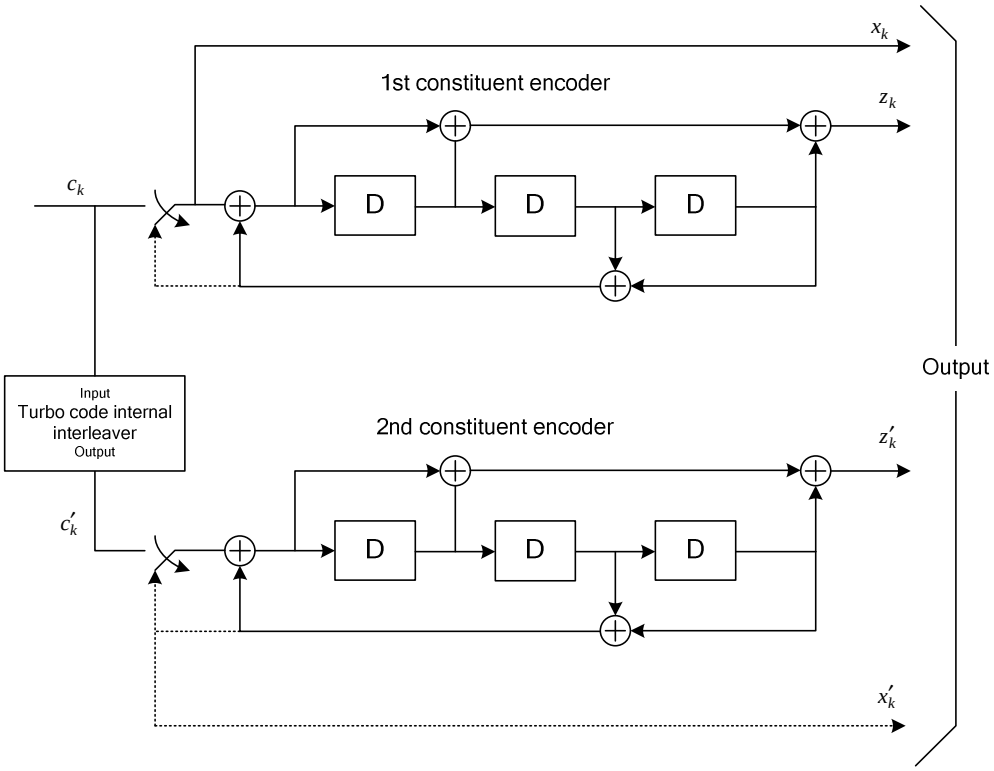

Figure 5-3 Structure of rate 1/3 turbo encoder
(dotted lines apply for trellis termination only) [**9**]

The turbo interleaver uses the $c'_i = c_{\Pi(i)}$ interleaver, where $\Pi(i) = \left(f_1 \cdot i + f_2 \cdot i^2\right) \bmod K$ and the parameters *K*, f_1, f_2, *i* are specified in Table 5.1.3-3 in [**9**].

The fifth block deals with the rate matching block, which takes the blocks x_k, z_k, z'_k and sends them through three sub-block interleavers, then the three obtained vectors are put in the bit collector block. The sub-block interleavers map accordingly the values into 32 columns and rows and pad with zeros if one final row does not have 32 values. The pattern *P(i)* for column permutation is described by Table 5-1:

Number of columns $C^{TC}_{subblock}$	**Inter-column permutation pattern** $< P(0), P(1), \ldots, P(C^{TC}_{subblock} - 1) >$
32	< 0, 16, 8, 24, 4, 20, 12, 28, 2, 18, 10, 26, 6, 22, 14, 30, 1, 17, 9, 25, 5, 21, 13, 29, 3, 19, 11, 27, 7, 23, 15, 31 >

Table 5-1 Inter-column permutation pattern for sub-block interleaver [**9**]

The permutation follows the rule $y_k = y_{\pi(k)}$ where $\pi(k)$ is given below:

$$\pi(k)=\left(P\left(\left\lfloor\frac{k}{R_{subblock}^{TC}}\right\rfloor\right)+C_{subblock}^{TC}\times\left(k \bmod R_{subblock}^{TC}\right)+1\right)\bmod K_{\Pi} \quad [5.1]$$

It is specified in the standard that the *pruning block* selects for transmission the data which is different from zero. This block has been implemented, but the output data that it produced could not be used afterwards for the Viterbi decoder in the receiver. Although several emails have been sent to 3GPP with questions about the use of this block, no reply has been received. Therefore, the solution adopted was the removal of this block and the transmission of the zeros also, as they were encoded by the turbo encoder and had to be recovered.

The sixth block is the modulation block that deals with the modulation schemes used for the PDSCH channel, which are quadrature phase shift keying (QPSK), 16 quadrature amplitude modulation (16QAM) and 64 quadrature amplitude modulation (64QAM) as specified in [**8**]. The mapping is done in the program depending on the value of "modulation_type", which acts as a flag: if it is equal to 1, QPSK is used, if it is 2, 16QAM is used, and if it is 3, 64QAM is used. The mapping is made according to the alphabet present in Tables 7.1.2-1, 7.1.3-1 and 7.1.4-1 of [**8**]. The default mapping of MatLab was not according to the standard, so a different constellation order had to be defined, and also a scaling factor.

The seventh block is the resource mapper block that maps the data into resource blocks of imposed dimensions, and also includes the synchronisation signals into the blocks. The resource mapper has three parameters which are shown in Table 5-2 .

Configuration		$N_{\text{sc}}^{\text{RB}}$	$N_{\text{symb}}^{\text{DL}}$
Normal cyclic prefix	$\Delta f = 15\,\text{kHz}$	12	7
Extended cyclic prefix	$\Delta f = 15\,\text{kHz}$		6
	$\Delta f = 7.5\,\text{kHz}$	24	3

Table 5-2 Physical resource blocks parameters [**9**]

The above mentioned parameters are implemented in MatLab code using flags for Δf and for "Normal cyclic prefix/Extended cyclic prefix" cases.

The eight block is the OFDM mapper block (orthogonal frequency multiplexing) that does the OFDM modulation and adds cyclic prefixes. The OFDM is done in inverse Fast Fourier Transform domain in N points; therefore a power scaling factor had to be used. The

cycling prefix is part of the modulated data that is put at the end of the block in order to avoid the inter-symbol interference. The data is mapped into OFDM symbols. Each OFDM symbol contains resource elements that are transmitted at the same time at different frequencies. $N_{\text{symb}}^{\text{DL}}$ OFDM symbols are transmitted during one downlink slot T_{slot}. In Figure 5-4 it is shown the transmitted signal, 10 blocks of data and synchronization signals.

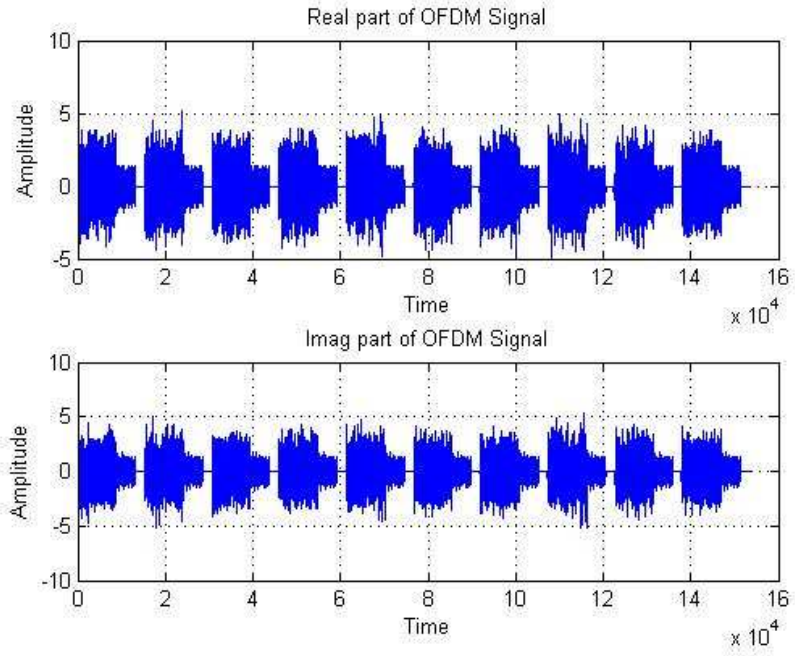

Figure 5-4 Real and imaginary part of the OFDM signal

For the simplicity of the implementation and the modeling of the air-interface in MatLab, the *Interpolator* block has been omitted in the transmitter. Using the interpolator, the lengths of the vectors would have been too long (millions of samples to be stored at once in a single vector in MatLab) for further signal processing. Therefore, the LTE transmitter is modeled with seven blocks (including the transmitter RF impairments block).

In order to have an accurate model of the system, the air interface is simulated by adding Gaussian noise and RF impairments, such as: I-Q mismatch (amplitude and phase), phase noise, DC offset, frequency offset and cubic nonlinearity.

The LTE receiver is implemented in the reverse order of the blocks that were created for the transmitter. The decimator block has been taken out, not only because of the lengthy processing times that it introduced, but also because the interpolator has not been used anymore.

The first block of the receiver is the OFDM de-mapper block, which does the Fast Fourier Transform (FFT) in N points. The useful data is to be found using the *depth* parameter, which is the length of the data before encoding.

The second block is the Viterbi channel equalizer block. This block uses a training sequence, the modulated constellation in order to equalize the noisy signals with correct data.

The third block is the resource de-mapper that separates the data from the synchronization signals and recovers the vectors of sent data from the sent blocks.

The fourth block is the modulation de-mapper that de-maps the modulated symbols to encoded data using the same defined constellations as for modulation.

The fifth block is the reverse rate matching block, which de-maps the big vector of encoded data into three vectors of data that are equal in length.

The sixth block is the Viterbi decoder that decodes the data using the same trellis that has been defined for the encoding. As the segmentation block did not segment any block, it is not needed in this study a block that would recover the segments.

The seventh block is the CRC de-mapper, which extracts the data from the data that has also CRC bits.

Throughout the MatLab program, conversions have been used: from decimal to binary and from binary to decimal, along with interleavers and de-interleavers, but these blocks are part of the implementation in code and do not need to be mentioned. However, there has been a continuous effort in implementing these not mentioned blocks correctly.

5.3 UMTS transceiver system design

UMTS is the acronym of *Universal Mobile Telecommunications System*. It appeared as a system improvement of Global System for Mobile communications (GSM), and allowed higher data rates and cost reductions for network operators, as the base stations could deal with more users at the same time and also offer faster internet and video communications.

It used techniques such as the more powerful Turbo encoding instead of the convolutional encoding, together with scrambling and spreading. The design of the UMTS transmitter is described at physical level in [**4**] for the High-Speed Downlink Shared Channel

(HS-DSCH). The implementation of the standard has been done in MatLab R2008b and followed the system implementation from Figure 5-5.

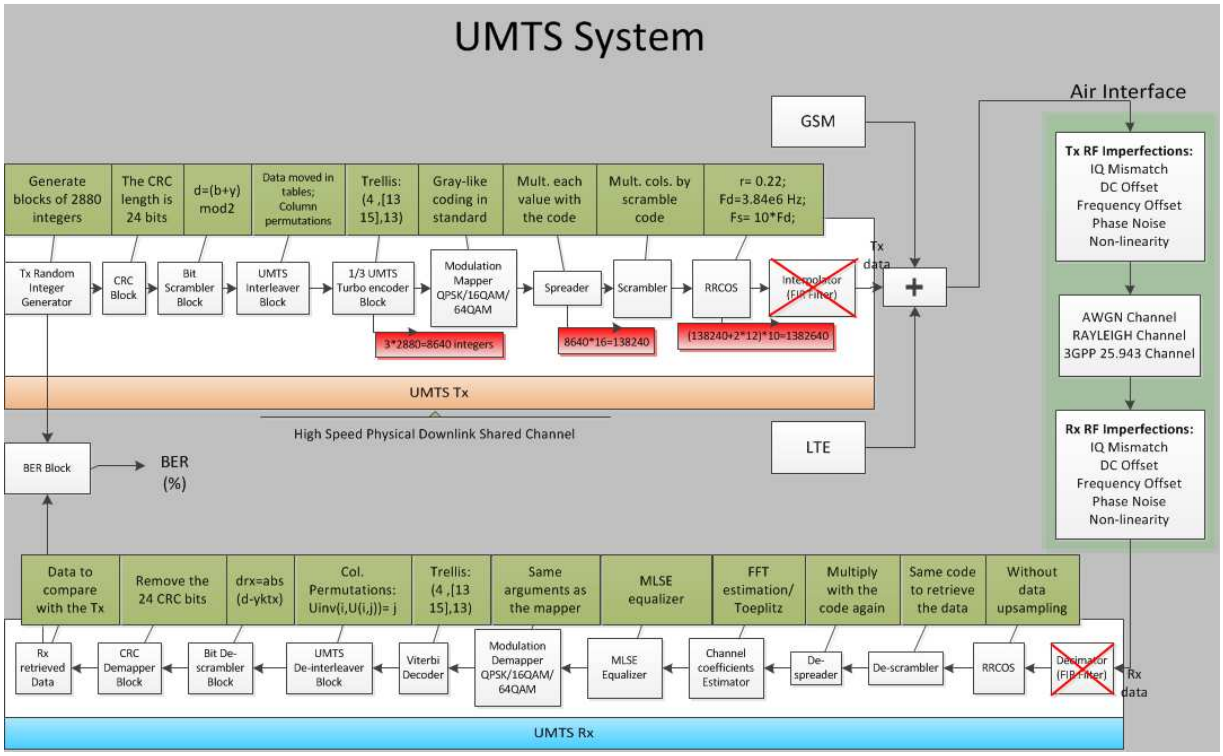

Figure 5-5 System implementation of UMTS

The first block is the *random integer generator*, which generates in a pseudo-random order the integers that will be used for encoding and transmission over the air interface. It is the data that will be transmitted and received, and which will be used to compute the bit error rate (BER) of the system.

The second block is the *CRC calculation block*, which adds CRC bits (*cyclic redundancy check*) to the data block, in order to help detecting the accidental changes on the data that was transmitted. It is described by a generation polynomial, and in the considered case, in which the downlink channel HS-DSCH (*High Speed Downlink Shared Channel*)/ HS-PDSCH (*High Speed Physical Downlink Shared Channel*) is used for downlink transmission, the CRC polynomial generator is:

$$g_{CRC24}(D) = [D^{24} + D^{23} + D^6 + D^5 + D + 1].$$

After the CRC block, the bits are scrambled according to [**10**] using the bit scrambler block. This is the third block.

The fourth block is the code segmentation block. Its purpose is to divide the generated block of data into blocks of a specified dimension *Z*. In case the last block has a length smaller than *Z*, then the block is filled with zero values. The same approach as for the LTE system has been considered.

The fifth block is the channel coding block. The bits are encoded using 1/3 rate turbo encoding. The turbo encoder uses a transfer function given by $G(D) = \left[1, \frac{g_1(D)}{g_0(D)}\right]$, where

$$g_0(D) = 1 + D^2 + D^3,$$

$$g_1(D) = 1 + D + D^3.$$

The polynomials above are defining the *octals* that define the trellis. The *octals* are defined as the coefficients of *D* in decreasing order, and taken in groups of three, adding zeros from left to right if not able to make groups of three, then convert each group from binary values to decimal values. For the above mentioned polynomials, the bits are converted to decimal:

$D^3\ D^2\ D^1\ D^0$→ zero add→grouping→decimal conversion:

$g_0(D) = 1 + D^2 + D^3$→1 0 1 1→**00** 1001→**00**1 001→13

$g_1(D) = 1 + D + D^3$→1 1 0 1→**00** 1101→**00**1 101→15

The turbo encoder is made of two feedback convolutional encoders and an interleaver (only for the second encoder). Each convolutional encoder has two outputs, one is the input data just copied at the output, and the other is the encoded data. These convolutional encoders give four outputs: x_k, z_k, z'_k, x'_k. Out of these four outputs, only the first three will be taken for transmission over the air. Details can be observed in Figure 5-6 [**10**]:

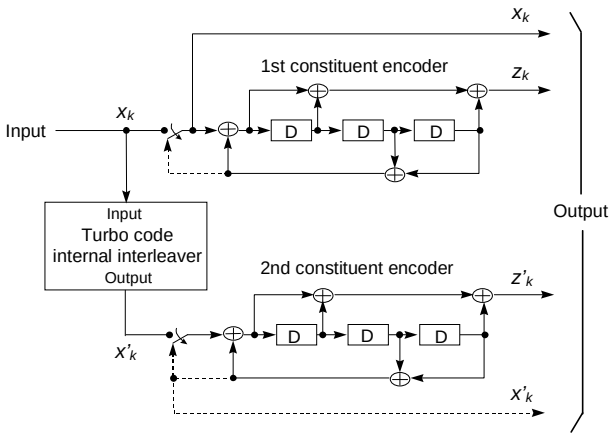

Figure 5-6 Structure of rate 1/3 Turbo coder
(dotted lines apply for trellis termination only) [**10**]

The turbo interleaver has a different implementation compared to the LTE implementation, in the sense that it uses intra-row and inter-row permutations instead of the parameters K, f_1 and f_2 values that would been have used for the generation of the new positions for the interleaver in the case of LTE. It uses a table with a list of prime number *p* and associated primitive root *v* which is shown in Table 5-3.

p	***v***	***p***	***v***	***p***	***v***	***p***	***v***	***p***	***v***
7	3	47	5	101	2	157	5	223	3
11	2	53	2	103	5	163	2	227	2
13	2	59	2	107	2	167	5	229	6
17	3	61	2	109	6	173	2	233	3
19	2	67	2	113	3	179	2	239	7
23	5	71	7	127	3	181	2	241	7
29	2	73	5	131	2	191	19	251	6
31	3	79	3	137	3	193	5	257	3
37	2	83	2	139	2	197	2		
41	6	89	3	149	2	199	3		
43	3	97	5	151	6	211	2		

Table 5-3 List of prime number *p* and associated primitive root *v* [**10**]

The inter-row permutation patterns for Turbo code internal interleaver is given in Table 5-4.

Number of input bits *K*	Number of rows *R*	Inter-row permutation patterns <*T*(0), *T*(1), …, *T*(*R* - 1)>
(40 ≤*K* ≤159)	5	<4, 3, 2, 1, 0>
(160 ≤*K* ≤200) or (481 ≤*K* ≤530)	10	<9, 8, 7, 6, 5, 4, 3, 2, 1, 0>
(2281 ≤*K* ≤2480) or (3161 ≤*K* ≤ 3210)	20	<19, 9, 14, 4, 0, 2, 5, 7, 12, 18, 16, 13, 17, 15, 3, 1, 6, 11, 8, 10>
K = any other value	20	<19, 9, 14, 4, 0, 2, 5, 7, 12, 18, 10, 8, 13, 17, 3, 1, 16, 6, 15, 11>

Table 5-4 Inter-row permutation patterns for Turbo code internal interleaver [**10**]

The sixth block deals with the interleaving block, which takes the blocks x_k, z_k, z'_k and sends them through three sub-block interleavers, which are specified in [**10**]. Their structure is shown in Figure 5-7.

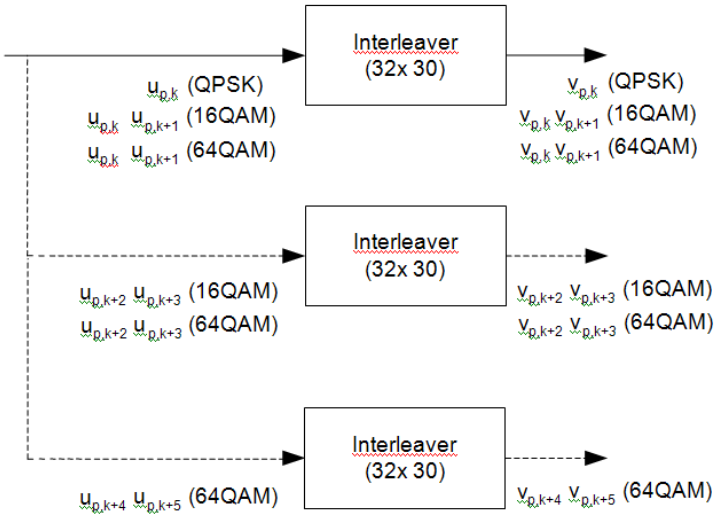

Figure 5-7 Interleaver structure for HS-DSCH [**10**]

The seventh block is the modulation block that deals with the modulation schemes used for the HS-DSCH channel, which are quadrature phase shift keying (QPSK), 16 quadrature amplitude modulation (16QAM) and 64 quadrature amplitude modulation (64QAM) as specified in the standard [**20**]. The mapping is done in the program depending on the value of “modulation_type”, which is like a flag: if it is equal to 1, QPSK is used, if it is 2, 16QAM is used, and if it is 3, 64QAM is used. The mapping is made according to the alphabet present in Tables 3B and 3C of [**20**] for 16QAM and 64QAM respectively. The default mapping of MatLab did not meet the standard; therefore a different constellation order had to be defined, together with the introduction of a scaling factor.

The eight block is the spreader block that spreads the data. As the spreading factor SF is 16, and k= SF/4, the data is spread according to the code $C_{ch,16,4}$ =[1 1 -1 -1 1 1 -1 -1 1 1 -1 -1 1 1 -1 -1] which is mentioned in chapter 4.3.1.2.1 of [**20**] for DPDCH (*Dedicated Physical Data Channel*). The spreading method is mentioned in Figure 5-8, where the modulation mapper is either QPSK, either 16QAM or 64QAM.

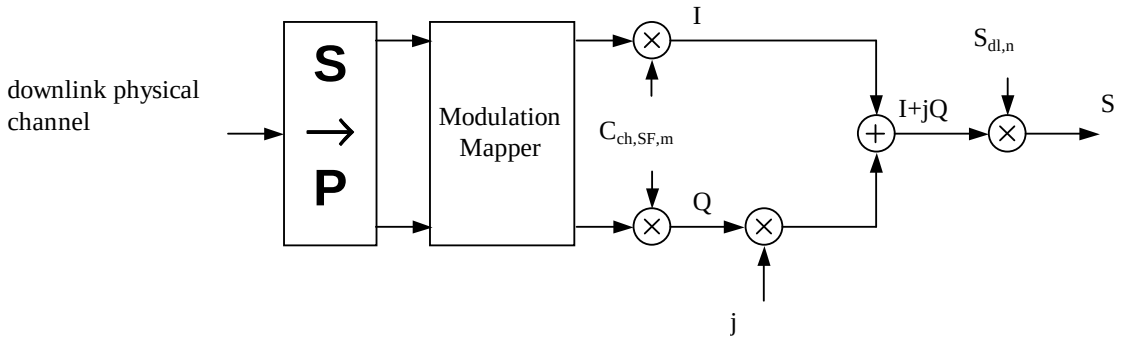

Figure 5-8 Spreading for all downlink physical channels except SCH [**20**]

The ninth block is the scrambler block. Its description is found in chapter 5.2.2 of [**20**]. Although it can be generated a maximum of 2^{18}-1 = 262,143 scrambling codes, there were generated 2^{8}-1 = 255 codes, because if the power of 2 would have been bigger, the necessary time for the simulation to run would have increased. However, not all the scrambling codes are used. The generated scrambling code is made of complex values of 1 plus or minus *i*.

The tenth block is the root raised cosine block (RRC), which is the block that implements a square root finite impulse response filter that filters the signal and makes oversampling. It is needed for transmission, as the filtered data has to be transmitted.

For the simplicity of the implementation and the modeling of the air-interface in MatLab, the *Interpolator* block has been omitted in the transmitter. Using the interpolator, the lengths of the vectors became too long (millions of samples) for further signal processing. Therefore, the UMTS transmitter is modeled with ten blocks instead of eleven (including the transmitter RF imperfections).

In order to have an accurate model of the system, the air interface is simulated by adding noise and imperfections, such as: I-Q mismatch (amplitude and phase), phase noise, DC offset, frequency offset and cubic nonlinearity.

The UMTS receiver is implemented in the reverse order of the blocks that were created for the transmitter. The decimator block has been taken out, not only because of

the lengthy processing times that it introduced, but also because the interpolator was not used anymore.

The first block of the receiver is the root raised cosine block, which is the block of the receiver that filters the data using a finite impulse response filter, but which does not do oversampling compared to the situation of the transmitter.

The second block of the receiver is the de-scrambler block. The de-scrambled data is obtained by dividing the output data of the second root raised cosine filter with the same scrambling sequence that was used for modulating the data block.

The third block is the de-spreader block, which is the block that de-spreads the signal. As the the spreader code $C_{ch,16,4}$ = [1 1 -1 -1 1 1 -1 -1 1 1 -1 -1 1 1 -1 -1] is used for de-spreading, it will be taken the first length ($code_{spreaded}$)/16 values, which are the recovered data. This is because the data has been multiplied with only two values, 1 or -1, therefore obtaining the value resulting from the multiplication of the two vectors is straightforward.

The fourth block is the Viterbi channel equalizer, which uses a modulated constellation (be it QPSK/16QAM/64QAM) as the training sequence. The estimation is not done actually, as the channel coefficients were taken with the same values. This is done as MatLab uses a separate program for estimation, and it has to run separately, as an add-on. However, it was shown in the help of the program that the results are very close, so the estimator works well. But the bit error rate (BER) cannot be computed using a loop in which also an add-on would work, therefore the channel coefficients were assumed to be properly estimated and only the channel equalization has been implemented.

The fifth block is the de-mapper block, which implements the QPSK/16QAM/64QAM de-modulations. It uses the same constellation that has been used for modulation.

The sixth block is the de-interleaver, which implements the inverse of the interleaver shown in Figure 5-7.

The seventh block is the Viterbi decoder, which uses the same trellis as the one that has been used for the convolutional encoders. In this case, only the first two of the three outputs x_k, z_k, z'_k have been used, so the data has been decoded using the output data given by the first convolutional encoder.

The eight block is the CRC removal block, which removes the CRC bits that have been added in the transmitter by the CRC block.

The ninth block is the block that contains the data that has been received and it is the same as the transmitted data in case no noise has been added.

Also in the case of the UMTS transceiver, conversions from decimal to binary and from binary to decimal have been used, along with interleavers and de-interleavers blocks. The decimal to binary conversion blocks have not been specified by the standard, but were necessary in order to use some functions of MatLab, such as "*convenc*" that only codes binary data. Therefore, such blocks had to be used throughout the program, but they have not been represented in the diagrams.

5.4 GSM/EDGE transceiver system design

GSM (acronym from *Global system for mobile communications*) is the system that is the most spread in the world. Part of the reasons for such a success are the possibility of changing the network operator without changing the phone, facilities such as SMS (*short message service*) and world-wide implemented roaming service. This system is considered the second generation of telecommunication systems (2G) as it is a clear upgrade of the 1st generation, the 1G systems that were not only analog instead of digital, but were moreover not spectrum efficient. The considered channel for transmission is the Full-rate traffic channel (TCH/F) is described in Figure 5-9.

As the GSM is the simplest system to implement, it also uses the simplest concepts and the smallest number of blocks. However, the system might be considered as a founding concept for the systems that followed afterwards (UMTS, LTE), as it was the first digital telecommunications system. These systems implemented several new techniques to deal with the spectrum requirements, and to higher data rates (OFDM modulation in the case of LTE or orthogonal spreading codes for improved efficiency use of the spectrum in case of UMTS). The considered channel is the full rate speech traffic channel (TCH/FS).

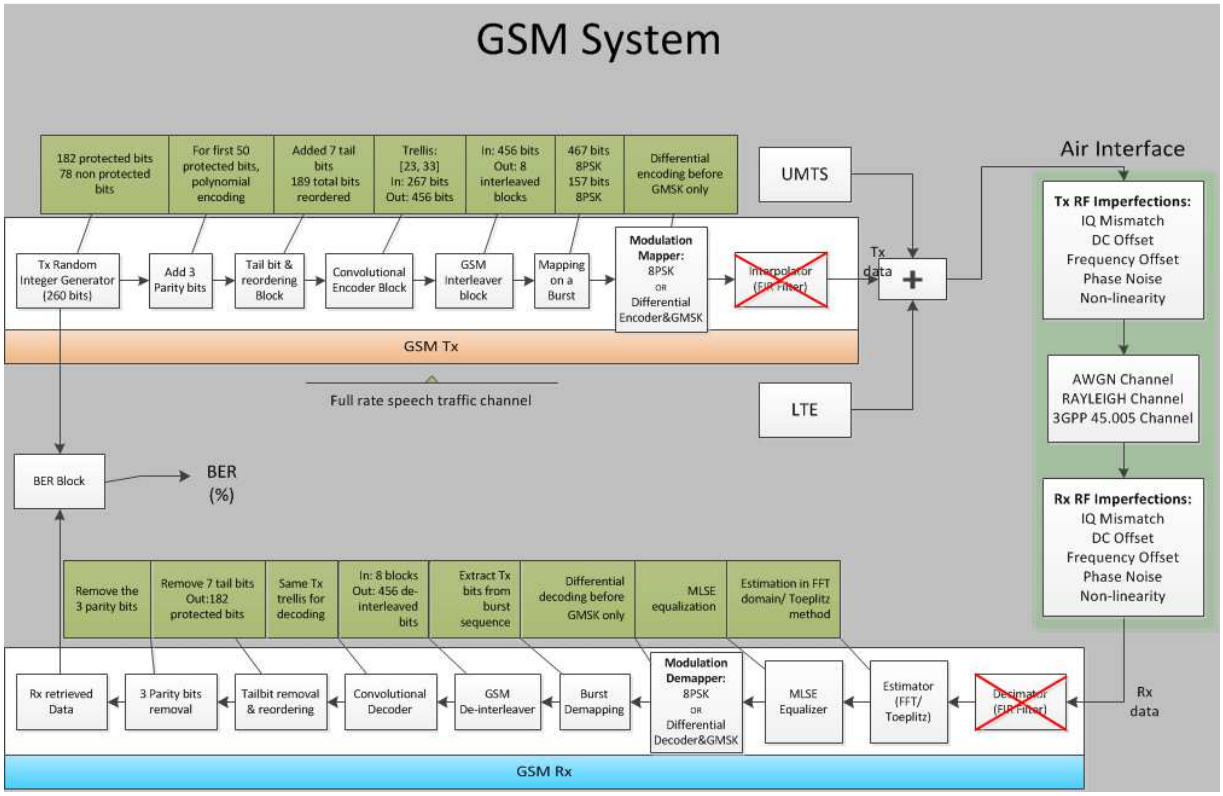

Figure 5-9 System implementation of GSM

The first block of the GSM transmitter is the speech generator frame block, which generates a frame of 260 bits.

The second block is the re-ordering block, which adds 3 parity bits and also tail bits and reorders the data.

The third block is the convolutional encoder, which uses a trellis for encoding. It has a ½ rate, so one bit of data is encoded with two bits at the output. The bits are encoded by the polynomials:

$$g_0(D) = 1 + D^3 + D^4$$

$$g_1(D) = 1 + D + D^3 + D^4 .$$

From these polynomials, octals can be defined by taking the powers of D in reverse order: 11001 read in reverse order is 10011 and as it is formed by only 5 digits, one zero has to be attached to the left. Therefore, the octal is formed by 010011 which taken in groups of three is 010 011 which is equivalent to 23.

The other polynomial is given by 11011 which read in reverse order is also 11011 which also needs a zero attached to the left to form a multiple of three, therefore the sequence becomes 011011 which is translated into an octal of 33. Therefore, the trellis of the GSM convolutional encoder is [23 33].

The fourth block is the interleaver, which permutes the 456 bits according to Table 1 of [**13**] standard. The bits are mixed using eight sub-blocks, using modulo 8 division by the formula j = 2((49k) mod 57) + ((k mod 8) div 4).

The fifth block is the normal burst mapper, which maps a sequence of data to a burst. The burst is formed of blocks of 57 bits, together with the signalling bits *hu* and *hl* that are flags that indicate the control channel signalling. Bits *hu* are 0 for the first 2 bursts and *hl* are 0 for the last 2 bursts.

The sixth block is the mapper block, which for the full rate speech traffic channel, can be either 8PSK (p*hase shift keying*) or GMSK (*gaussian minimum shift keying*). In case the signal is modulated using 8PSK, the values are determined by groups of three bits, and mapped to a constellation of 8 values. This constellation is specified in Table 1 in [**14**]. In case GMSK modulation is used, each data value {0, 1} is first differential encoded using $\hat{d}_i = d_i \oplus d_{i-1}$, where $\oplus$ denotes modulo 2 addition. Therefore, the modulating data value α_i input to the modulator is:

$$\alpha_i = 1 - 2\hat{d}_i \qquad (\alpha_i \in \{-1, +1\}).$$

Afterwards, the data is filtered that has the impulse response defined by $g(t) = h(t) * rect\left(\frac{t}{T}\right)$ where the function $rect\left(\frac{t}{T}\right)$ is defined by:

$$rect\left(\frac{t}{T}\right) = \begin{cases} \frac{1}{T} & for\ |t| < \frac{T}{2} \\ 0 & otherwise \end{cases}$$

and * means convolution.

The signal is then transmitted over the air interface and is detected by the antenna of the receiver.

The GSM receiver follows the same steps as the transmitter for decoding, just that the order is reversed.

The first block of the receiver is the Viterbi channel equalizer, which equalizes the received signal with the modulated constellation (either 8PSK or GMSK) in order to recover the transmitted data.

The second block is the demapper, which is either using the constellation of 8PSK, or the one of GMSK, depending on which one has been used for transmission. If GMSK is used, the demodulation is followed by differential decoding.

The third block is the burst demapping, that extracts the sent data from the received bursts.

The fourth block is the 456 bits de-interleaver, which permutes the bits of the 8 blocks back to the original order.

The fifth block is the Viterbi decoder, which uses the same trellis for decoding as it has been used for the convolutional encoding. The data that enters the Viterbi decoder is double length, after decoding, therefore the data will be the same length as it was when it was convolutionally encoded in the GSM transmitter.

The sixth block is the Rx reordering block, which removes the tail bits and does the reordering of the bits back to their original positions as they were before the reordering of the transmitter block. This block also removes the 3 parity bits.

The seventh block is the receiver information data, which is the vector to be compared with the frame of 260 bits that has been generated in the transmitter.

5.5 Conclusion

Chapter 5 described in detail the block components of each of the standards, LTE, UMTS and GSM/EDGE. Some of the most important blocks have been described in detail (interleaver, spreader, scrambler, channel coding block). As one will see in chapter 6, the completion of the systems has been followed by a code validation that ensured that the simulated BER graphs match the theoretical BER graphs, for each of the modulations used.

This proves to be a very important aspect, as the systems (LTE, UMTS and GSM/EDGE) have to have the same signal power level at the output of each block, equal to a mean power value of 0 dBm. Thus, the systems implemented the RF imperfections in a correct way, making feasible a comparison between their tolerances to RF impairments.

The wireless standards treated in this chapter show that the evolution from GSM/EDGE to LTE went through different steps: first, the Gaussian filter has been replaced with a Raised Root Cosine filter, the modulations of GSM (GMSK and 8PSK) have been replaced with QAM modulations because of the easier spectrum requirements and higher capacity offered; blocks like Spreader and Scrambler appeared in order to have orthogonality between different Tx and tolerance to perturbations; however these affected the spectrum efficiency, therefore have been replaced with the OFDM modulation in the case of LTE.

6. Simulation of LTE, UMTS & GSM/EDGE wireless systems in the AWGN channel (uncoded bits and MLSE equalization)

The transmission channel can be modeled as noisy. The frequently used type of noise is the *additive white Gaussian noise* (AWGN). It has a constant spectral density and a Gaussian distribution in amplitude. The addition of this noise is made in order to observe the BER plots for the three systems. The BER is computed comparing the transmitted vector of data with the received vector, and counting the numbers of bits that differ. This number is divided by the length of the block. As it is usually expressed in percents, a multiplication with 100% is necessary. For better accuracy, more blocks are transmitted in order to compute the BER in a more precise manner.

The results of the BER are shown in plots, for each wireless system, and for each modulation type. The SNR values are taken differently for each modulation, as from one point on, the BER is 0. For the simulations, the signal to noise ratio (SNR) is swept over 0 to 15 for QPSK, over 0 to 20 for 16QAM and over 0 to 25 for 64QAM. The plot is made for energy per bit (E_b/N_0), and the conversion is E_b/N_0= SNR-10*$\log_{10}(\log_2(M))$, where M is the number of constellation points (4 for QPSK, 16 for 16QAM and 64 for 64QAM).

6.1 BER Results for LTE (classic I-Q Tx)

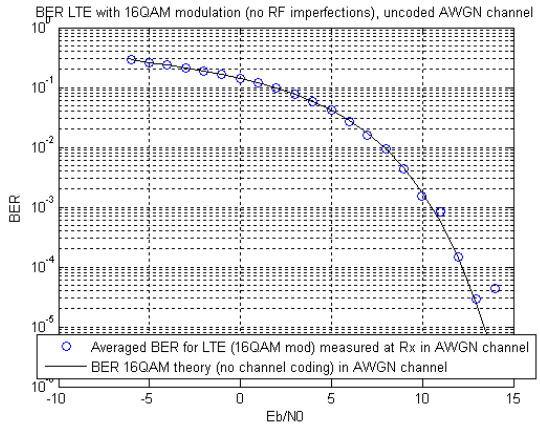

Figure 6-1 BER versus E_b/N_0 for LTE with QPSK modulation

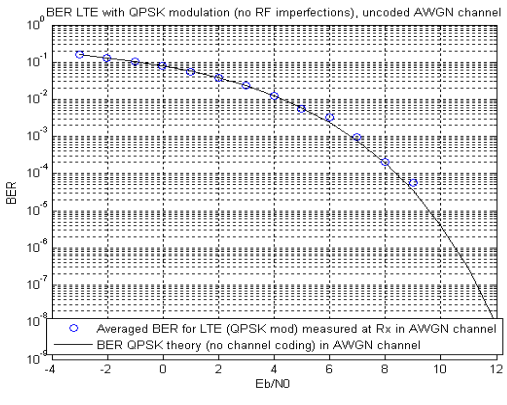

Figure 6-2 BER versus E_b/N_0 for LTE with 16QAM modulation

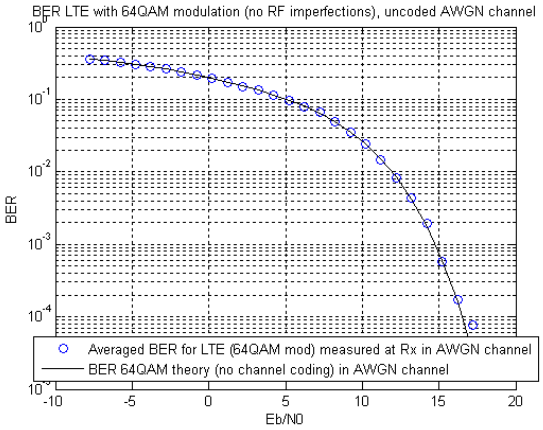

Figure 6-3 BER versus E_b/N_0 for LTE with 64QAM modulation

Figure 6-1-Figure 6-3 show that the LTE wireless model of the system is validated, and that there is no difference between the results from theory and the results of the simulations. An article of interest about this subject is [**37**].

6.2 BER Results for UMTS (classic I-Q Tx)

It is shown in this chapter that the simulated BER curve matches the theoretical BER curve that is found in theory for the QPSK/16QAM/64QAM modulations. Compared to LTE, it is made use of the spread code $C_{ch,16,4}$ = [1 1 -1 -1 1 1 -1 -1 1 1 -1 -1 1 1 -1 -1] for both spreading and de-spreading, accounting for the noise that is averaged (therefore the noise has to be increased with a $10*\log_{10}$(length(spread code)) value). The spreading takes place in the transmitter. In the considered case, the 8640 symbols are spread in the following way: each symbol is multiplied with the spread code of 16 unary values. A matrix of 16*8640 values results. Then, in the receiver, de-spreading takes place: the matrix is reshaped in a vector and has its values grouped in blocks of 16 values. These are multiplied with the transposed spread code. The obtained value is divided by the length of the spread code, currently 16, and thus an average value is obtained.

With the shift of wireless generations from 3G (UMTS) to 4G (LTE), the use of the spreader-despreader blocks has been discontinued, the reason being the inefficient spectrum use. It is shown in Figure 6-4-Figure 6-6 the graphs for the BER. The code is validated through the addition of a $10*\log_{10}$(length(spread code)) term to the SNR value used for the generation of the white Gaussian noise. This addition is necessary in order to take into account the averaging of the noise when dispreading.

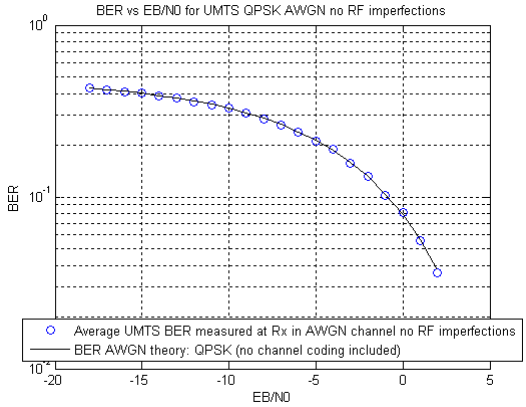

Figure 6-4 BER versus E_b/N_0 for UMTS with QPSK modulation

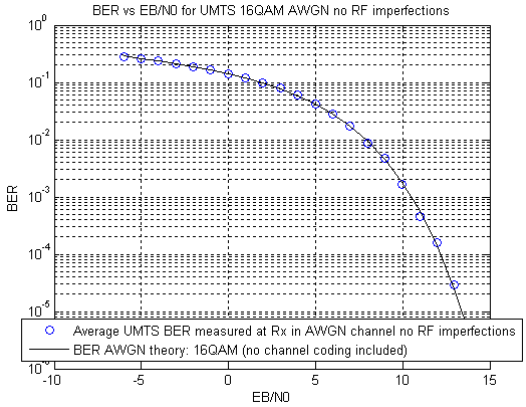

Figure 6-5 BER versus E_b/N_0 for UMTS with 16QAM modulation

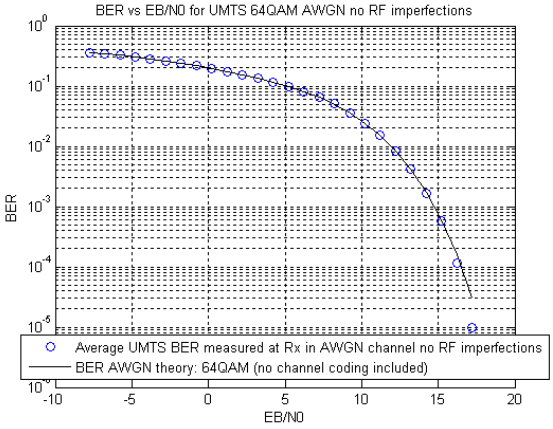

Figure 6-6 BER versus E_b/N_0 for UMTS with 64QAM modulation

6.3 BER Results for GSM/EDGE (classic I-Q Tx)

The GSM/EDGE system does not use the blocks of the UMTS system, the spreader and de-spreader. The BER for the 8PSK modulation matches the theory. In case of GMSK, the BER curve is compared to theoretical MSK. In general, the BER curve for GMSK is degraded because of the inter-symbol interference (ISI) by the Gaussian filter [**15**]. The theoretical curve plotted in Figure 6-8 is for MSK modulation with coherent detection and precoding given by '*berawgn*' function of the MatLab software. In [**15**] it is given the theoretical formula for the BER of GMSK: $BER = erfc(\sqrt{2\beta \frac{E_b}{N_0}})$. It depends on the degradation factor β that is due to the pre-modulation filter, on the E_b/N_0. It makes use of

the *erfc* function that gives an error for negative values of the E_b/N_0, as it expects positive input values. It has been studied for the positive values, considering various values for the degradation factor β. A comparison has been made between the values given by the MatLab computed function *berawgn* and the one from [**15**], and the results shown were different, the formula in the book showing better BER until a E_b/N_0 value when the BER seemed to flatten.

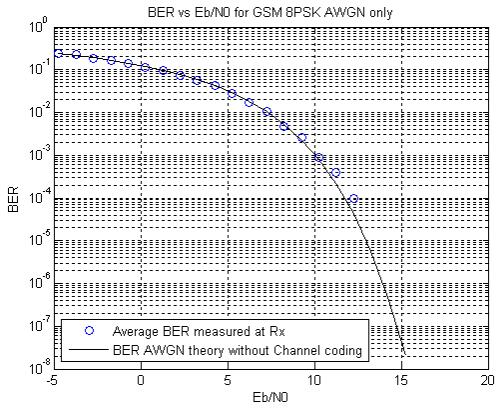

Figure 6-7 BER versus E_b/N_0 for GSM/EDGE with 8PSK modulation

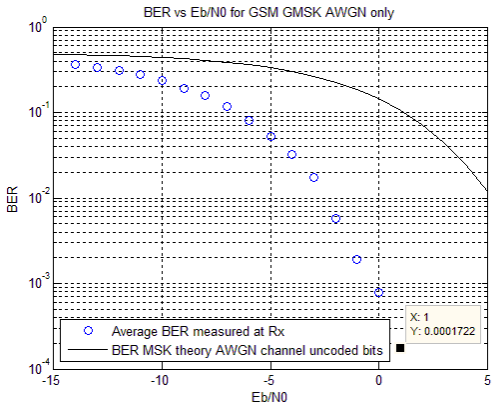

Figure 6-8 BER versus E_b/N_0 for GSM/EDGE with GMSK modulation

6.4 Conclusions

The LTE transceiver system has been simulated and the ideal case (with no RF imperfections) has been compared with the theoretical curve. The results match almost perfectly; this ensures a proper calibration of the system.

In the case of the GSM transceiver, it is shown that for the 8PSK modulation, the theoretical BER curve matches the simulated curve; therefore the system is properly calibrated. However, for GMSK, the simulated curve is obtained, but it cannot accurately be compared to the theoretical GMSK curve because of the degradation due to the inter-symbol interference by the Gaussian filter.

It has been shown that the transceivers follow the ideal curve in general.

7. Modeling of RF impairments

7.1 DC offset

The DC offset appears because of IC processing [**18**]. As part of the local oscillator (LO) signal leaks into the radio frequency (RF) port because of the finite isolation, the down-converter shows at its output a DC offset given by the mixing of the LO leakage signal with the LO signal. A second cause is the leakage from the transmitter, from the output of the power amplifier (PA). A third cause is the interference from other transceivers. DC offset has to be removed or cancelled in the direct-conversion receiver, in order for the receiver to work. The methods used for removing the time invariant DC offset are alternative current (AC) coupling or high pass filtering in the base band (BB) block, together with storing the data at the input of the low noise amplifier (LNA) in a memory. Another method is averaging the digitized signal containing the modulation schemes with zero mean (QPSK, 16QAM, 64QAM). Values for DC offset have been determined, in order to have a 3 dB BER offset from the ideal curve.

As the input signal is of I-Q type, this translates into the following formulas [**40**]

$$s_{input}(t)= s_{real}(t)+j*s_{imag}(t) \quad [7.1]$$

where

$$s_{real}(t)= \mathrm{Re}\ \{s_{input}(t)\} \quad [7.2]$$

$$s_{imag}(t)= \mathrm{Imag}^{6}\ \{s_{input}(t)\} \quad [7.3]$$

and therefore, the DC offset signal results after the addition of I_{DC} and Q_{DC} ($I_{DC}= Q_{DC}$)

$$s_{DC\ offset}(t)= s_{real}(t)+ I_{DC} +j*[s_{imag}(t)+ Q_{DC}] \quad [7.4]$$

[6] Re and Imag are notations for the real and imaginary part of the signal

7.1.1 DC offset for LTE

For LTE, the modulation 16QAM is the most sensitive to this type of RF impairments, contrary to the expectations (64QAM was expected to be the most sensitive). For LTE, the range thats give a 3 dB difference for the BER curve is 5-17 mV. The results are shown in Figure 7-1-7-3.

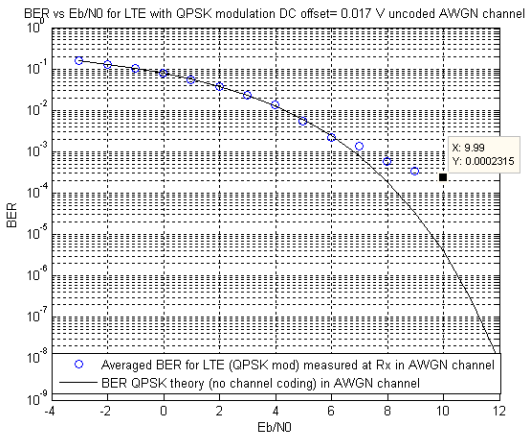

Figure 7-1 BER versus E_b/N_0 for LTE with QPSK modulation, 17 mV DC offset

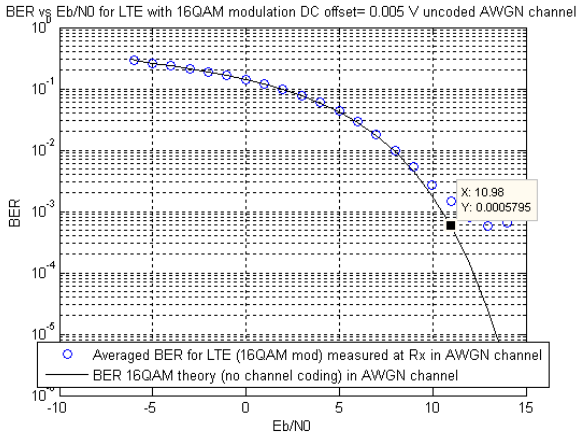

Figure 7-2 BER versus E_b/N_0 for LTE with 16QAM modulation, 5 mV DC offset

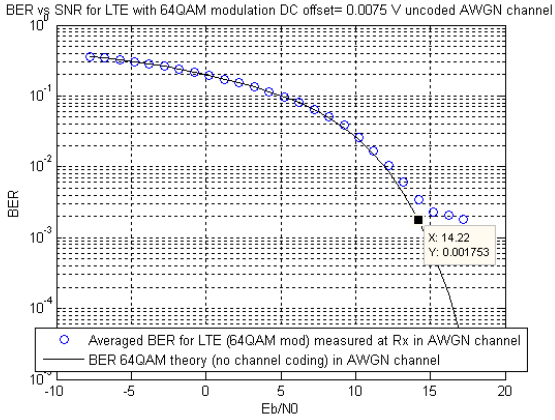

Figure 7-3 BER versus E_b/N_0 for LTE with 64QAM modulation and 7.5 mV DC offset

7.1.2 DC offset for UMTS

In Figure 7-4-Figure 7-6, the effect of the DC offset has been studied for the UMTS wireless system. The 3 dB offset in terms of the BER values is observed in comparison with the ideal case, for which the values have been stored in a vector and plotted on the same

graph for convenience. The modulation most sensitive to DC offset is the 64QAM, with 100mV. The DC offset range for UMTS is between 125 mV and 1000 mV, therefore UMTS is more tolerant to DC offset compared to LTE.

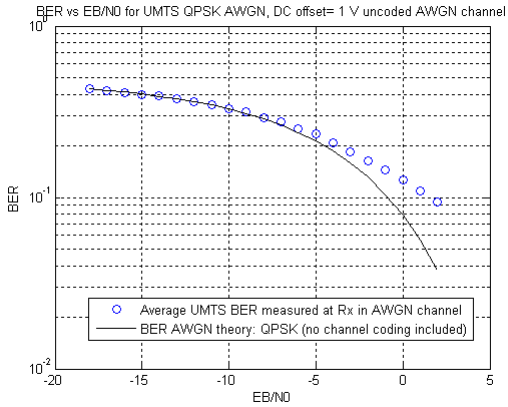

Figure 7-4 BER versus E_b/N_0 for UMTS with QPSK modulation, 1 V DC offset

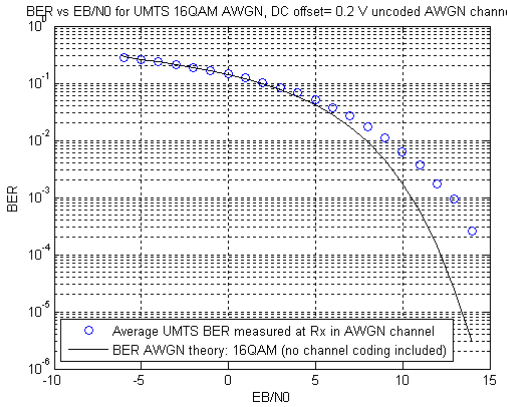

Figure 7-5 BER versus E_b/N_0 for UMTS with 16QAM modulation, 0.2 V DC offset

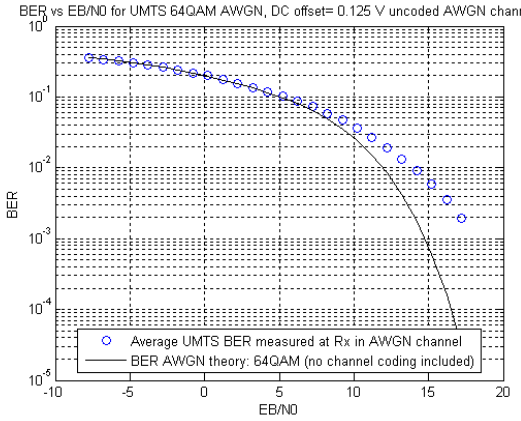

Figure 7-6 BER versus E_b/N_0 for UMTS with 64QAM modulation, 0.125 V DC offset

7.1.3 DC offset for GSM/EDGE

The DC offset effect has been studied on GSM/EDGE also. The values differ for the two modulation types used for the system, however it seems that GMSK is more tolerant to DC offset than 8PSK. That translates into a bigger sensitivity for EDGE (that uses 8PSK) compared to GSM (that uses GMSK). In Figure 7-7 and Figure 7-8 are shown the results for the two systems.

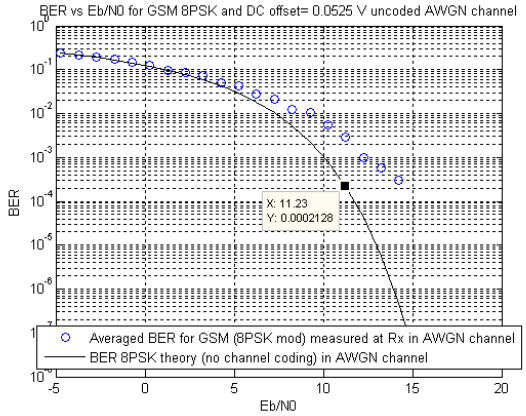

Figure 7-7 BER versus E_b/N_0 for GSM with 8PSK modulation, 52.5 mV DC offset

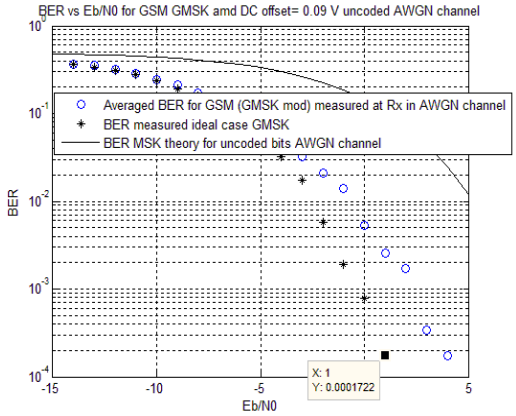

Figure 7-8 BER versus E_b/N_0 for GSM with GMSK modulation, 90 mV DC offset

7.2 I-Q amplitude mismatch

The received RF signal is directly down-converted into two quadrature base band signals, named I and Q. These signals propagate and are amplified in separate I and Q paths. As such, the amplitude varies, because of the gain imbalance of the two separate paths, even when using the-state-of-the-art integrated RF circuits. Considering the same input signal s(t), the amplitude mismatch affected signal results as:

$$s_{I-Q\ ampl}(t) = 10^{0.5*\frac{Ia}{20}} * \mathrm{s_{real}(t)} + j * 10^{-0.5*\frac{Ia}{20}} * \mathrm{s_{imag}(t)} \qquad [7.5]$$

7.2.1 I-Q amplitude mismatch for LTE

The amplitude mismatch varies with the modulation type. For QPSK, the amplitude imbalance is 3 dB, for 16QAM is 1.12 dB, while the strictest is for 64QAM with 0.55 dB. In Figure 7-9-Figure 7-11 are shown the effects of different DC offsets for different modulations for the 3 dB offset from the ideal BER curve.

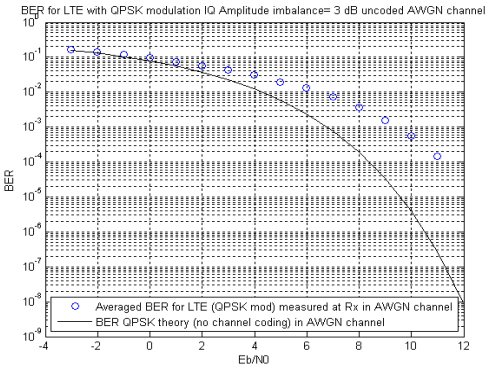

Figure 7-9 BER versus E_b/N_0 for LTE with QPSK modulation, 3 dB imbalance

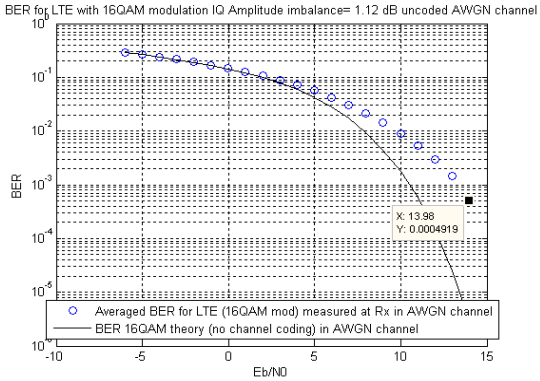

Figure 7-10 BER versus E_b/N_0 for LTE with 16QAM modulation 1.12 dB imbalance

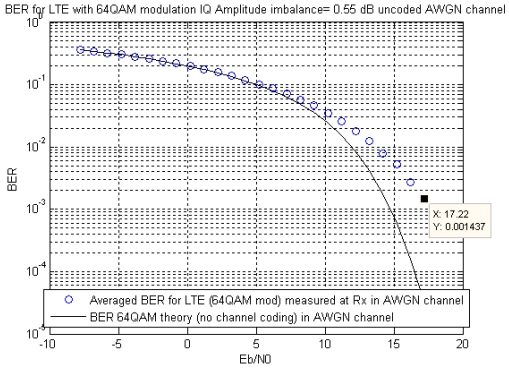

Figure 7-11 BER versus E_b/N_0 for LTE with 64QAM modulation, 0.55 dB imbalance

7.2.2 I-Q amplitude mismatch for UMTS

Compared to LTE, UMTS is more tolerant to I-Q amplitude mismatch, as for QPSK one needs 11.5 dB amplitude mismatch compared to 3 dB in order to produce a 3 dB offset from the ideal curve, 3 dB instead of 1.12 dB for 16QAM and 1.75 dB compared to 0.55 dB for 64QAM. As expected, the 64QAM modulation is the most sensitive to I-Q amplitude mismatch. The results are shown in Figure 7-12-Figure 7-14.

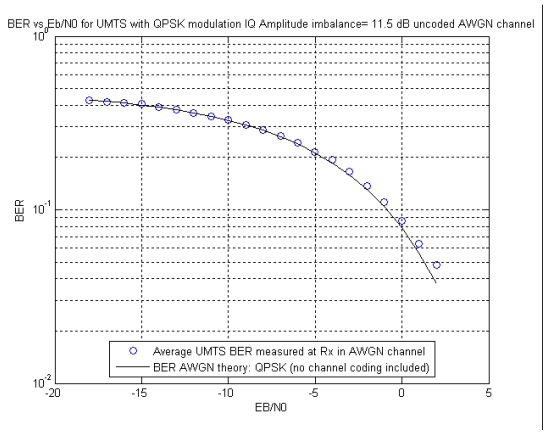

Figure 7-12 BER versus E_b/N_0 for UMTS with QPSK modulation, 11.5 dB imbalance

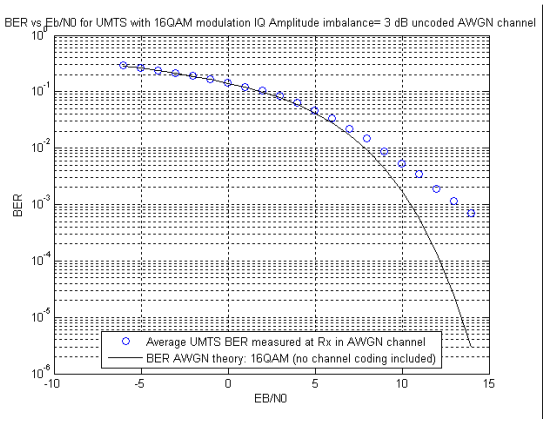

Figure 7-13 BER versus E_b/N_0 for UMTS with 16QAM modulation, 3 dB imbalance

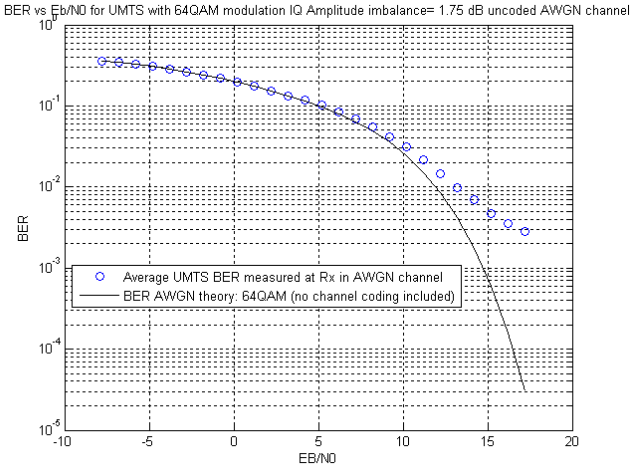

Figure 7-14 BER versus E_b/N_0 for UMTS with 64QAM modulation, 1 dB imbalance

7.2.3 I-Q amplitude mismatch for GSM/EDGE

The GSM/EDGE system is also sensitive to I-Q amplitude mismatch. A 3 dB BER offset is ensured by an amplitude mismatch equal to 1.5 dB for 8PSK and to 3.5 dB for GSMK. EDGE is more sensible than GSM in this case also. This is shown in Figure 7-14-Figure 7-15 and in Figure 7-16.

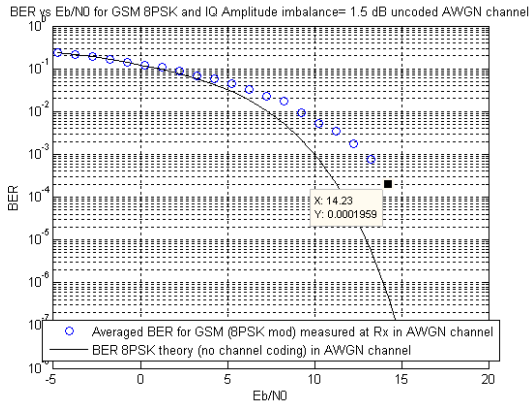

Figure 7-15 BER versus E_b/N_0 for GSM/EDGE with 8PSK modulation, 1.5 dB imbalance

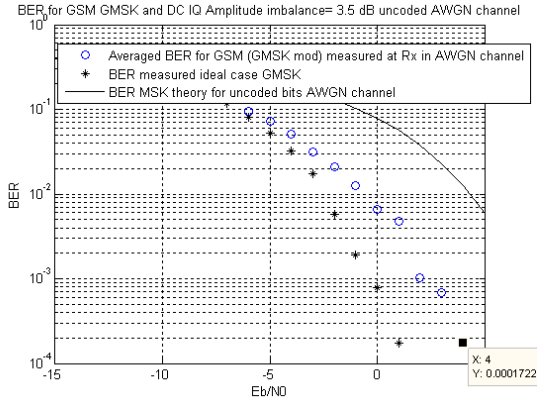

Figure 7-16 BER versus E_b/N_0 for GSM/EDGE with GMSK modulation, 3.5 dB imbalance

7.3 I-Q phase mismatch

Aside from I-Q amplitude mismatch, the two different propagation paths ensure also a phase mismatch. To minimize the effect of I-Q mismatch in general, a better synchronization of the gain controls of the analog base band block has to be obtained. The expression of the phase mismatch affected signal is given in formula (7.6), partly described in [**40**]:

$$s_{I-Q\ phase}(t) = 10^{-0.5*j*\pi*\frac{Ip}{180}} * \mathrm{s_{real}(t)} + j * 10^{(\frac{\pi}{2}+0.5*j*\pi*\frac{Ip}{180})} * \mathrm{s_{imag}(t)} \qquad [7.6]$$

7.3.1 I-Q phase mismatch for LTE

A 3 dB offset for the BER curve has been aimed for. The values that offer this offset are 20°, 7.5° and 3.5° for QPSK, 16QAM and 64QAM respectively. The 64QAM modulation is the most sensitive to phase imbalance. The results follow in Figure 7-17- Figure 7-19.

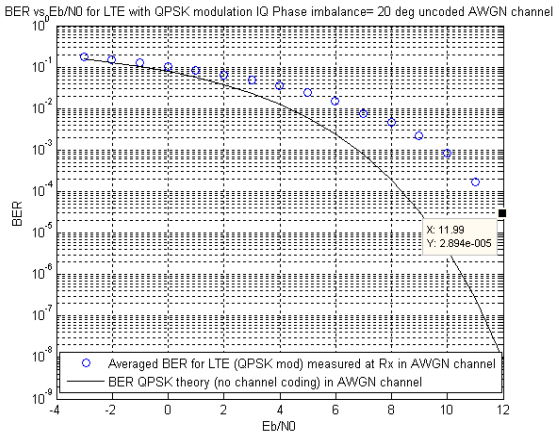

Figure 7-17 BER versus E_b/N_0 for LTE with QPSK modulation, 20º imbalance

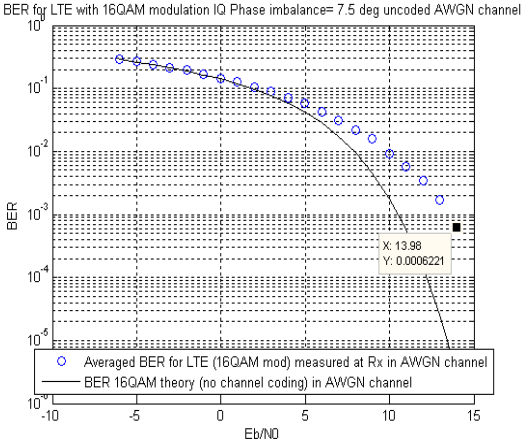

Figure 7-18 BER versus E_b/N_0 for LTE with 16QAM modulation, 7.5º imbalance

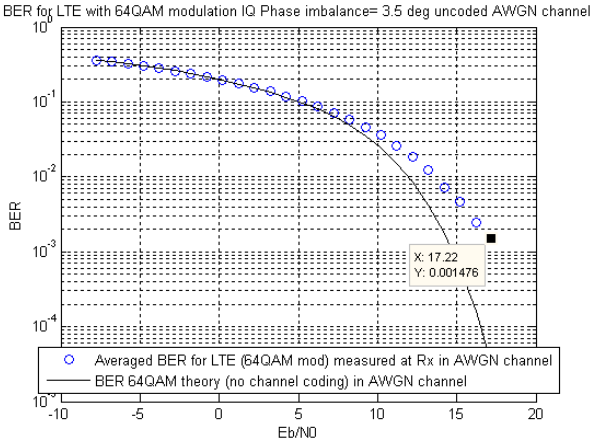

Figure 7-19 BER versus E_b/N_0 for LTE with 64QAM modulation, 3.5º imbalance

7.3.2 I-Q phase mismatch for UMTS

As the UMTS did not show influence of the I-Q amplitude mismatch variation, for QPSK, a similar results was expected also for the phase mismatch in the case of QPSK. It is shown in Figure 7-20-Figure 7-22 the comparison between the phase mismatch affected signal and the ideal signal (no RF imperfections). The UMTS system shows a better tolerance to both the amplitude and phase mismatch compared to the LTE system, for all modulations types: QPSK, 16QAM, 64QAM.

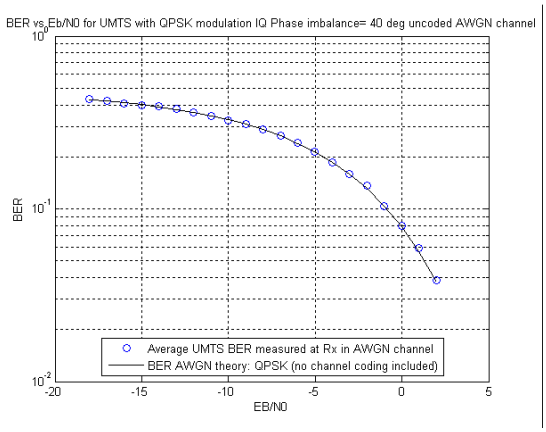

Figure 7-20 BER versus E_b/N_0 for UMTS with QPSK modulation, 40° imbalance

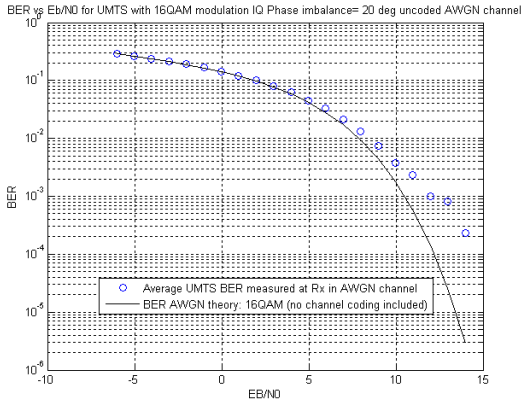

Figure 7-21 BER versus E_b/N_0 for UMTS with 16QAM modulation, 20° imbalance

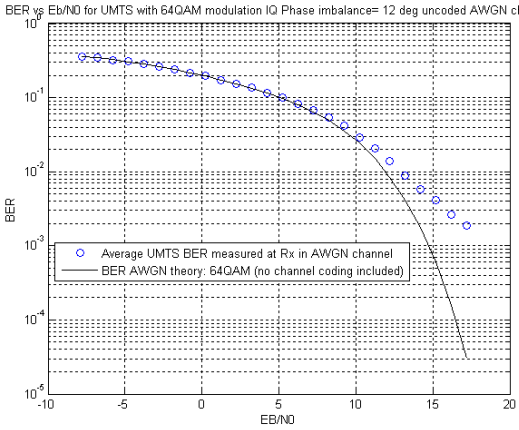

Figure 7-22 BER versus E_b/N_0 for UMTS with 64QAM modulation, 12° phase imbalance

7.3.3 I-Q phase mismatch for GSM/EDGE

The I-Q phase mismatch of 10° for 8PSK and of 30° for GMSK will give a 3 dB offset for the BER curve. This translates into the EDGE system being more sensitive to phase mismatch than the GSM system. The results are shown in Figure 7-23 and in Figure 7-24.

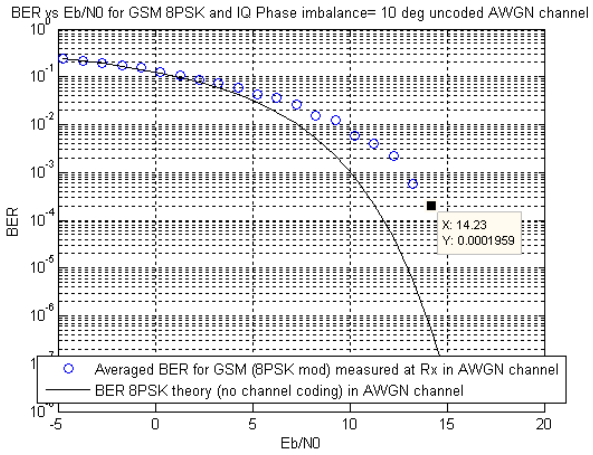

Figure 7-23 BER versus E_b/N_0 for GSM/EDGE with 8PSK modulation, 10° imbalance

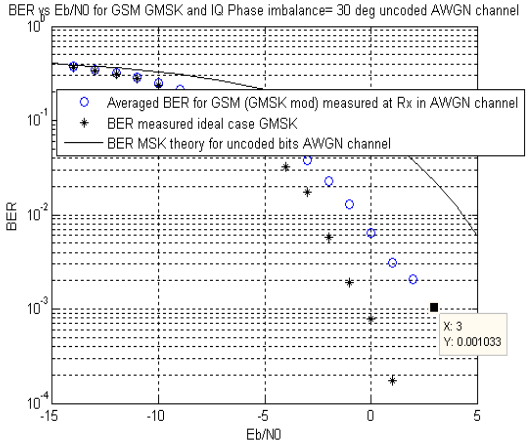

Figure 7-24 BER versus E_b/N_0 for GSM/EDGE with GMSK modulation, 30° imbalance

7.4 Nonlinearity: IIP_2 and IIP_3 on AM2AM

The systems are sensitive to nonlinearity. This happens when a device has weak linearity, and higher order terms have to be taken into consideration. The cubic nonlinearity is studied in this work. As the even mode distortion is suppressible by the common-mode rejection of the differential circuits, the important distortion is the differential mode. The given input for the simulation is the IIP_3 parameter in dBm. The signal has the form in (7.7):

$$s(t)= a_1s^1(t)+a_2s^2(t)+a_3s^3(t) \quad [7.7]$$

and

$$IIP_3[dBm] = \sqrt{\frac{4}{3}\left|\frac{a_1}{a_3}\right|} \quad [7.8]$$

$$IIP_2[dBm] = \left|\frac{a_1}{a_2}\right| \quad [7.9]$$

Then IIP_3 and IIP_2 are converted from dBm to V using the formula (7.10):

$$IIP_{2,3}[V] = \sqrt{10^{\frac{IIP_{2,3}[dBm]-30}{10}}} \quad [7.10]$$

The value of a_1 is assumed to be 1, and the value of a_2 and a_3 are computed using (7.11-12):

$$a_2 = \frac{a_1}{IIP_2[V]} \quad [7.11]$$

$$a_3 = \frac{4}{3}\frac{a_1}{IIP_3[V]} \quad [7.12]$$

7.4.1 Nonlinearity for LTE

The IIP_3 parameter is equal to 33.5 dBm for QSPK, 38 dBm for 16QAM and 41.5 dBm for 64QAM (thus 64QAM is most sensitive). The results are shown in Figure 7-25-Figure 7-27.

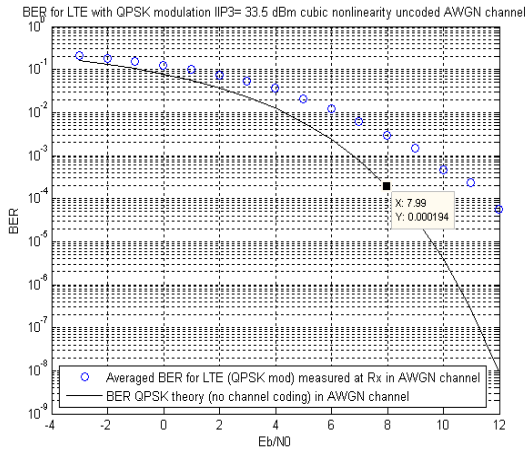

Figure 7-25 BER versus E_b/N_0 for LTE with QPSK modulation, 33 dBm IIP_3

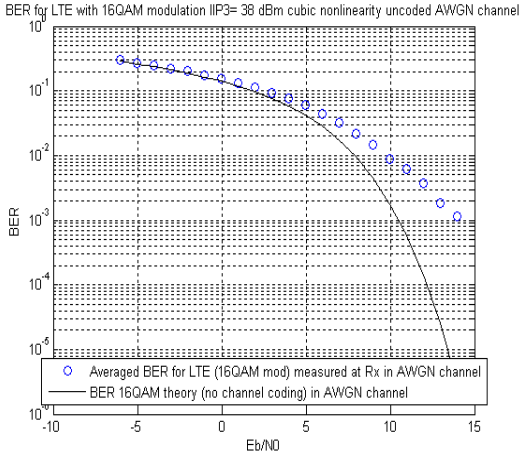

Figure 7-26 BER versus E_b/N_0 for LTE with 16QAM modulation, 38 dBm IIP_3

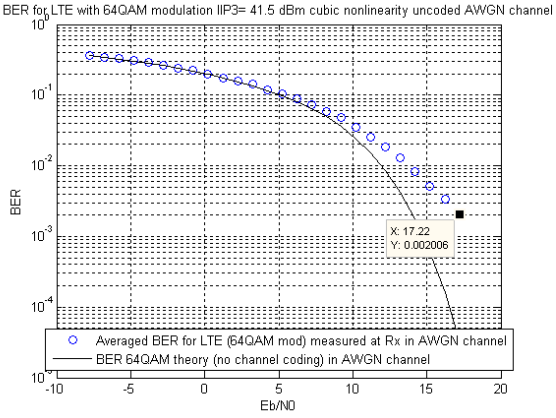

Figure 7-27 BER versus E_b/N_0 for LTE with 64QAM modulation, 41.5 dBm IIP_3

7.4.2 Nonlinearity for UMTS

Compared to LTE, the IIP_3 for UMTS has smaller values, which translates into better tolerance to the nonlinearity RF imperfection. The IIP_3 values are 32.5 dBm, 36.75 dBm and

40 dBm, values that are 1- 1.5 dB lower than for the LTE wireless systems. The results follow in Figure 7-28-Figure 7-30.

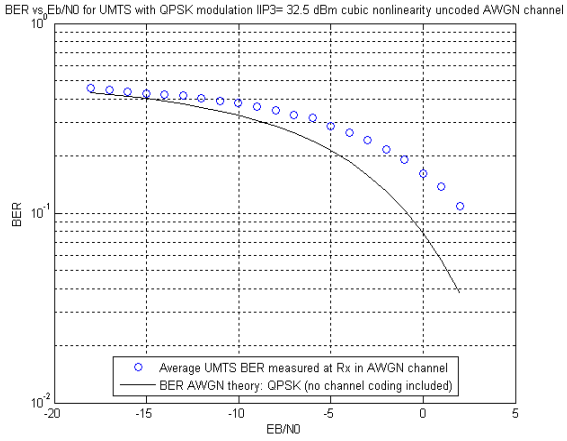

Figure 7-28 BER versus E_b/N_0 for UMTS with QPSK modulation, 32.5 dBm IIP_3

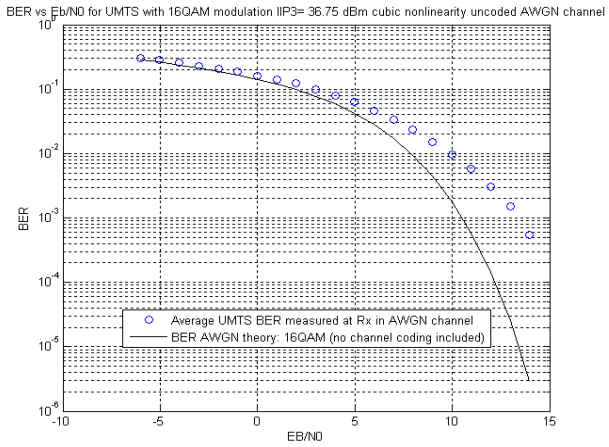

Figure 7-29 BER versus E_b/N_0 for UMTS with 16QAM modulation, 36.75 dBm IIP_3

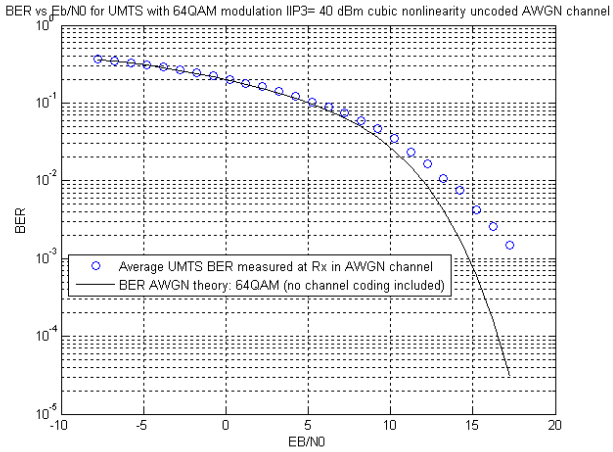

Figure 7-30 BER versus E_b/N_0 for UMTS with 64QAM modulation, 40 dBm IIP_3

7.4.3 Nonlinearity for GSM/EDGE

Compared to both LTE and UMTS, the IIP_3 for GSM/EDGE has smaller values, which translates into better tolerance to the nonlinearity RF imperfection. The IIP_3 values are 36.5 dBm in both cases, at least 1 dBm lower than in both cases mentioned above. The results follow in Figure 7-31-Figure 7-32.

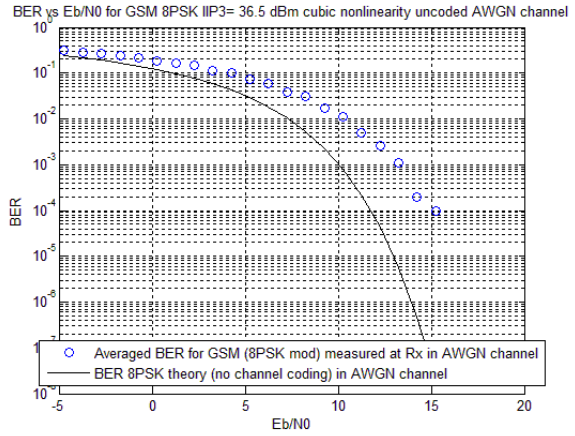

Figure 7-31 BER versus E_b/N_0 for GSM with 8PSK modulation, 36.5 dBm IIP_3

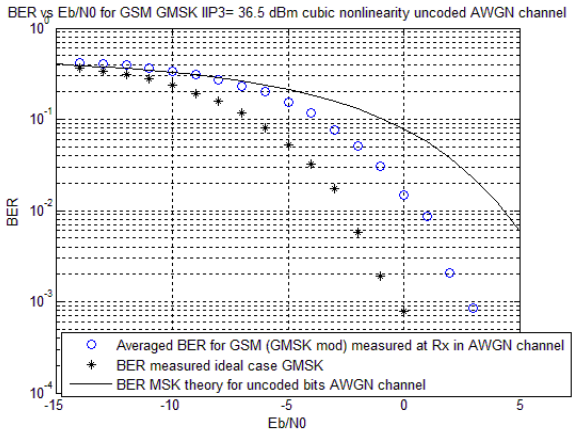

Figure 7-32 BER versus E_b/N_0 for GSM with GMSK modulation, 36.5 dBm IIP_3

7.5 Frequency offset

In order to ensure a good signal quality, the receiver has to tune itself on the transmitter frequency, otherwise reception quality problems would appear because of the inter symbol interference (ISI). In practice, there is an offset between the two because of the imperfect synchronization; therefore the frequency offset influence on the three wireless systems has been studied. The offset frequency is applied to the signal s(t) using the formula (7.13):

$$s_{freq\ offset}(t) = s(t) * e^{j*2\pi*f_{offset}*t} \quad [7.13]$$

where $t = 0{:}T_s{:}\frac{signal_{length}}{f_{carrier}} - T_s$ and where $T_s = \frac{1}{42.2\ GHz}$ is the sampling period and $f_{carrier=2.1\ GHz}$. If the time frame will be longer, but the step bigger, the offset will have a stronger influence.

7.5.1 Frequency offset for LTE

In case of LTE, the frequency offset that ensures a 3 dB offset from the two BER curves is 672 kHz for QPSK, 315 kHz for 16QAM and 168 kHz for 64QAM. The most sensitive to frequency offset is the 64QAM modulation. The results follow in Figure 7-33-Figure 7-35.

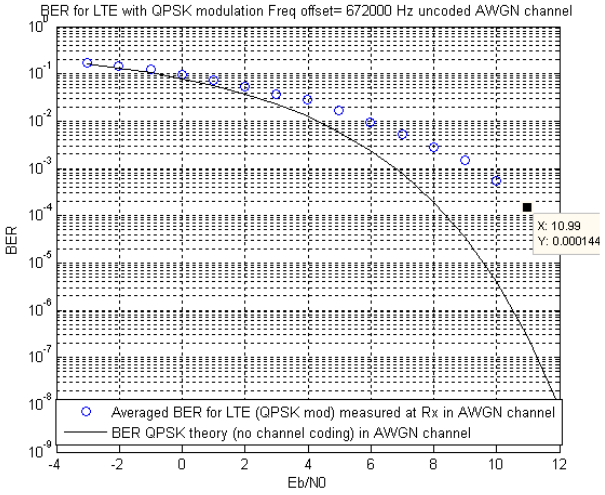

Figure 7-33 BER versus E_b/N_0 for LTE with QPSK modulation, 672 kHz f_{offset}

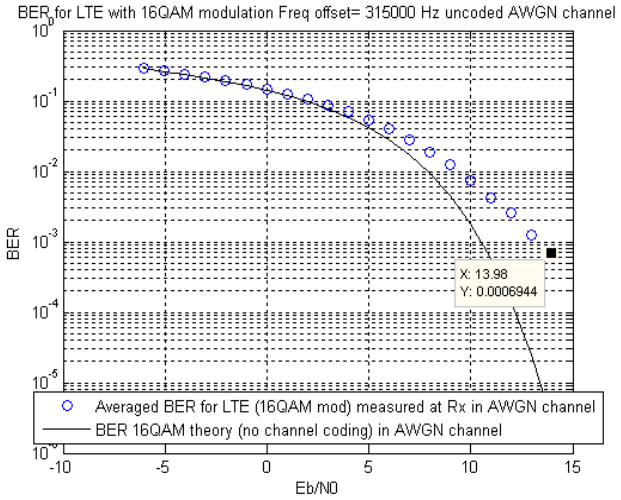

Figure 7-34 BER versus E_b/N_0 for LTE with 16QAM modulation, 315 kHz f_{offset}

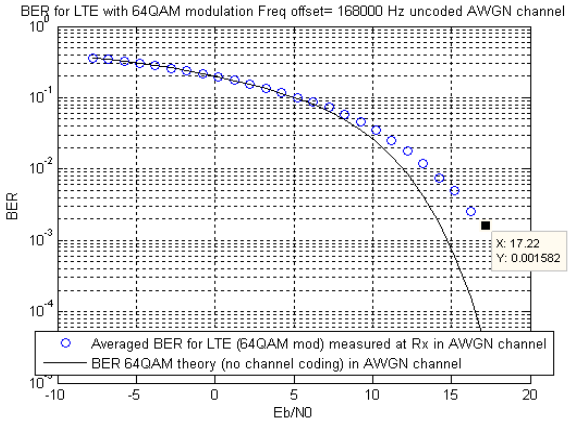

Figure 7-35 BER versus E_b/N_0 for LTE with 64QAM modulation, 168 kHz f_{offset}

7.5.2 Frequency offset for UMTS

Compared to LTE, UMTS is very sensitive to frequency offset. A frequency offset of 185 Hz for 64QAM deviates with 3 dB the BER curve of the ideal one instead of 168 kHz. The values obtained for QSPK and 16QAM are 1.8 kHz and 420 Hz. The results follow in Figure 7-36-Figure 7-38.

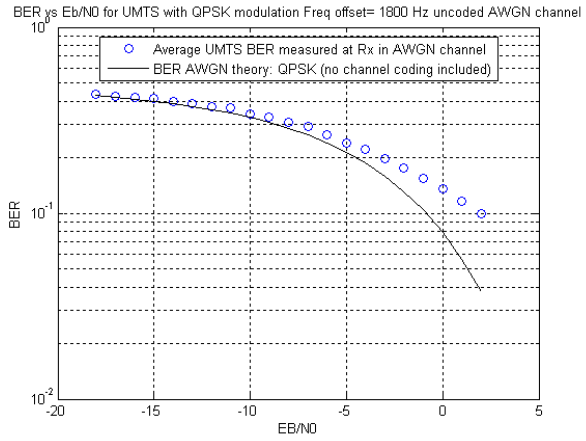

Figure 7-36 BER versus E_b/N_0 for UMTS with QPSK modulation, 1.8 kHz f_{offset}

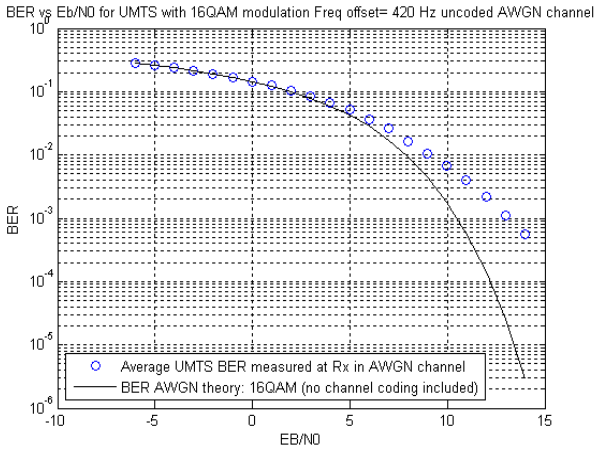

Figure 7-37 BER versus E_b/N_0 for UMTS with 16QAM modulation, 420 Hz f_{offset}

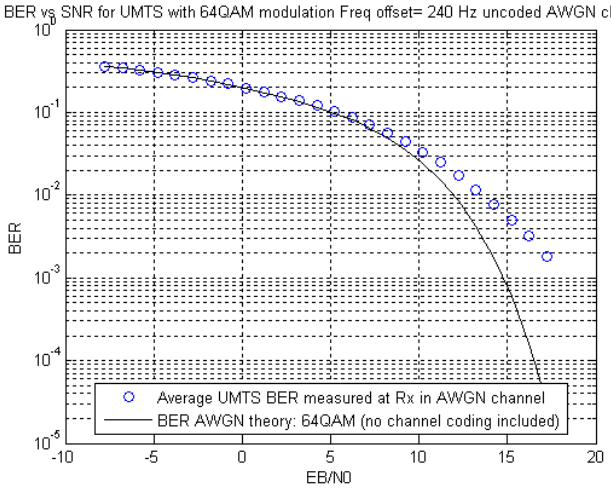

Figure 7-38 BER versus E_b/N_0 for UMTS with 64QAM modulation, 240 Hz f_{offset}

7.5.3 Frequency offset for GSM/EDGE

The frequency offset for EDGE is 135 kHz. For GSM, the frequency offset considered is 234 kHz, and as in sensitivity level, is in-between the LTE and EDGE. The results are shown in Figure 7-39-Figure 7-40.

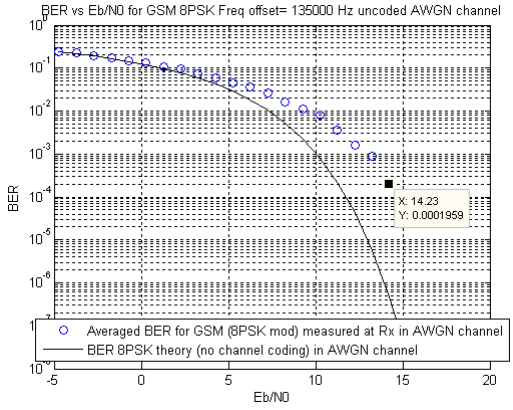

Figure 7-39 BER versus E_b/N_0 for GSM/EDGE with 8PSK modulation, 135 kHz f_{offset}

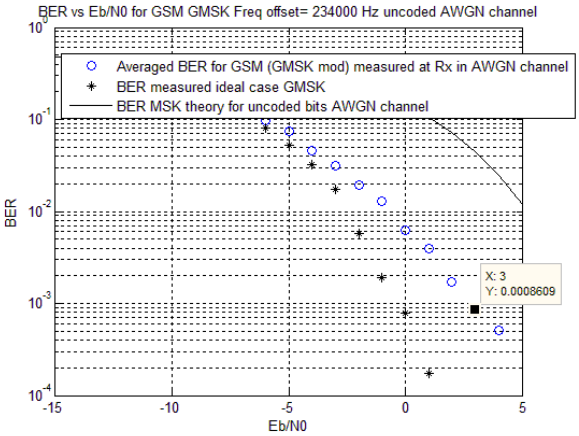

Figure 7-40 BER versus E_b/N_0 for GSM/EDGE with GMSK modulation, 234 kHz f_{offset}

7.6 Phase noise

The phase noise is defined using a phase noise mask, which specifies power limits at different frequency offsets. The phase noise mask used throughout this study is given below:

```
Phase_frequencies= [1E3,10E3,100E3,1E6,5E6]; %Frequency offset from carrier [Hz]
Phase_power limit= [-84,-100,-96,-109,-174]; %Power[dBc/Hz]
```

The phase noise has been implemented in the transmitter and in the receiver in separate cases, using the same mask for the frequencies and power limits. If one would like to have the same results and implement the phase noise mask only in one branch (the transmitter or the receiver), he should increase the power limit phase noise mask by 3 dBm for each of the values in the vector.

7.6.1 Phase noise for LTE

In Figure 7-41- Figure 7-43 it is shown that the phase noise affects the 64QAM the most. The QPSK modulation is hardly affected by noise. The BER curve shows some irregularities, and the reason for this could be the randomness of the phase noise in the spectrum, it is bigger or smaller depending on the frequencies it has to affect.

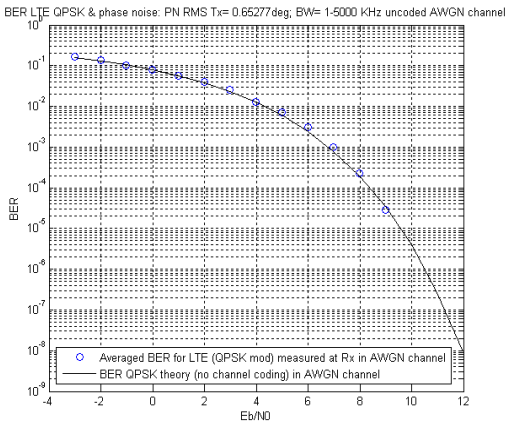

Figure 7-41 BER versus E_b/N_0 for LTE with QPSK modulation, phase noise mask

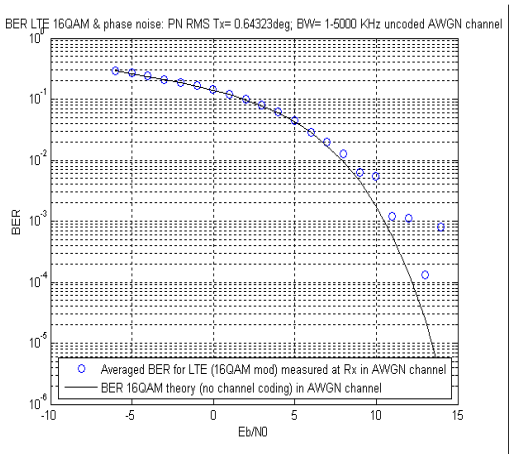

Figure 7-42 BER versus E_b/N_0 for LTE with 16QAM modulation, phase noise mask

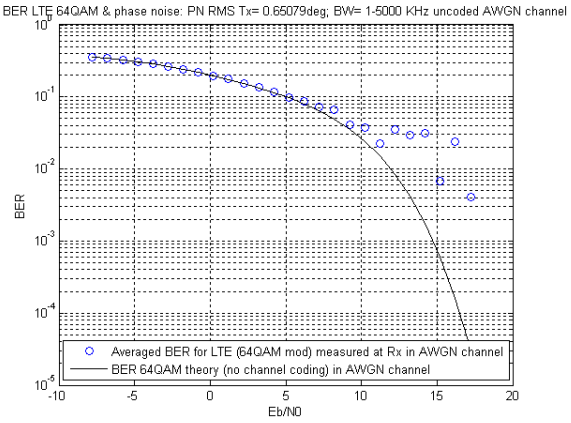

Figure 7-43 BER versus E_b/N_0 for LTE with 64QAM modulation and phase noise mask

The phase noise root mean square is 0.65° approximately, and it is approximately the same for all the modulation types, as the phase noise mask is the same, and the white Gaussian noise power remains at the same level. The interpolation of the phase noise mask points is done in the logarithmic domain. For example, the linear interpolation of the points between 1 kHz and 10 kHz is done after the conversion of the frequency points into $\log_{10}$ values.

7.6.2 Phase noise for UMTS

In Figure 7-44-Figure 7-46 are shown the effects of the phase noise addition for the UMTS wireless systems. Although the BER results do not overlay for all the SNR values, the the curves match in a good measure.

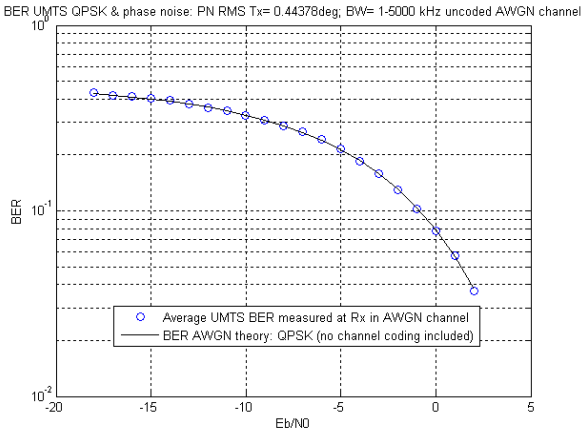

Figure 7-44 BER versus E_b/N_0 for UMTS with QPSK modulation and PN_{mask}

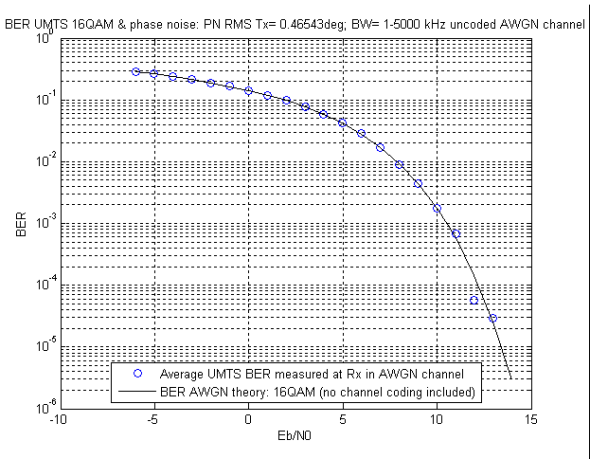

Figure 7-45 BER versus E_b/N_0 for UMTS with 16QAM modulation and PN_{mask}

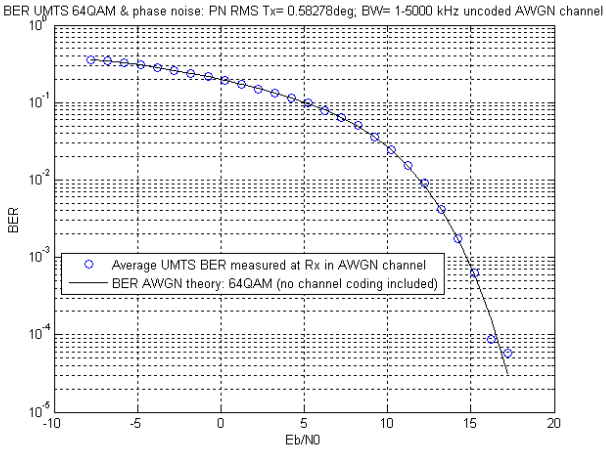

Figure 7-46 BER versus E_b/N_0 for UMTS with 64QAM modulation, and PN_{mask}

7.6.3 Phase noise for GSM/EDGE

In Figure 7-47 and Figure 7-48, the effect of phase noise on the GSM system with 8PSK and GMSK modulations is shown. The curve drift is almost the same as in the case in which the systems are ideal, without any RF impairments added in the transmission path, be it transmitter or receiver.

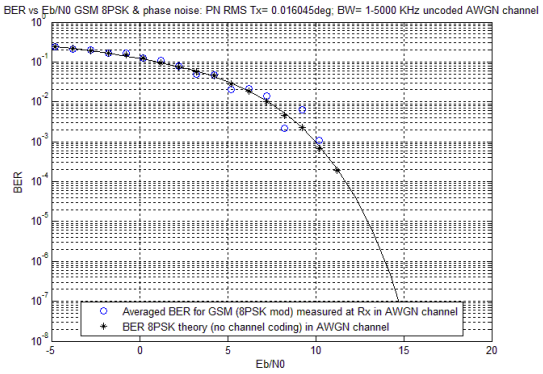

Figure 7-47 BER versus E_b/N_0 for GSM/EDGE with 8PSK modulation, AWGN channel and phase noise mask

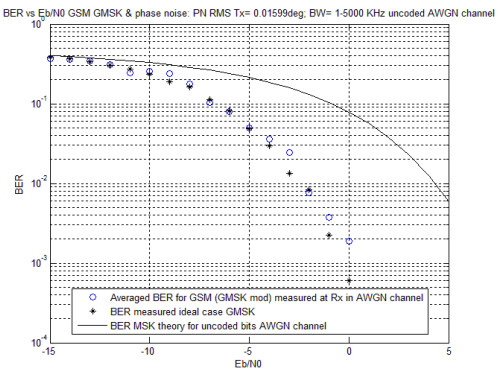

Figure 7-48 BER versus E_b/N_0 for GSM/EDGE with GMSK modulation, AWGN channel and phase noise mask

7.7 All RF impairments in a chain

7.7.1 All RF impairments in a chain for LTE

In Figure 7-49-Figure 7-51, the effect of the RF impairments modeled consecutively in a chain is showed. The added RF imperfections have been tuned in such a way that the total offset of the BER curve is 3 dB from the ideal BER curve. As the I-Q amplitude imbalance, I-Q phase imbalance, DC offset and frequency offset are the smallest in the case of 64QAM, together with the maximum value of IIP_3 of 43 dBm for this case, the 64QAM modulation is the most sensitive to RF imperfections. The RF imperfections have been only implemented for the transmitter, however, one should divide the values in two if the receiver imperfections are to be considered, and the IIP_3 value should be increased by 3 dBm.

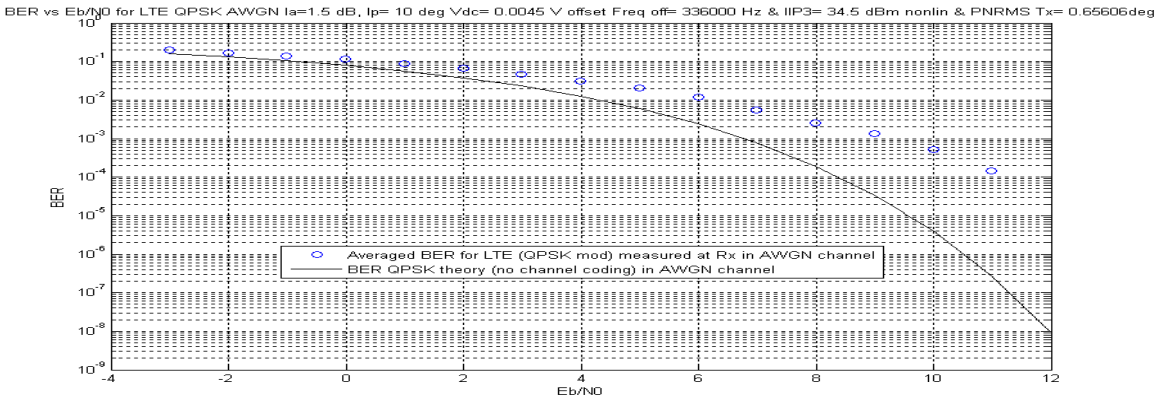

Figure 7-49 BER versus E_b/N_0 for LTE with QPSK modulation, AWGN channel and all RF imperfections

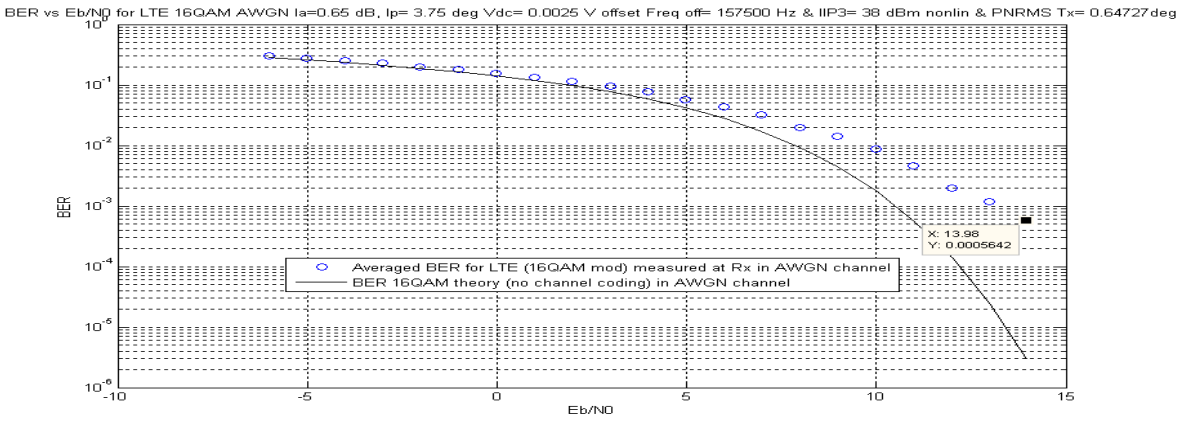

Figure 7-50 BER versus E_b/N_0 for LTE with 16QAM modulation, AWGN channel and all RF imperfections

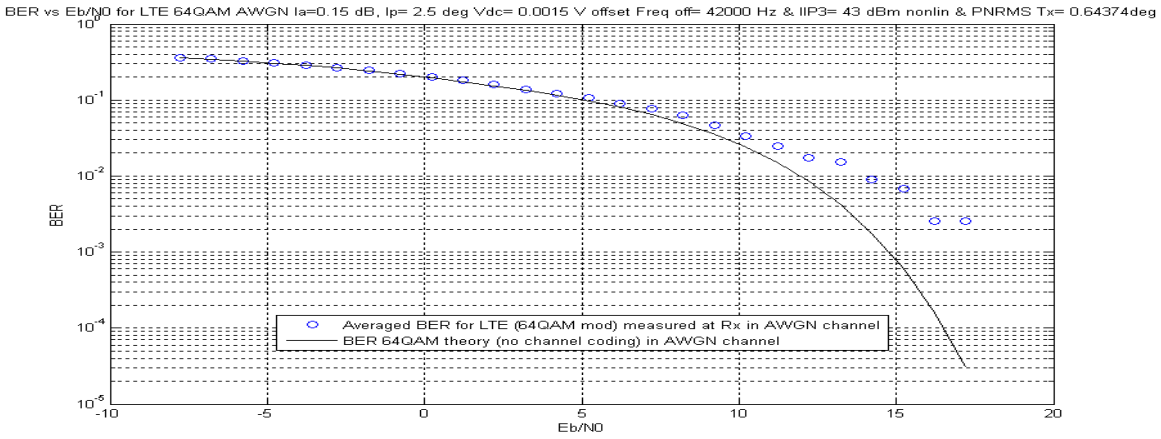

Figure 7-51 BER versus E_b/N_0 for LTE with 64QAM modulation, AWGN channel and all RF imperfections

7.7.2 All RF impairments in a chain for UMTS

In Figure 7-52-Figure 7-54, the effect of the RF imperfections implemented in a chain is shown for the UMTS wireless system for the QPSK, 16QAM and 64QAM.

Comparing the values of the RF imperfections, one discovers that the 64QAM system is the most sensitive to RF imperfections, as in the case of the LTE wireless system.

The set of parameters that gives the 3 dB offset for the BER curve in case of the 64QAM modulation is given here: I-Q amplitude imbalance of 0.25 dB, I-Q phase imbalance of 0.5^o, DC offset of 60 mV, a frequency offset of 50 Hz and an IIP_3 of 41.75 dBm.

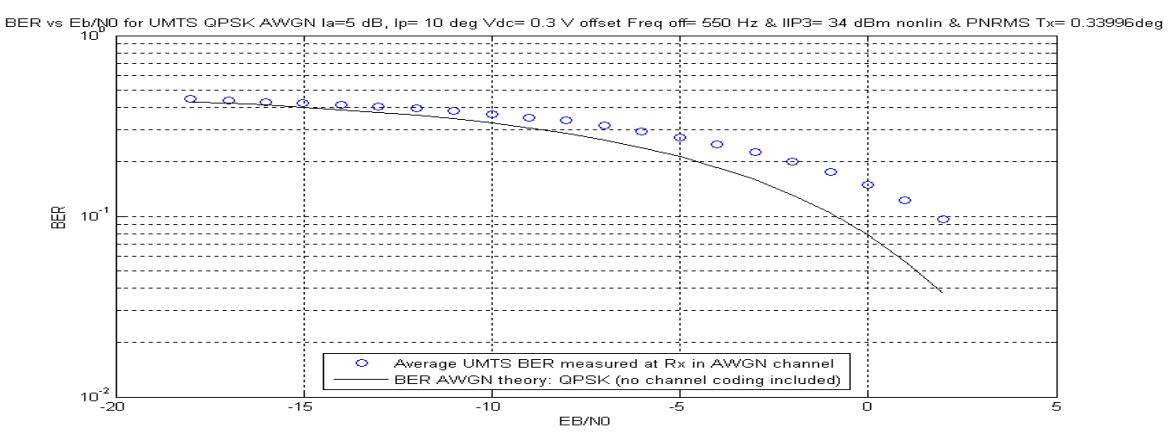

Figure 7-52 BER versus E_b/N_0 for UMTS with QPSK modulation, AWGN channel and all RF imperfections

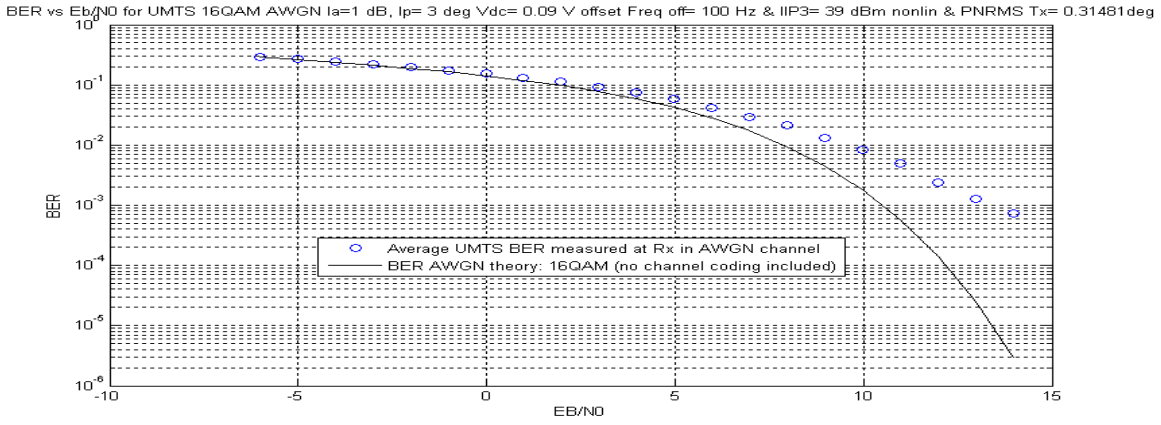

Figure 7-53 BER versus Eb/N0 for UMTS with 16QAM modulation, AWGN channel and all RF imperfections

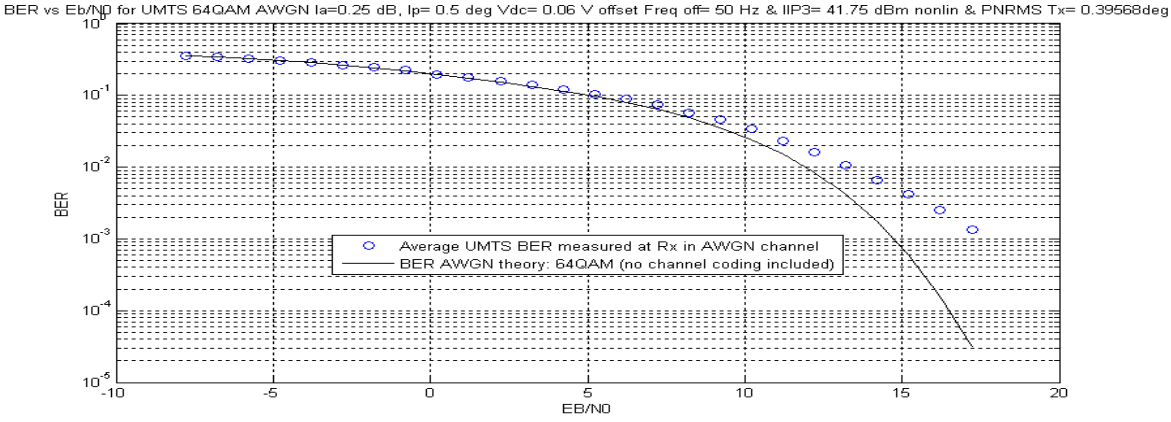

Figure 7-54 BER versus E_b/N_0 for UMTS with 64QAM modulation, AWGN channel and all RF imperfections

7.7.3 All RF impairments in a chain for GSM/EDGE

In Figure 7-55-Figure 7-56, the effect of all RF impairments in a chain on the GSM and EDGE systems is studied. Comparing the two modulation types, 8PSK and GMSK, one can see that the 8PSK is more sensitive to I-Q mismatch (both amplitude and phase), but more tolerant to frequency offsets (742.5 kHz for 8PSK compared to 126 kHz for GMSK) for the same level of nonlinearity of IIP_3= 38.5 dBm.

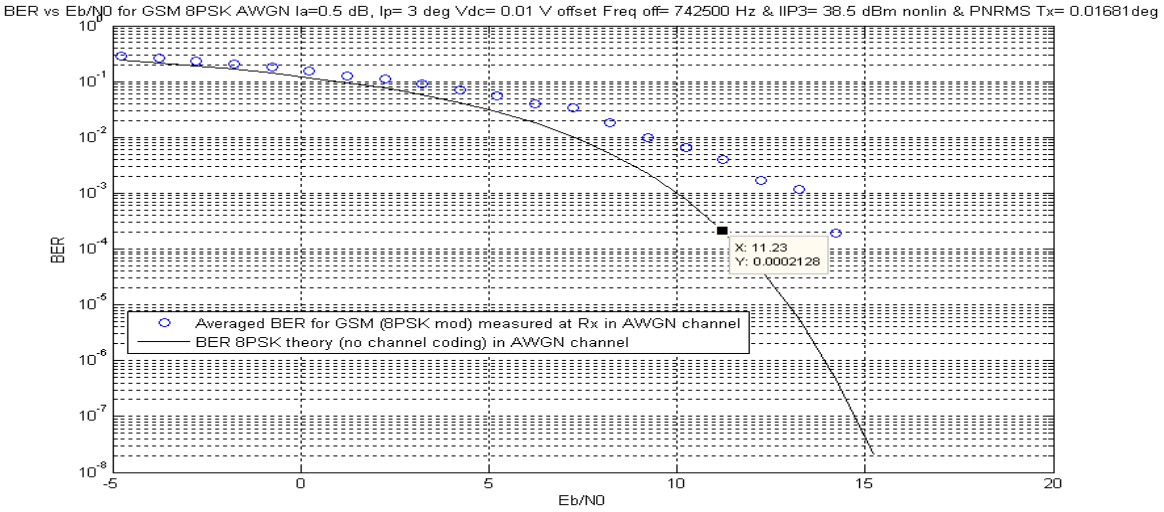

Figure 7-55 BER versus E_b/N_0 for GSM/EDGE with 8PSK modulation, AWGN channel and all RF imperfections

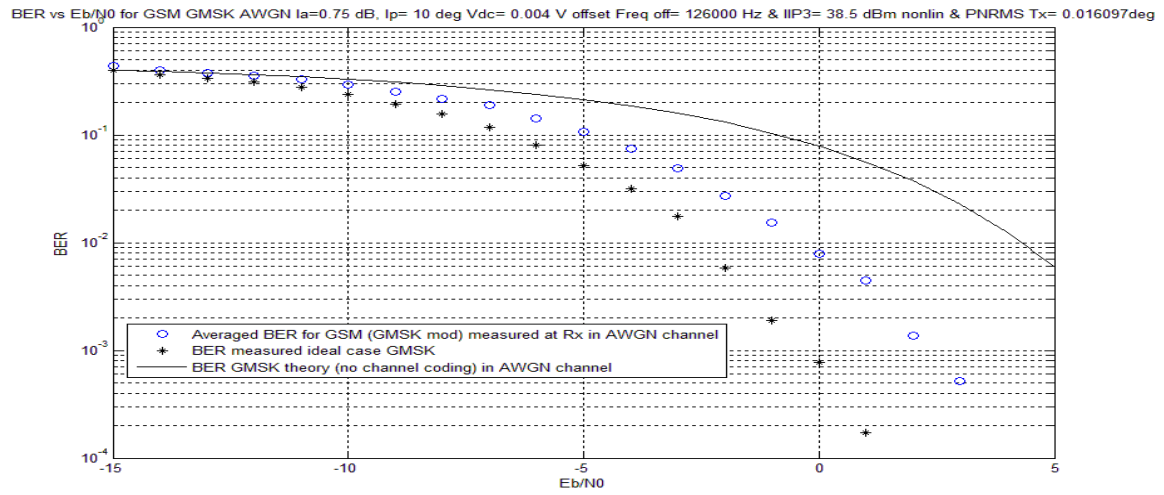

Figure 7-56 BER versus E_b/N_0 for GSM/EDGE with GMSK modulation, AWGN channel and all RF imperfections

7.8 Conclusions

In Table 7-1, a synthesis of all the results in chapter 7 is given. It appears that the most sensitive system to RF impairments in terms of BER performance is LTE (64QAM is the most intolerant). In bold are printed the most demanding results extracted from the results of Table 7-1. The IIP_3 values found in the table are more relaxed compared to the values found in Chapter 3, as the signals considered are not observed at the antenna, but at the output of the transmitters.

		GSM		UMTS			LTE		
Nr.	RF Imperfection	8PSK	GMSK	QPSK	16QAM	64QAM	QPSK	16QAM	64QAM
1	DC offset [mV]	52.5	90	1000	200	125	17	**10**	15
2	I-Q amplitude [dB]	1.5	3.5	11.5	3	1.75	3	1.12	**0.55**
3	I-Q phase [deg]	10	30	40[6]	20[6]	12[7]	20	7.5	**3.5**
4	IIP_3 [dBm]	36.5	36.5	32.5	36.75	40	33.5	38	**41.5**
5	Frequency offset [Hz]	135000	234000	1800	420	**240**	6720000	3150000	1680000
6	PN [RMS]	0.0158	0.016	0.46	0.453	0.453	**0.65606**	0.64727	0.6437
7	Chain of RF impairments:								
	DC offset [mV]	10	4	300	90	60	4.5	2.5	**1.5**
	I-Q amplitude [dB]	0.5	0.75	5	1	0.25	1.5	0.65	**0.15**
	I-Q phase [deg]	3	10	10	3	**0.5**	10	3.75	2.5
	IIP_3 [dBm]	38.5	38.5	34	39	41.75	34.5	38	**43**
	Frequency offset [Hz]	742500	120000	550	100	**50**	336000	157500	42000
	PN RMS [deg]	0.0168	0.0166	0.39	0.379	0.363	**0.65606**	0.64727	0.64374

Table 7-1 Tolerance to RF imperfections for GSM/EDGE, UMTS and LTE

[7] The values considered for the phase imbalance in case of UMTS are taken the same as for LTE

8. LTE transmitter configurations and their comparison

8.1 Classic outphasing transmitter

[Confidential]

8.2 Improved efficiency outphasing transmitter (threshold angle implementation)

[Confidential]

8.3 RF imperfections in the three transmitter systems

[Confidential]

8.3.1 RF imperfections characteristic for outphasing Tx only

[Confidential]

8.3.2 RF imperfections results compared for the three Tx types

8.3.2.1 DC Offset

[Confidential]

8.3.2.2 I-Q amplitude mismatch

[Confidential]

8.3.2.3 I-Q phase mismatch

[Confidential]

8.3.2.4 Nonlinearity

[Confidential]

8.3.2.5 Frequency offset

[Confidential]

8.3.2.6 Phase noise

[Confidential]

8.3.2.7 All RF impairments in a chain

[Confidential]

8.4 Conclusions

[Confidential]

9. Future research directions

9.1 Multipath channel modeling

This study has been taking into account the most simplified case of a transmission, that is the transmission in an AWGN channel. In reality, there is multipath because of reflections in the environment. An attempt has been made to simulate the Rayleigh channel, that is a type of channel widely used to simulate the multipath characteristic. The estimation has been assumed to be perfect. The generation of values has been done randomly, respecting the Rayleigh distribution. The time delay vector and power delay vector have been taken from the simplified version of the transmission paths model from the standard [**23**].

```
t_delay= [0 130.2e-9 260.4*1e-9 380.6*1e-9 520.891*1e-9]; %s
P_dB=    [-2.748 -4.413 -11.052 -18.5 -18.276];           %dBm
```

The power values have been converted from dBm to W and then a Rayleigh distribution has been generated for the powers vector. This distribution is then multiplied point by point with the other power vector in order to have a Rayleigh distributed power vector. The channels coefficients are then obtained after the multiplication of the Rayleigh distributed powers vector with each of the elements of the t_{delay} vector. The formula applied is (9.1):

$$Chan\_coef_{Rayleigh} = P.*(\cos(omega*t_{delay})+j*\sin(omega*t_{delay}));\%channel\ coef \qquad [9.1]$$

where omega is the channel bandwidth, for LTE is equal to $2*\pi*f_{BW}$ where $f_{Bw}= 3.84\ MHz$.

In Figure 9-1 it is shown the BER result for QPSK, in the case of LTE.

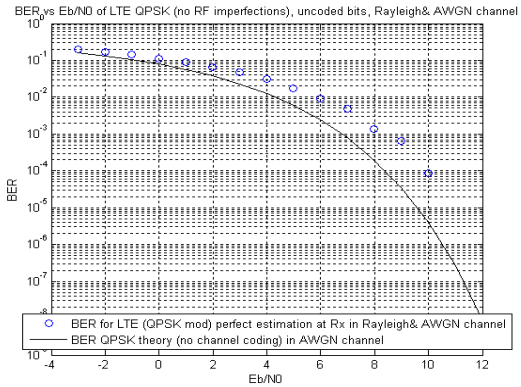

Figure 9-1 BER for LTE with QPSK modulation and Rayleigh distributed channel coefficients

It is shown that the Rayleigh distribution affects the BER rate, as the simulated curve does not match the theoretical one, compared to the case in which the channel was AWGN only. The simulation has been done for QPSK because it takes less time to simulate compared to 16QAM or 64QAM. However, in Figure 9-2 it is shown the result for the 16QAM simulation:

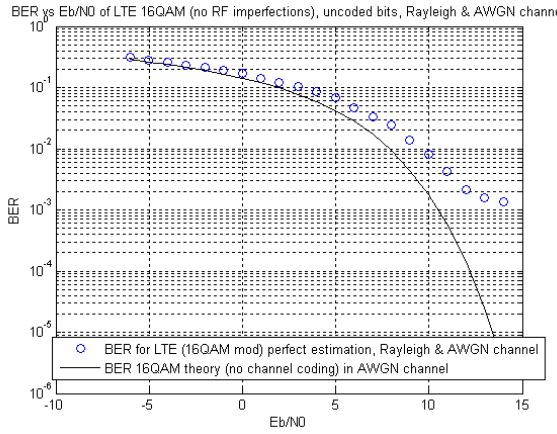

Figure 9-2 BER for LTE with 16QAM modulation and Rayleigh distributed channel coefficients

The BER values seem to flatten near the BER value of 0.1% for 16QAM. The 64QAM modulation has not been simulated because of the lengthy simulation time needed by the equalizer. To conclude, the Rayleigh channel affects the BER performance, the main reason being the incapacity of the equalizer to deal with the distorted information in the case of higher order modulations.

9.2 Doppler shift in Rayleigh channel

The Rayleigh channel has not taken into account the Doppler shift that might appear because of the moving user. A special function of MatLab has been used for the generation of the Doppler affected channel coefficients, that is the `rayleighchan.DopplerSpectrum` property of the `rayleighchan` function. The equalizer had to run in a *continuous* mode in order to equalize the data received for each of the path gains of the vector `rayleighchan.PathGains`. As the simulation took approximately 10 hours for each E_b/N_0 for the two transmitted blocks, the results are plotted only for several values, and not for the entire range. A paper that treats the channel estimation for the fading systems is [**31**]. The equalization aspect is treated in [**43**]. In Figure 9.3 it is shown the graph of the BER for the Rayleigh fading channel that is affected by Doppler shifts.

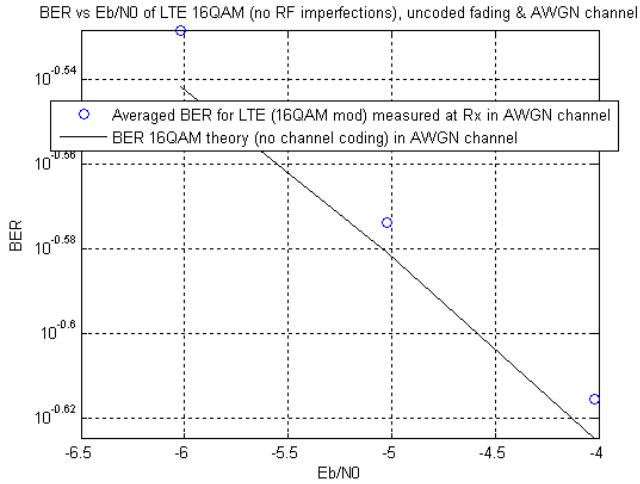

Figure 9-3 BER for LTE with 16QAM modulation and fading Rayleigh channel

In conclusion, the Doppler shift affected the transmission, but the time it took for the equalizer to deal with the Doppler affected values was so high that it has been decided at that time that it is better to proceed with the study of the RF impairments instead of the Rayleigh or Rayleigh fading channel. However, articles of interest on this topic are [**35**, **36**].

9.3 Estimation methods for the channel coefficients

Throughout this study it has been assumed that the estimation of the channel coefficients is perfect, in other words that the channel coefficients are known when the transmission takes place. However, this is not true in reality, as the user mobile has to estimate these coefficients in the receiver and improve the BER, thus the quality of the signal.

Numerous authors have studied the problem of estimation in OFDM systems [**24-34**]. One estimation method used in this study is the one proposed in [**24**], the discrete Fourier transform (DFT) domain based interpolation. The method is straightforward, but time consuming. A cyclic prefix is taken from the last part of the transmitted signal. This prefix is then filtered using the same channel coefficients. Then the fast Fourier transform (FFT) is computed for both the cyclic prefix (and one obtains the numerator) and for the transmitted signal (and one obtains the denominator), then the transfer function *H* is determined from the division of the numerator with the denominator. The last step is the inverse Fourier transform on this transfer function, that gives the channel coefficients.

The second estimation method is using the Toeplitz matrix. Its properties [**30**] make it useful for the estimation of the channel coefficients. The method used for estimation is the following: a Toeplitz matrix is created using the `X= toeplitz(R,C)` function of MatLab 2008, where R is made of five values of the signal to be transmitted, and C is made from the next twenty five values. Vector B is the received C vector, and the estimated channel coefficients are found by dividing the numerator X by the denominator B. This method is on average four times faster than the FFT estimation, and although it does not provide the same accuracy, the simulation time is much shorter. In Figure 9-4 and Figure **9-5** it is shown the performance of the Toeplitz estimator compared to the one of perfect estimation for five coefficients channel for LTE and UMTS respectively.

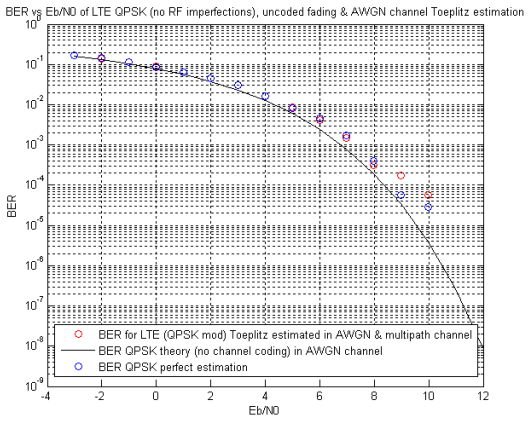

Figure 9-4 BER for LTE with QPSK modulation and fading Rayleigh channel, Toeplitz estimation

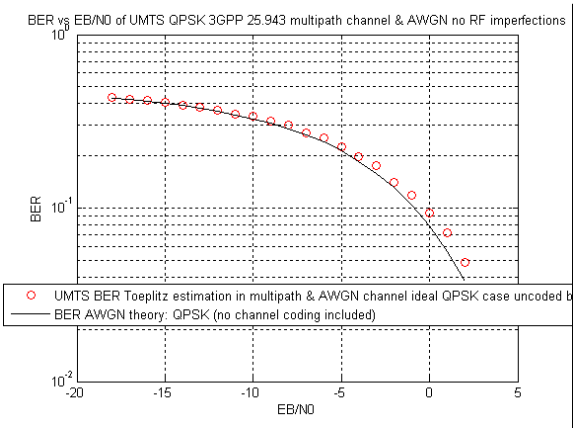

Figure 9-5 BER for UMTS with QPSK modulation and fading Rayleigh channel, Toeplitz estimation

9.4 Other future research directions and considerations

It has been a true challenge to implement some of the specifications found in the standards. For example, the UMTS standard [**11**], chapters 5.1.1.2 and 5.1.1.3 presented a different constellation (16QAM and 64QAM only) compared to the ones from the LTE standard [**8**], and the power of the modulated signals was not zero dBm in that case. Therefore, the constellations mentioned in the LTE standard had to be implemented instead of the ones mentioned for UMTS.

Moreover, the authors did not obtain the expected graph for the 8PSK pulse shaping filter defined in [**14**] when implementing the written code, nor from the direct import of the filter coefficients from MatLab 2010b (TU Delft student license) with a modified default function. The system has been considered as such, without 8PSK pulse shape filtering.

The MLSE equalizer has been preferred to the linear equalizers as its performance is the best among all equalizers analyzed according to Figure A-17.

The number of bits transmitted for one system has been calculated to be the same for all the three systems: LTE, UMTS and GSM/EDGE in order to have the BER computed for the same amount of bits.

Although in this study the BER implementation considered has been done only for the uncoded bits, the implementations took into account both the Turbo coding and the decoding.

An important thing worth mentioning is that the signals have not been up converted, thus they have not been mapped on a carrier.

An approximation has been considered on the following subject: the pruning of the bits. In the standard for LTE [**9**] chapter 5.1.4.2.2, it is specified that there is a pruning block that selects the bits for transmission and prunes the others. Doing so, the decoding in the receiver could not work properly, as the generated zero symbols were pruned and thus one will miss parts of the transmitted information in the receiver.

10. Conclusions

In this thesis, the study of the impact of RF imperfections on base stations transmission and reception performance has been done. The work has been based on the 3GPP standards for GSM/EDGE, UMTS and LTE, and IEEE standards for WiMax phase noise derivations. The requirements for linearity and phase noise have been derived, together with the multi-standards requirements. In chapters 5, the implementation of principle for the LTE, UMTS and GSM/EDGE wireless systems has been presented. In chapter 6, the BER performance of the three systems is analyzed in an AWGN channel. The study shows that UMTS presents better performance in general to RF impairments compared to LTE. In chapter 7, RF imperfections are considered and added to the three systems. Their tolerance to RF imperfections is observed and the most sensitive to RF imperfections proves to be, in general, LTE with 64QAM modulation. Chapter 8 is presenting the comparison between the classical I-Q transmitter, the classical outphasing transmitter and the improved outphasing transmitter with a 77^{o} threshold angle. This chapter also briefly treated another type of RF imperfection specific only to the outphasing transmitter, the delay between the two branches together with an amplitude mismatch.

A comparison is done not only between GSM/EDGE, UMTS and LTE, but also between the three types of transmitters for LTE. The main objective is to observe the tolerance to RF impairments of the wireless systems and of the transmitter types. The results showed that the LTE system is the least tolerant to RF imperfections in general, with its 64QAM modulation the most demanding case of all modulations. An important note of this study is the fact that even if the uncoded bits have been used for the simulations of BER, EVM, ACPR and other parameters, the programs are fully implemented according to the standards, that is including Turbo coding.

At the end of the study, future research directions are briefly indicated: the study of the propagation of the wireless signals in a Rayleigh channel, in a Rayleigh channel with Doppler shifts together with the estimation methods in these two cases. It has been the intention of estimating the channel coefficients, rather than deciding which method of estimation is the most convenient. This should be the subject of a further study.

Bibliography

[1] Qureshi, J.H.; Pelk, M.J.; Marchetti, M.; Neo, W.C.E.; Gajadharsing, J.R.; van der Heijden, M.P.; de Vreede, L.C.N.; , "A 90-W Peak Power GaN Outphasing Amplifier With Optimum Input Signal Conditioning," *Microwave Theory and Techniques, IEEE Transactions on* , vol.57, no.8, pp.1925-1935, Aug. 2009

[2] 3GPP TS 37.104 V9.2.0 “E-UTRA, UTRA and GSM/EDGE; Multi-Standard Radio (MSR) Base Station (BS) radio transmission and reception”

[3] 3GPP TS 36.104 V9.4.0 “Evolved Universal Terrestrial Radio Access (E-UTRA); Base Station (BS) radio transmission and reception”

[4] 3GPP TS 25.104 V9.4.0 “Base Station (BS) radio transmission and reception (FDD)”

[5] 3GPP TS 45.005 V9.4.0 “Radio transmission and reception”

[6] 3GPP TS 51.021 V9.2.0 “Base Station System (BSS) equipment specification; Radio aspects”

[7] IEEE Std 802.16™-2009 “IEEE Standard for Local and metropolitan area networks, Part 16: Air Interface for Broadband Wireless Access Systems”

[8] 3GPP TS 36.211 V9.1.0 “Evolved Universal Terrestrial Radio Access (E-UTRA); Physical channels and modulation”

[9] 3GPP TS 36.212 V9.2.0 “Evolved Universal Terrestrial Radio Access (E-UTRA); Multiplexing and channel coding”

[10] 3GPP TS 25.212 V10.0.0 “Multiplexing and channel coding (FDD)”

[11] 3GPP TS 25.213 V9.1.0 “Spreading and modulation (FDD)”

[12] 3GPP TS 25.104 V9.4.0 “Base Station (BS) radio transmission and reception (FDD)”

[13] 3GPP TS 45.003 V9.0.0 “Channel coding”

[14] 3GPP TS 45.004 V9.1.0 “Modulation”

[15] Vijay Garg, “Wireless communications and networking”, 1st edition, Morgan Kauffmann publishers, 2007

[16] http://www.3gpp.com/About-3GPP

[17] http://www.3gpp.com/specification-numbering

[18] Gu, Q., ”RF system design of transceivers for wireless communications”, Springer, 2005

[19] Mogensen, P. et al., “LTE Capacity compared to the Shannon Bound”, IEEE 65th Vehicular Technology Conference 2007. 22-25 April 2007, pages 1234 – 1238

[20] 3GPP 25.213 V9.1.0 “Spreading and modulation (FDD)”

[21] Hamedi-Hagh, S.; Salama, C.A.T.; "CMOS wireless phase-shifted transmitter," *Solid-State Circuits, IEEE Journal of* , vol.39, no.8, pp. 1241- 1252, Aug. 2004

[22] Schiller, J., “Mobile communications”, Pearson Education Limited, Second Edition, 2003, Great Britain

[23] 3GPP 25.943 V9.1.0 “Deployment aspects”

[24] Weng F.; Yin C.; Luo T.; "Channel estimation for the downlink of 3GPP-LTE systems," *Network Infrastructure and Digital Content, 2010 2nd IEEE International Conference on*, vol., no., pp.1042-1046, 24-26 Sept. 2010

[25] Mehlfuhrer, C.; Caban, S.; Rupp, M.; "An accurate and low complex channel estimator for OFDM WiMAX," *Communications, Control and Signal Processing, 2008. ISCCSP 2008. 3rd International Symposium on*, vol., no., pp.922-926, 12-14 March 2008

[26] Weng F.; Yin, C.; Luo, T.; "Channel estimation for the downlink of 3GPP-LTE systems," *Network Infrastructure and Digital Content, 2010 2nd IEEE International Conference on*, vol., no., pp.1042-1046, 24-26 Sept. 2010

[27] Rajeswari, K.; Sangeetha, T.; Natchammai, A.P.; Nandhini, M.; Thiruvengadam, S.J.; "Performance analysis of pilot aided channel estimation methods for LTE system in time-selective channels," *Industrial and Information Systems (ICIIS), 2010 International Conference on* , vol., no., pp.113-118, July 29 2010-Aug. 1 2010

[28] Maechler, P.; Greisen, P.; Felber, N.; Burg, A.; "Matching pursuit: Evaluation and implementation for LTE channel estimation," *Circuits and Systems (ISCAS), Proceedings of 2010 IEEE International Symposium on* , vol., no., pp.589-592, May 30 2010-June 2 2010

[29] van de Beek, J.-J.; Edfors, O.; Sandell, M.; Wilson, S.K.; Borjesson, P.O.; "On channel estimation in OFDM systems," *Vehicular Technology Conference, 1995 IEEE 45th*, vol.2, no., pp.815-819, 25-28 Jul 1995

[30] R. M. Gray, "Toeplitz and circulant matrices: A review," Tech. Rep., Inform. Syst. Lab., Stanford Univ., Stanford, CA, 1971

[31] Z. Xiaoping , Y. Fang, "Compressed sensing based channel estimation for fast fading OFDM systems", *Journal of Systems Engineering and Electronics*, vol. 21, no.4, pp. 550-556, August 2010

[32] Wirfalt, P.; Jansson, M.; "On Toeplitz and Kronecker structured covariance matrix estimation," *Sensor Array and Multichannel Signal Processing Workshop (SAM), 2010 IEEE* , vol., no., pp.185-188, 4-7 Oct. 2010

[33] Qian Yu; Gaonan Zhang; Guoan Bi; "Improved blind channel estimation method with Toeplitz displacement for long code DS-CDMA," *Signal Processing Advances in Wireless Communications, 2003. SPAWC 2003. 4th IEEE Workshop on*, vol., no., pp. 224-228, 15-18 June 2003

[34] Kung, S.; Lo, C.; Foka, R.; "A Toeplitz approximation approach to coherent source direction finding," *Acoustics, Speech, and Signal Processing, IEEE International Conference on ICASSP '86.* , vol.11, no., pp. 193- 196, Apr 1986

[35] Deergha Rao, K.; "A comparative theoretical BER performance analysis of wireless communication techniques in Rayleigh fading channel," *Signal Processing (ICSP), 2010 IEEE 10th International Conference on*, vol., no., pp.1642-1645, 24-28 Oct. 2010
[36] Uysal, M.; "Maximum achievable diversity order for cascaded Rayleigh fading channels, " *Electronics Letters* , vol.41, no.23, pp. 1289- 1290, 10 Nov. 2005

[37] van Wyk, J.; Linde, L.; "Bit error probability for a M-ary QAM OFDM-based system," *AFRICON 2007*, vol., no., pp.1-5, 26-28 Sept. 2007

[38] Priyanto, B.E.; Sorensen, T.B.; Jensen, O.K.; Larsen, T.; Kolding, T.; Mogensen, P.; , "Impact of polar transmitter imperfections on UTRA LTE uplink performance," *Norchip, 2007* , vol., no., pp.1-4, 19-20 Nov. 2007

[39] Yijun Zhou; Chia, M.Y.-W.; "A Novel Alternating and Outphasing Modulator for Wireless Transmitter," *Microwave Theory and Techniques, IEEE Transactions on*, vol.58, no.2, pp.324-330, Feb. 2010

[40] Huttunen, A.; Kaunisto, R.; "A 20-W Chireix Outphasing Transmitter for WCDMA Base Stations," *Microwave Symposium, 2007. IEEE/MTT-S International*, vol., no., pp.1437-1440, 3-8 June 2007

[41] Jau-Horng Chen; "An Efficiency-Improved Outphasing Power Amplifier Using RF Pulse Modulation," *Microwave and Wireless Components Letters, IEEE*, vol.20, no.12, pp.684-686, Dec. 2010

[42] Helaoui, M.; Boumaiza, S.; Ghannouchi, F.M.; "On the outphasing power amplifier nonlinearity analysis and correction using digital predistortion technique," *Radio and Wireless Symposium, 2008 IEEE* , vol., no., pp.751-754, 22-24, Jan. 2008

[43] Myburgh H.C., Olivier J.C., “Low Complexity MLSE equalization in Highly Dispersive Rayleigh Fading Channels”, EURASIP Journal on Advances in Signal Processing, vol. 2010

[44] United States Patent US7729445

A. Appendix

Tx EVM [%]		LTE classic I-Q Tx		
Nr.	**Due to RF Imperfection**	**QPSK**	**16QAM**	**64QAM**
1	Ideal	0.00	0.00	0.00
2	DC offset [mV]	1.06	1.06	1.06
3	I-$Q_{\text{amplitude mismatch}}$ [dB]	17.36	6.44	3.16
4	I-Q_{phase} mismatch [deg]	17.38	6.52	3.06
5	IIP_3 [dBm]	49.6	14.94	6.32
6	Frequency offset [Hz]	23.43	11.10	5.91
7	Phase noise [RMS]	3.69-6.97	3.7-6.9	3-7.3
8	Chain of All RF impairments	**18.9-20**	**9.2-11.6**	**5-8.8**

Table A-1 EVM values for the LTE classic I-Q Tx (no equalization)

Tx EVM [%]		LTE classic I-Q Tx		
Nr.	**Due to RF Imperfection**	**QPSK**	**16QAM**	**64QAM**
1	Ideal	0.00	0.00	0.00
2	DC offset [mV]	0.00	0.00	0.00
3	I-$Q_{\text{amplitude mismatch}}$ [dB]	0.00	0.00	0.00
4	I-Q_{phase} mismatch [deg]	0.00	0.00	0.00
5	IIP_3 [dBm]	0.00	0.00	0.00
6	Frequency offset [Hz]	0.00	0.00	0.00
7	Phase noise [RMS]	0.00	0.00	0-5.5
8	Chain of All RF impairments	**0**	**0-0.82**	**0-7.42**

Table A-2 EVM values for the LTE classic I-Q Tx (after equalization)

Tx EVM [%]		LTE classic outphasing Tx		
Nr.	**Due to RF Imperfection**	**QPSK**	**16QAM**	**64QAM**
1	Ideal	2.6E-14	2.9534E-14	2.517E-14
2	DC offset [mV]	2.40	1.41	2.13
3	I-$Q_{\text{amplitude mismatch}}$ [dB]	17.37	6.44	3.16
4	I-Q_{phase} mismatch [deg]	17.4	6.5	3.046
5	IIP_3 [dBm]	29.14	10.34	4.62
6	Frequency offset [Hz]	11.76	5.54	2.97
7	Phase noise [RMS]	5.13-10.6	5.38-11.14	5.44-11.36
8	Chain of All RF impairments	**21.8-22.8**	**11.8-14.88**	**6.36-11.7**

Table A-3 EVM values for the LTE classic outphasing Tx (no equalization)

Tx EVM [%]		LTE classic outphasing Tx		
Nr.	**Due to RF Imperfection**	**QPSK**	**16QAM**	**64QAM**
1	Ideal	0.00	0.00	0.00
2	DC offset [mV]	0.00	0.00	2.71
3	I-$Q_{\text{amplitude mismatch}}$ [dB]	0.00	0.00	0.00
4	I-Q_{phase} mismatch [deg]	0.00	0.00	0.00
5	IIP_3 [dBm]	0.00	0.00	0.00
6	Frequency offset [Hz]	0.00	0.00	0.00
7	Phase noise [RMS]	0.00	0-3	1.8-9.4
8	Chain of All RF impairments	0.00	0-8.12	1.96-11.87

Table A-4 EVM values for the LTE classic outphasing Tx (after equalization)

Tx EVM [%]		LTE improved outphasing Tx		
Nr.	**Due to RF Imperfection**	**QPSK**	**16QAM**	**64QAM**
1	Ideal	2.6E-14	2.9534E-14	2.517E-14
2	DC offset [mV]	2.40	1.41	2.13
3	I-$Q_{\text{amplitude mismatch}}$ [dB]	17.37	6.44	3.16
4	I-Q_{phase} mismatch [deg]	17.4	6.5	3.046
5	IIP_3 [dBm]	29.14	10.34	4.62
6	Frequency offset [Hz]	11.76	5.54	2.97
7	Phase noise [RMS]	5.13-10.6	5.38-11.14	5.44-11.36
8	Chain of All RF impairments	21.8-22.8	11.8-14.88	6.36-11.7

Table A-5 EVM values for the LTE improved outphasing Tx (no equalization)

Tx EVM [%]		LTE improved outphasing Tx		
Nr.	**Due to RF Imperfection**	**QPSK**	**16QAM**	**64QAM**
1	Ideal	0.00	0.00	0.00
2	DC offset [mV]	0.00	0.00	2.76
3	I-$Q_{\text{amplitude mismatch}}$ [dB]	0.00	0.00	0.00
4	I-Q_{phase} mismatch [deg]	0.00	0.00	0.00
5	IIP_3 [dBm]	0.00	0.00	0.00
6	Frequency offset [Hz]	0.00	0.00	0.00
7	Phase noise [RMS]	0.00	0-1.18	0.33-7.42
8	Chain of All RF impairments	**0-0.76**	**3.61-23.58**	**10.73-18.26**

Table A-6 EVM values for the LTE improved outphasing Tx (after equalization)

$\underline{ACPR_{Tx}}$ [dBc]		LTE classic I-Q Tx		
Nr.	**RF Imperfection**	**QPSK**	**16QAM**	**64QAM**
1	Ideal	-79.19	-78.57	-78.31
2	DC offset [mV]	-79.20	-78.53	-78.92
3	I-$Q_{amplitude\ mismatch}$ [dB]	-79.39	-78.61	-78.41
4	I-Q_{phase} mismatch [deg]	-79.13	-78.31	-78.48
5	IIP_3 [dBm]	-36.41	-42.76	-46.57
6	Frequency offset [Hz]	-48.97	-41.92	-44.74
7	Phase noise [RMS]	-53.83	-48.36	-52.20
8	Chain of All RF impairments	-32.22	-38.47	-48.08

Table A-7 ACPR values for the LTE classic I-Q Tx

$\underline{ACPR_{Rx}}$ [dBc]		LTE classic I-Q Rx		
Nr.	**RF Imperfection**	**QPSK**	**16QAM**	**64QAM**
1	Ideal	-79.19	-78.57	-78.31
2	DC offset [mV]	-79.19	-78.43	-78.08
3	I-$Q_{amplitude\ mismatch}$ [dB]	-79.65	-78.52	-78.36
4	I-Q_{phase} mismatch [deg]	-78.97	-78.20	-78.33
5	IIP_3 [dBm]	-18.07	-29.55	-38.50
6	Frequency offset [Hz]	-36.13	-38.72	-35.78
7	Phase noise [RMS]	-43.07	-43.72	-44.09
8	Chain of All RF impairments	NA	NA	NA

Table A-8 ACPR values for the LTE classic I-Q Rx

$\underline{ACPR_{Tx}}$ [dBc]		LTE classic outphasing Tx		
Nr.	**RF Imperfection**	**QPSK**	**16QAM**	**64QAM**
1	Ideal	-79.19	-78.57	-78.31
2	DC offset [mV]	-79.20	-78.85	-78.20
3	I-$Q_{amplitude\ mismatch}$ [dB]	-79.41	-78.40	-78.53
4	I-Q_{phase} mismatch [deg]	-79.15	-78.68	-78.55
5	IIP_3 [dBm]	-77.42	-78.08	-78.13
6	Frequency offset [Hz]	-34.83	-42.55	-43.83
7	Phase noise [RMS]	-35.53	-33.43	-33.80
8	Chain of All RF impairments	-23.09	-24.89	-25.29

Table A-9 ACPR values for the LTE classic outphasing Tx

$\underline{ACPR_{Rx}}$ [dBc]		LTE classic outphasing Rx		
Nr.	**RF Imperfection**	**QPSK**	**16QAM**	**64QAM**
1	Ideal	-79.19	-78.57	-78.31
2	DC offset [mV]	-79.18	-78.38	-77.94
3	I-$Q_{amplitude\ mismatch}$ [dB]	-79.42	-78.36	-78.40
4	I-Q_{phase} mismatch [deg]	-79.06	-78.64	-78.28
5	IIP_3 [dBm]	-37.02	-40.32	-46.54
6	Frequency offset [Hz]	-30.81	-39.66	-39.29
7	Phase noise [RMS]	-27.76	-25.45	-27.18
8	Chain of All RF impairments	NA	NA	NA

Table A-10 ACPR values for the LTE classic outphasing Rx

$\underline{ACPR_{Tx}}$ [dBc]		LTE improved outphasing Tx		
Nr.	**RF Imperfection**	**QPSK**	**16QAM**	**64QAM**
1	Ideal	-79.20	-78.67	-78.59
2	DC offset [mV]	-79.20	-78.50	-78.33
3	I-$Q_{amplitude\ mismatch}$ [dB]	-79.28	-78.53	-78.41
4	I-Q_{phase} mismatch [deg]	-79.11	-78.47	-78.43
5	IIP_3 [dBm]	-22.26	-28.35	-33.13
6	Frequency offset [Hz]	-47.96	-50.16	-38.48
7	Phase noise [RMS]	-40.36	-39.17	-37.40
8	Chain of All RF impairments	-18.01	-24.07	-28.62

Table A-11 ACPR values for the LTE improved outphasing Tx

$\underline{ACPR_{Rx}}$ [dBc]		LTE improved outphasing Rx		
Nr.	**RF Imperfection**	**QPSK**	**16QAM**	**64QAM**
1	Ideal	-79.20	-78.67	-78.59
2	DC offset [mV]	-79.20	-78.28	-78.67
3	I-$Q_{amplitude\ mismatch}$ [dB]	-79.57	-78.70	78.29
4	I-Q_{phase} mismatch [deg]	-79.22	-78.31	-78.28
5	IIP_3 [dBm]	-20.60	-28.63	-31.79
6	Frequency offset [Hz]	-31.51	-36.40	-36.12
7	Phase noise [RMS]	-33.07	-32.29	-32.14
8	Chain of All RF impairments	NA	NA	NA

Table A-12 ACPR values for the LTE improved outphasing Rx

Two tone analysis of a 5 kHz sinusoid

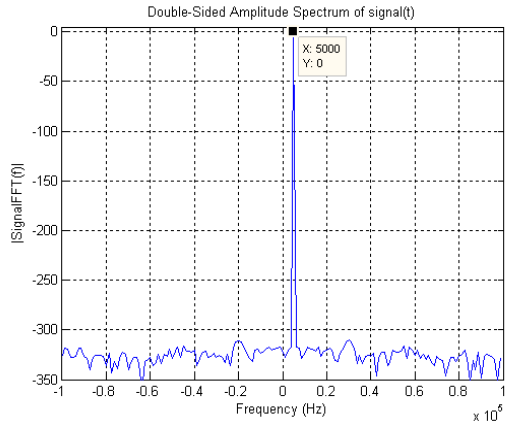

Figure A-1 FFT of the original sinusoid

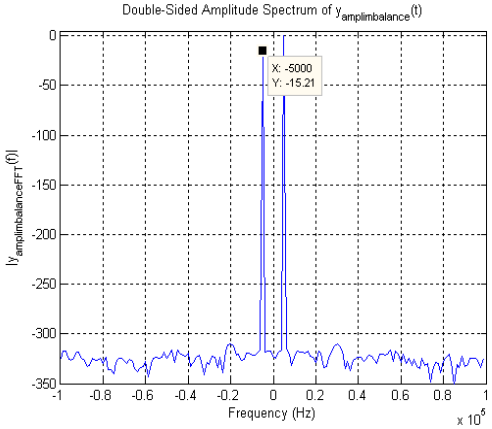

Figure A-2 FFT of the 3dB I-$Q_{A\ mismatch}$ affected sine

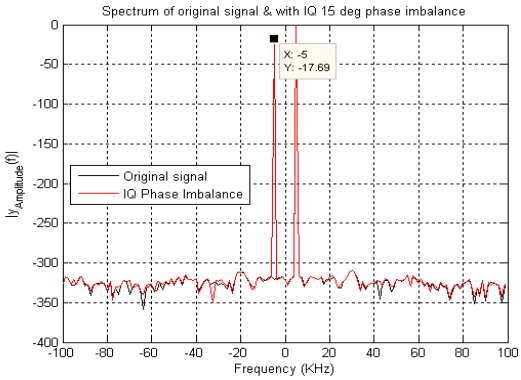

Figure A-3 FFT of the 15^{o} I-$Q_{phase\ mismatch}$ affected sine

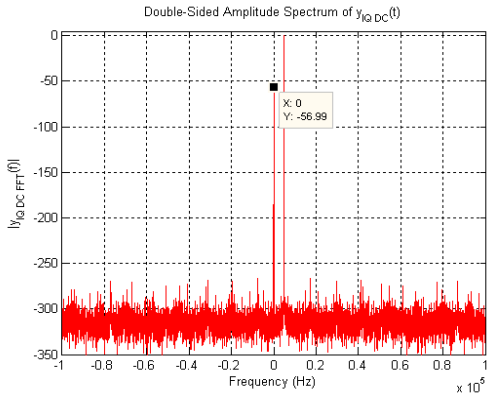

Figure A-4 FFT of the 1 mV DC_{offset} affected sine

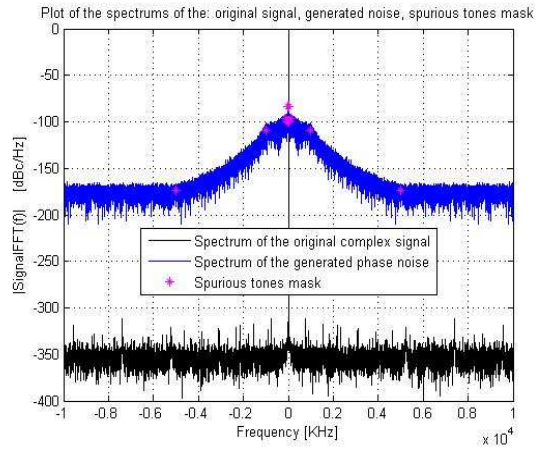

Figure A-5 FFT of the phase noise affected sine

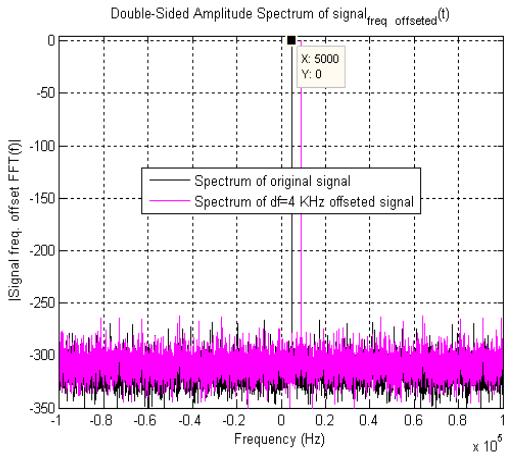

Figure A-6 FFT of the 4 kHz f_{offset} affected sine

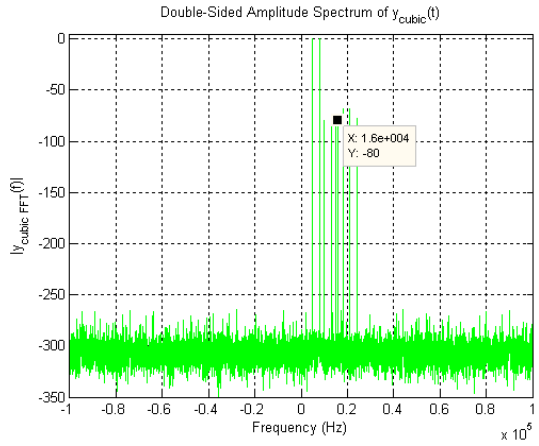

Considered values:

IIP_3= 40 dBm;

IIP_2= 80 dBm;

$s(t)= a_1s^1(t)+a_2s^2(t)+a_3s^3(t)$;

The determined vector of coefficients is:

$[a_1\ a_2\ a_3]$= [1 1E-4 1.33E-4]

Figure A-7 FFT of the cubic nonlinearity affected sine

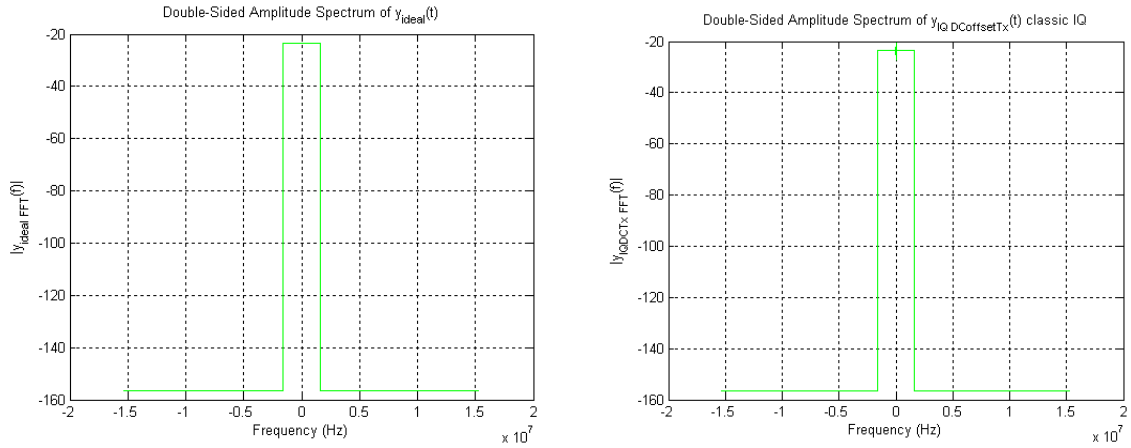

Figure A-8 FFT spectrum for the ideal case and for 17 mV DC_{offset} LTE QPSK Tx

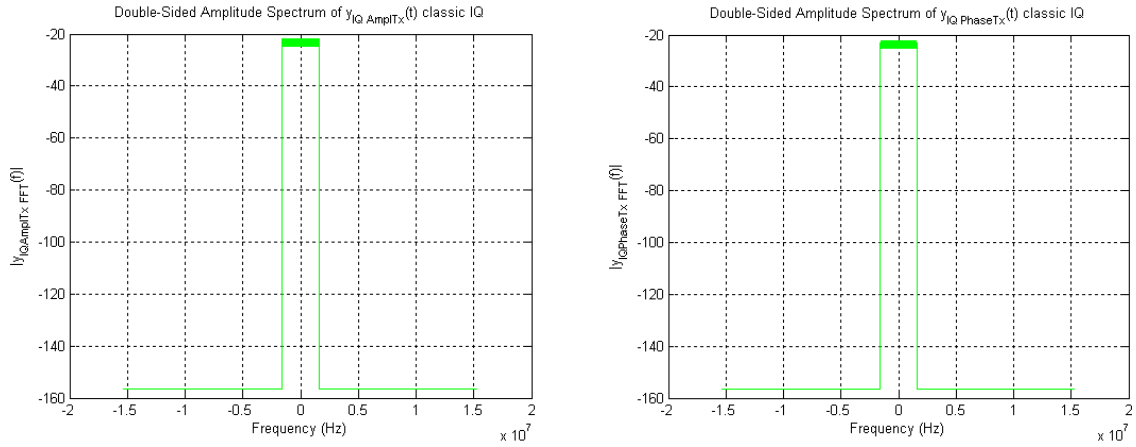

Figure A-9 FFT spectrum for the 3 dB amplitude mismatch and 20^o phase mismatch LTE QPSK Tx

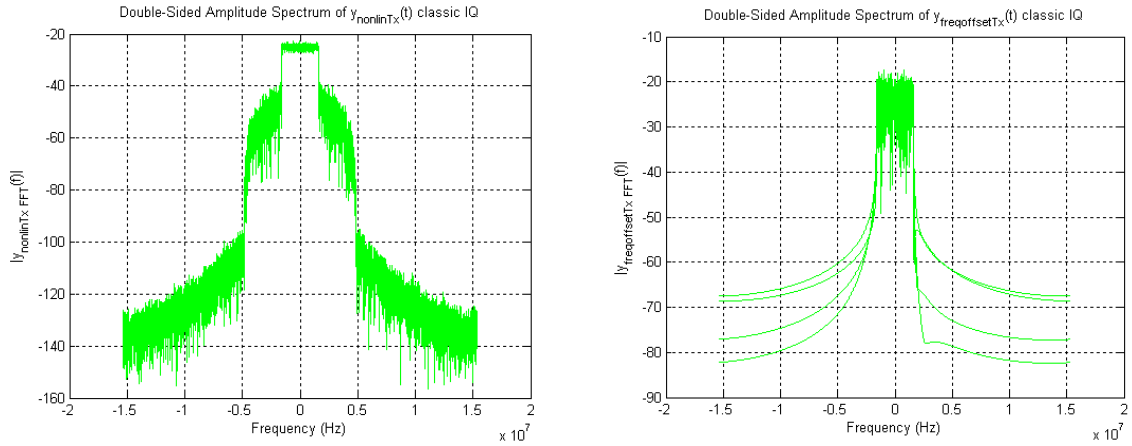

Figure A-10 FFT spectrum for IIP_3= 33.5 dBm cubic nonlinearity and 6.72 MHz $frequency_{offset}$ LTE QPSK Tx

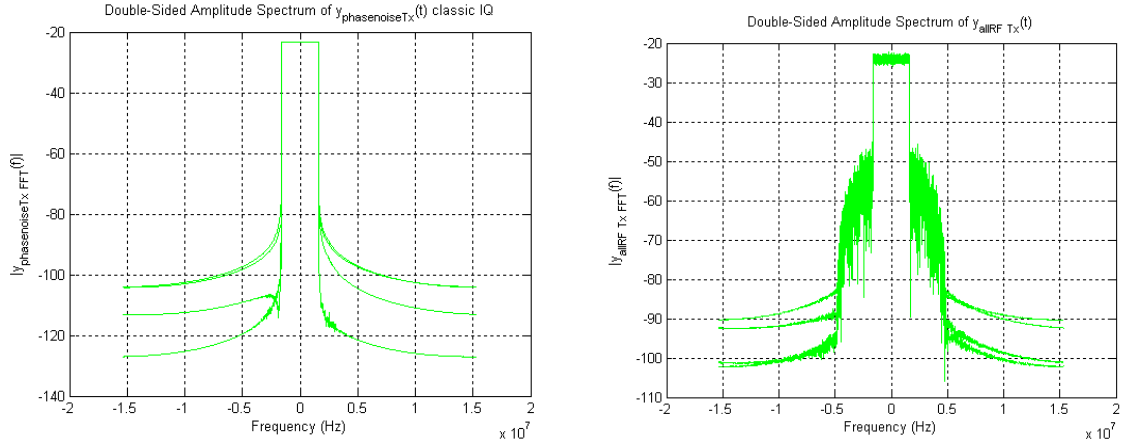

Figure A-11 FFT spectrum for phase noise mask and all RF imperfections LTE QPSK Tx

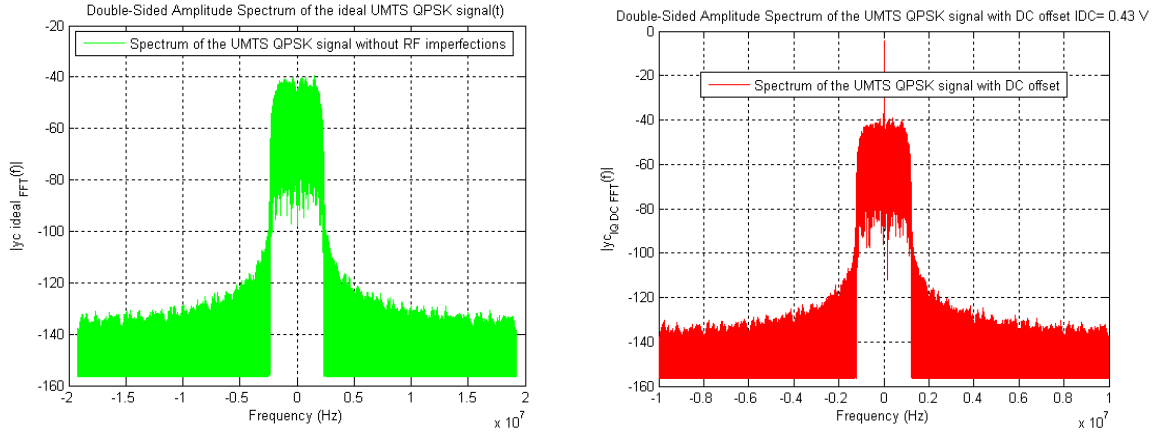

Figure A-12 FFT spectrum for ideal case and 430 mV DC_{offset} UMTS QPSK Tx

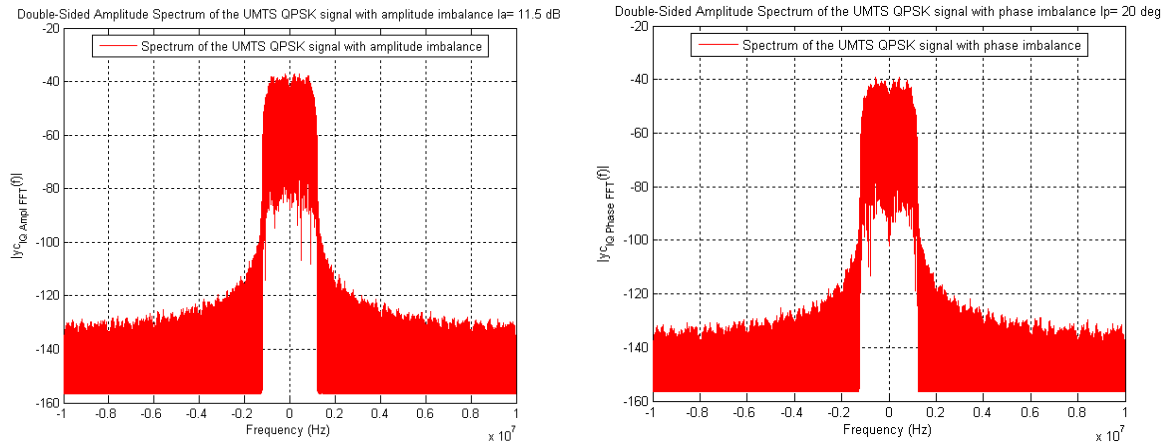

Figure A-13 FFT spectrum for 11.5 dB amplitude imbalance and 20^{o} phase imbalance UMTS QPSK Tx

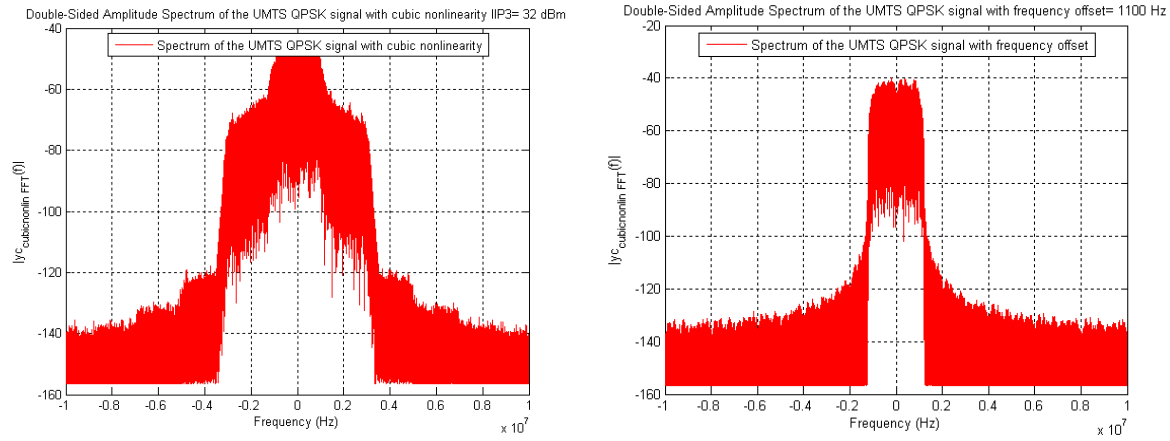

Figure A-14 FFT spectrum for 32 dBm cubic nonlinearity and 1100 Hz frequency offset UMTS QPSK Tx

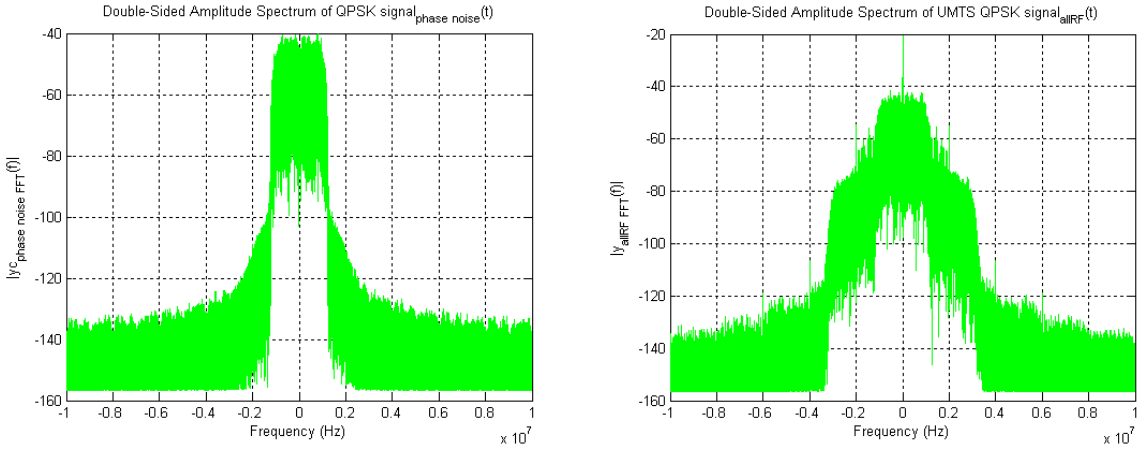

Figure A-15 FFT spectrum for phase noise mask and all RF imperfections UMTS QPSK Tx

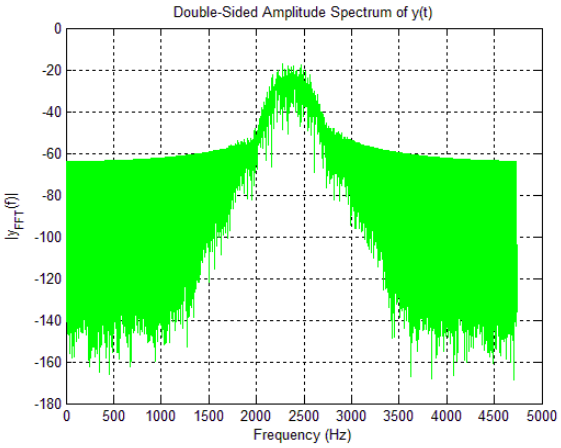

Figure A-16 FFT spectrum for ideal GSM GMSK Tx

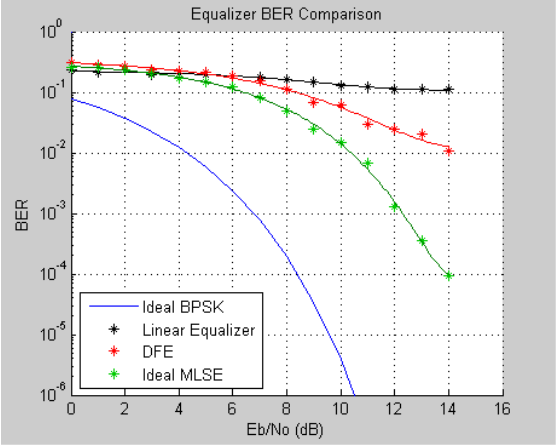

Figure A-17 BER performance of different equalizers for a BPSK modulated signal
(MatLab2008b figure from the Help of the program, chapter “BER performance of different equalizers”)